

General Disclaimer

One or more of the Following Statements may affect this Document

- This document has been reproduced from the best copy furnished by the organizational source. It is being released in the interest of making available as much information as possible.
- This document may contain data, which exceeds the sheet parameters. It was furnished in this condition by the organizational source and is the best copy available.
- This document may contain tone-on-tone or color graphs, charts and/or pictures, which have been reproduced in black and white.
- This document is paginated as submitted by the original source.
- Portions of this document are not fully legible due to the historical nature of some of the material. However, it is the best reproduction available from the original submission.

E.W. Urban
ES63

(NASA-CR-171392) INFRARED TELESCOPE Final
Technical Report (Alabama Univ.,
Huntsville.) 151 p EC A08/EF A01 CSCI 03A

185-26465

Unclas
G3/89 21186

FINAL TECHNICAL REPORT
NASA CONTRACT NAS8-32818
INFRARED TELESCOPE

by

Gerald R. Karr and John B. Hendricks

to

National Aeronautics and Space Administration
George C. Marshall Space Flight Center
Marshall Space Flight Center, Alabama, 35812

from

The University of Alabama in Huntsville
Huntsville, Alabama, 35899

FINAL TECHNICAL REPORT
NASA CONTRACT NAS8-32818
INFRARED TELESCOPE

by

Gerald R. Karr and John B. Hendricks

to

National Aeronautics and Space Administration
George C. Marshall Space Flight Center
Marshall Space Flight Center, Alabama, 35812

from

The University of Alabama in Huntsville
Huntsville, Alabama, 35899

TABLE OF CONTENTS

	<u>Page</u>
Preface	iii
I. Transfer Assembly Development	1
II. Cryostat Development	19
III. IRT Flow Meters	26
IV. Low Pressure Transfer Of Liquid Helium	44
V. Burst Disks For IRT	48
VI. Flow Of Helium Gas In The IRT	59
VII. Cold Finger Testing Results	66
VIII. Design And Testing Of The Rotating Connection For IRT	73
IX. Porous Plug Development	78
X. Thermal Modelling And Heat Exchanger Design	81
XI. Results and Conclusions	86

APPENDICES

APPENDIX A.	A Cryogenic Helium II System For Spacelab	A-1
APPENDIX B.	Spacelab 2 Infrared Telescope Cryogenic System	B-1
APPENDIX C.	Cryogenic Sub-System Performance Of The Infrared Telescope For Spacelab 2	C-1
APPENDIX D.	Performance Of The Helium II Dewar Sub-System For The Spacelab 2 Infrared Telescope	D-1
APPENDIX E.	Cryogenic Performance Testing Of The Infrared Telescope (IRT) For Spacelab 2	E-1
APPENDIX F.	Design And Performance Of Transfer Assembly For The Infrared Telescope For Spacelab 2	F-1
APPENDIX G.	The Infrared Telescope On Spacelab 2	G-1

PREFACE

This is the Final Technical Report on the effort at the University of Alabama in Huntsville in the development of the Infrared Telescope for Spacelab 2. The PI's at UAH undertook the design, development, and testing required to interface a stationary superfluid helium dewar with a scanning cryostate capable of operating in the zero-g environment in the space shuttle bay. Other than the PI's, a number of others at UAH that had significant roles in the successful development of IRT. In particular, John Medlen who was the UAH machine shop foreman, enabled the manufacture of many unique components which makes up the transfer assembly. All the transfer assembly was manufactured in the UAH shop under the direction of John Medlen.

The mechanical design of the internal parts of the Transfer assembly was the responsibility of Paul Clemons, consultant to the UAH IRT effort. All drawings of the Transfer assembly were originally prepared by Paul Clemons and later modified to be recorded in the MSFC archives. Many unforeseen problems with interfacing with the dewar and cryostate were successfully solved by designs prepared by Paul.

Mark Tcherneshoff was employed under this effort while pursuing an undergraduate degree in engineering. His effort was directed to the assembly and testing of the various components of the IRT. In particular, the MLI insulation blankets required extreme care in the layup. Mark was also responsible for most of the final assembly of the Transfer-Assembly.

The UAH-IRT effort was supported through the MSFC Space Science Laboratory under the direction of Dr. Eugene Urban. All of the UAH effort was performed with the close cooperation and invaluable input of Dr. Urban who was involved in all phases of the design development and testing of the IRT.

Gerald R. Karr

John B. Hendricks

I. Transfer Assembly Development

1. Critical Design Review

A presentation was made on May 21 at the Critical Design Review for the Transfer Assembly. The presentation consisted of the four tables attached to this report. Table 1 reviews the functions of the T.A., Table 2 lists the major components of the T.A., Table 3 lists the valve positions required for various operations, and Table 4 lists the assembly sequence required to assemble the T.A. onto the dewar.

The major results of the CDR was identification of (1) the need to provide locks and indicators for valves, (2) the problem of alignment of the cryostat during assembly, (3) the need to determine the maximum angular deflection of the helix to be allowed, and (4) the need to determine the impact of design options on the thermal performance of the system including (a) the location of the transfer tube heat shield on either the coldest or next coldest shield, (b) the effect of radiation down the holes for the valve actuators, and (c) the effect of the thermal shorting of the teflon spacer between the valve assembly and the coldest heat shield.

2. Major Testing and Fabrication Needs

The following list has been developed of the major tests and fabrications which are needed for the T.A. development:

a. Porous Plug Assembly

- b. Flow Meters
- c. Burst Disk
- d. Helix
- e. Plumbing
 - 1. Valve Assembly
 - 2. Heat Exchanger Manifolds
- f. Electrical Feedthroughs at Cold Temperatures
- g. Dewar-T.A. Thermal Performance Test
- 3. Assembly Sequence of T.A.

The following assembly sequence has been developed for assembling the T.A. onto the dewar:

- A. Assembly Sequence of T.A.
 - 1. Cut dewar tubes and weld conflat
 - 2. Pack MLI around neck tube
 - 3. Attach mount rings
 - 4. Attach outer shell
 - 5. Attach outer (largest) shield tub
 - 6. Attach second largest shield tub
 - 7. Attach transfer line shield
 - 8. Attach inner (smallest) shield tub
 - 9. Attach valve assembly support plate
 - 10. Attach depth probe assembly
 - 11. Attach valve assembly to plate
 - 12. Attach helix to valve assembly
 - 13. Attach fill and vent outer valves
 - 14. Make up internal plumbing
 - 15. Attach cryostat substitute line to helix

16. Make up electrical connections
17. Attach shield-tub lids
18. Attach dome
19. Attach valve actuator cover.

4. Cryostat Thermal Performance Data

The data obtained in the cryostat thermal performance tests was reviewed to find periods during which the system had come to a steady state for known values of inlet temperature and flow rates.

5. Dewar Design Information

The desing of the flight dewar was reviewed to obtain information needed for input to the computer program. The following information was obtained for the dewar as delivered by the manufacturer:

Item	Radiation Area (in) ²	Conduction		Material
		Area (in) ²	Length (in)	
Liquid vessel	3200			Aluminum
Liquid vessel neck support to first heat shield		$\pi(9.75)(.12)$	9	Fiberglas
Liquid vessel bottoms support to first heat shield		$.437(.05)(2)(3)$	1.8	Fiberglas
First heat shield	4119			Aluminum
First heat shield neck support to second heat shield		$\pi(9.75)(.12)$	3	Fiberglas
First heat shield bottom support to second heat shield		$.437(.05)(2)(3)$	3.2	Fiberglas
Second heat shield	4606			Aluminum

Item	Radiation Area (in) ²	Conduction		Material
		Area(in) ²	Length(in)	
Second heat shield neck support to third heat shield		$\pi(10.0)(.12)$	3.75	Fiberglas
Second heat shield bottom support to outer shell		$\pi 37(.05)(2)(3)$	4.9	Fiberglas
Third heat shield	5129			Aluminum
Third heat shield neck tube support to outer shell		$\pi(10.0)(.12)$	5.75	Fiberglas

6. Transfer Assembly Layout

The attached figures show two views of the plumbing layout for the transfer assembly. This layout is preliminary and for planning purposes only. The separate subassemblies are designed to attach to the three lines which interface with the dewar and the cold gas line which delivers gas to the IRT cryostat.

The fill-subassembly consists of:

- (a) a flange which attaches to the fill line which penetrates into the dewar storage volume
- (b) a flange which attaches to the fill line from outside the transfer assembly
- (c) a fill line valve which controls the fill process and seals the dewar after filling, and
- (d) a fill line burst disk which is designed to exhaust out through the outside fill line.

The superfluid-subassembly consists of:

- (a) a flange which attaches to the line which will bring superfluid liquid helium from the helium storage volume
- (b) a flange which attaches to the line that sends cold gas back to cool the dewar vapor cooled shields
- (c) a flange which attaches to the helix subassembly
- (d) a valve which bypasses the superfluid plug to allow for additional venting during fill and pump down operations.
- (e) a superfluid plug device which will serve as a phase separator of the liquid and vapor helium, and
- (f) a burst disk which is designed to exhaust out through the two vapor lines.

The helix-subassembly consists of:

- (a) a flange which attaches to the appropriate flange on the superfluid subassembly
- (b) a helical coil designed to serve as a passage for cold helium gas and as a torsional spring to take up the relative rotation between the helium dewar and the IRT cryostat, and
- (c) a flange or pipe fitting which will connect the helix exhaust to the IRT inlet pipe.

The three subassemblies can be made up and tested separately and arranged on a common support for final attachment to the three-tube interface of the helium dewar and the transfer line to the IRT experiment. The preliminary layout shows the total package to fall within a 6 to 7 inch radius which is within the limits required in the transfer assembly design.

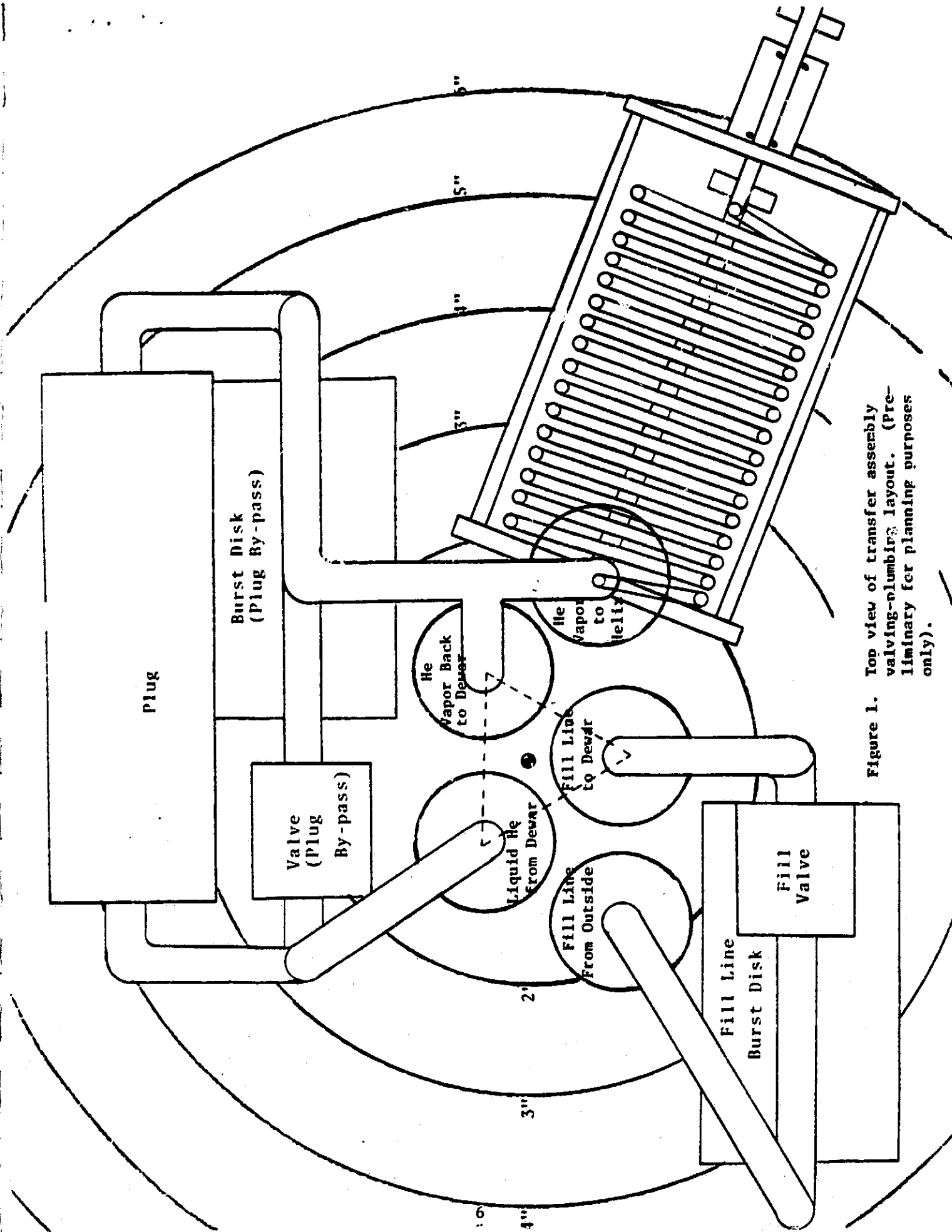


Figure 1. Top view of transfer assembly valving-plumbing layout. (Preliminary for planning purposes only).

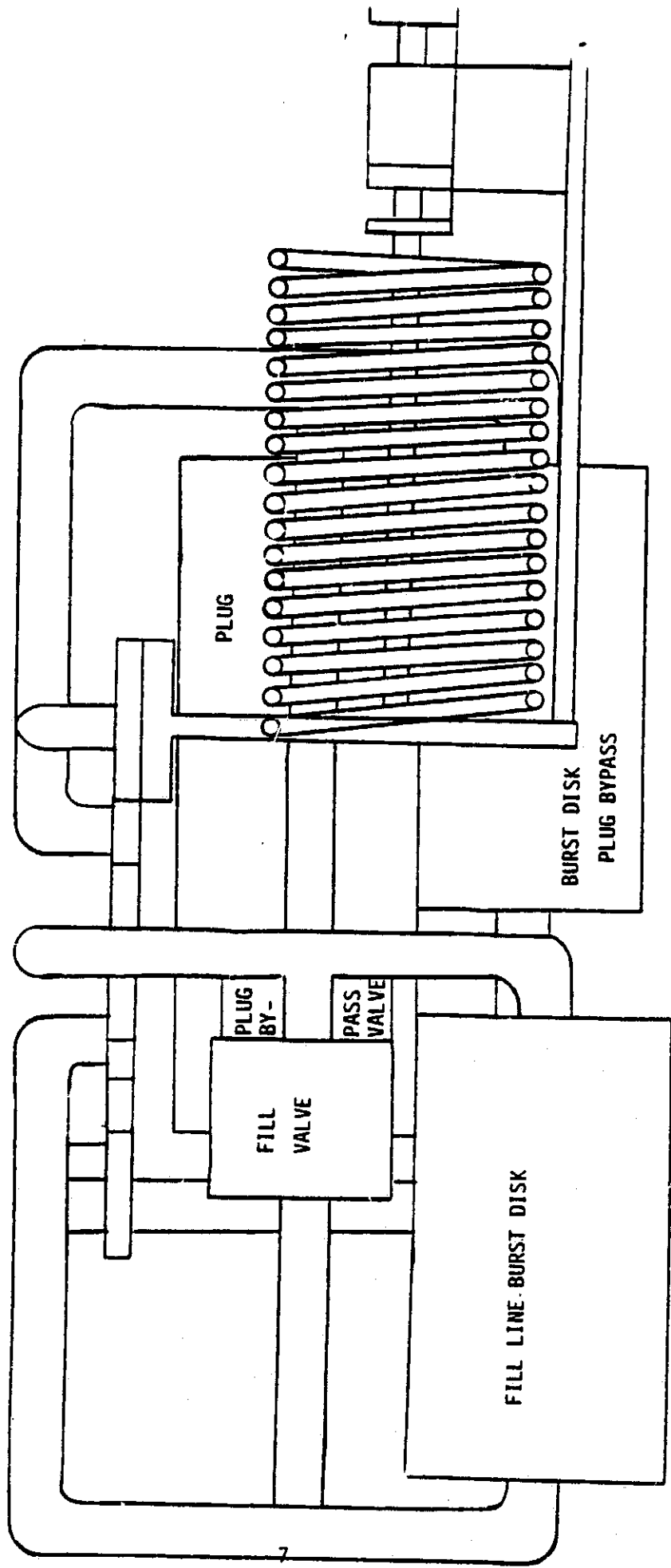


Figure 2. Side view of transfer assembly valving-plumbing layout. (Preliminary for planning purposes only).

7. Critical Design Review

The CDR for the IRT was held at MSFC on August 14 and 15, 1979. Dr. Karr made a presentation on the design of the transfer assembly which included Tables 1, 2, 3, and 4. Table 1 gives the functions of the T.A., Table 2 shows the major components of the T.A., Table 3 shows the valve positions for the control valves of the T.A., and Table 4 gives the assembly sequence of the T.A.

A list prepared by Paul Clemons of materials, weights, and supplies was provided at the CDR and is attached to this report.

TABLE 1

FUNCTIONS OF THE TRANSFER ASSEMBLY, T.A.

1. TO PROVIDE FOR FILLING OF STORAGE DEWAR
2. TO PROVIDE FOR VENTING OF VAPOR CRYOGEN DURING FILLING AND DURING PUMP DOWN
3. TO PROVIDE FOR PHASE SEPARATION IN ZERO -g
4. TRANSFER CRYOGEN FROM STORAGE DEWAR TO THE CRYOSTAT
 - (a) COOL DETECTORS
 - (b) PROVIDE COOLING OF VAPOR COOLED SHIELDS
5. TO PROVIDE COOLING OF STORAGE DEWAR VAPOR COOLED SHIELDS
6. ACCOMMODATE ROTARY MOTION OF CRYOSTAT w.r.t. T.A. AND DEWAR

TABLE 2

MAJOR COMPONENTS OF T.A.

COLD VALVES	
FILL	- V7
PLUG BYPASS	- V5
DEWAR BYPASS	- V17
WARM VALVES	
FILL BAYONET	- V6
VENT BAYONET	- V13
RELIEF (FILL)	- V15 (RV4)
RELIEF (VENT)	- V16 (RV3)
VALVE ACTUATORS	- RETRACTABLE, VACUUM SEALED
HEAT EXCHANGERS	- 20K, 60K, 120K
MLI	- BETWEEN ALL SHIELDS
HELIX	- 1/8" S.S. TUBE
FERROFLUIDIC SEAL	-
SUPERFLUID PLUG	- 3" DIAMETER, 1/4" THICK, 2 μ m PORE SIZE

TABLE 3

VALVE POSITIONS FOR T.A. OPERATIONS

VALVE	DEWAR FILL	PRE-COOL PRIOR TO TOP-OFF	PUMP DOWN	NORMAL OPERATION
COLD FILL, V7	OPEN	OPEN	CLOSED	CLOSED
DEWAR BYPASS, V17	CLOSED	OPEN	CLOSED	CLOSED
PLUG BYPASS, V5	OPEN	OPEN	OPEN	CLOSED
GHE VENT, V13	OPEN	OPEN	OPEN	OPEN
LHE FILL, V6	OPEN	OPEN	CLOSED	OPEN
RELIEF (FILL) RV4	REMOVED	REMOVED	REMOVED	IN-PLACE
RELIEF (VENT) RV3	REMOVED	REMOVED	REMOVED	IN-PLACE

TABLE 4

ASSEMBLY SEQUENCE OF T.A.

1. CUT DEWAR TUBES AND WELD CONFLATS
2. PACK MLI AROUND NECK
3. ATTACH MOUNT RING
4. ATTACH OUTER SHELL
5. ATTACH OUTER SHIELD
6. ATTACH MIDDLE SHIELD
7. ATTACH TRANSFER LINE SHIELD
8. ATTACH CENTER SHIELD
9. ATTACH VALVE ASSEMBLY PLATE
10. ATTACH DEPTH PROBE ASSEMBLY
11. ATTACH VALVE ASSEMBLY TO PLATE
12. ATTACH HELIX TO VALVE ASSEMBLY
13. ATTACH FILL AND VENT OUTER VALVES
14. MAKE UP INTERNAL PLUMBING
15. ATTACH CRYOSTAT LINE TO HELIX
16. MAKE UP ELECTRICAL CONNECTIONS
17. ATTACH SHIELD LIDS
18. ATTACH DOME
19. ATTACH VALVE ACTUATOR COVER

TRANSFER ASSEMBLY WEIGHTS

<u>Part</u>	<u>Wt. (lbs.)</u>
Plumbing Assembly	12.98
Helix	2.39
Inside Shield .125 Thk/.062 Thk	6.63/3.70
Middle Shield .125 Thk/.062 Thk	9.75/5.93
Outside Shield .125 Thk/.062 Thk	12.93/8.02
Outside Shell (including cover with Valve Activators)	31.29
Inside Lid	.62
Middle Lid	.92
Outer Lid	1.29
Inner Shield Mount Ring	.29
Middle Shield Mount Ring	.48
Outside Shield Mount Ring	.69
Fill Line	1.22
Fill Valve Assembly	1.00
Vent Valve Assembly	1.25
Ferrofluidic Seal Assembly (Estimated)	4.00
Wire Suspension System	.10
Insulation (Estimated)	5.00
Mount Blocks (Tube to Manifold)	.72
Transfer Assembly with .125 Shields	93.55
Transfer Assembly with .062 Shields	81.89

PLUMBING ASSEMBLY

<u>Part</u>	<u>Size</u>	<u>Material</u>	<u>Co. Name</u>
Tubing	.500 dia. X .035 wall	CRES	
Elbows	.500 Tube Size	CRES	Parker-Hannifin Corp. 2407 Memorial Pkwy. S. Huntsville, AL
Tees	.500 Tube Size	CRES	Parker-Hannifin Corp.
Cross	.500 Tube Size	CRES	Parker-Hannifin Corp.
Valves	SS-6TW-SW-CU		Nupro Co. 15635 Saranac Rd. Cleveland, OH 44110
Burst Disk	A-4593-1		Fike Metal Prod. Corp. 7045 10th St. Blue Springs, MO 64015
Plug	In-House Design of CRES		
Aluminum to CRES Transitions - 1/2" tube size			Bi-Braze Corp. 4 Railroad Ave. Glen Head, N.Y. 11545
Vacuum Flange	Mini-conflat 954-5139 Rotatable 954-5136 Non-Rotatable	CRES	Varian Vacuum Div. 611 Hansen Way Palo Alto, CA 94303

HELIX

Housing & Mount Assembly		AL	
End Cap	.25 Thk	AL	
Bearing		Teflon	
Tubing	.125 OD X .035 wall	CRES	
Vacuum Flange	same as for Plumbing Assembly		

INSIDE SHIELD

<u>Part</u>	<u>Size</u>	<u>Material</u>	<u>Co. Name</u>
Base and Side	.062 or .125 Thk	AL sheet	
Manifold	.50 X 1.50 X .062 wall Die No. MH-2957	AL	Mideast Aluminum Corp. Rt. 130 Dayton, NJ 08810
Crossover	.50 X .50 X .058 wall Sq. tube	AL	Tube Sales 175 Tubeway Forest Park, GA 30050
Tubing	.375 OD X .035 wall	AL	
Lid Ring	.25 Thk	AL	

MIDDLE SHIELD

Base and Side	.062 or .125 Thk	AL	
Manifold (Rec. Tube)	.50 X 3.0 X .094 wall Die No. MH-2888		Mideast Aluminum Corp.
Crossover Tube - same as inner shield			
Tubing	.375 OD X .035 wall	AL	
Lid Ring	.256 Thk	AL	
Helix Tube Shield	1" OD X .020 wall	AL	

OUTER SHIELD

Base and Side	.062 or .125 Thk	AL	
Manifold (Rec. Tube)	.50 X 4.00 X .094 wall Die No. MH-2891		Mideast Aluminum Corp.
Crossover - Same as inner shield			
Tubing	.375 OD X .035 wall	AL	
Lid Ring	.25 Thk	AL	

OUTSIDE SHIELD

<u>Part</u>	<u>Size</u>	<u>Material</u>	<u>Co. Name</u>
Base	.375 Thk plate	AL	
Side	.125 Thk	AL	
Flange (to cover)	.375 Thk	AL	
Formed Disk	.125 Thk	AL	
Wire Port Tube	1.50 OD X .125 wall	AL	
Wire Port Tube Flanges	.25 Thk	AL	
Fill Valve Tube	2.00 OD X .125 wall	AL	
Fill Valve Flange	.25 Thk	AL	
Vent Valve Tube	4.00 OD X .125 wall	AL	
Vent Valve Flange	.25 Thk	AL	
Ferrofluidic Seal Ball	3.00 dia. X .75 Thk	AL	

INSIDE LID

Lid	.062 Thk	AL	
Valve Guide Tube	.312 OD X .049 wall	AL	

MIDDLE LID

Lid	.062 Thk	AL	
Valve Guide Tube - Same as Inside Lid			

OUTER LID

Lid	.062 Thk	AL	
Valve Guide Tube	.312 OD X .049 wall	AL	

INNER SHIELD MOUNT RING

	.75 Thk	AL	
--	---------	----	--

MIDDLE SHIELD MOUNT RING

<u>Part</u>	<u>Size</u>	<u>Material</u>	<u>Co. Name</u>
	.75 Thk	AL	

OUTSIDE SHIELD MOUNT RING

	.75 Thk	AL	
--	---------	----	--

FILL LINE

Tube	.500 OD X .035 wall	CRES	
------	---------------------	------	--

Flange - Same as other Varian Flanges

FILL VALVE ASSEMBLY

Valve	CV9-84-5W1 (Part No.)	CRES	Cryolab Box 6003 Los Osos, CA 93402
-------	-----------------------	------	---

Flange to Outer Shell	.25 Thk	CRES	
-----------------------	---------	------	--

Flange on line - Same as other Varian Flanges

Tubing	.500 OD x .035 wall	CRES	
--------	---------------------	------	--

VENT VALVE ASSEMBLY

Valve - Same as on Fill Valve Assembly

Flange to outer shell	.50 Thk	CRES	
-----------------------	---------	------	--

Flange on line - Same as other Varian Flanges

Tubing	.500 OD x .035 wall	CRES	
--------	---------------------	------	--

FERROFLUIDIC SEAL ASSEMBLY

Ferrofluidic Seal - per UAH drawings

Bellows - TBD

Flange to Outside Shell	.25 Thk	CRES	
-------------------------	---------	------	--

WIRE SUSPENSION SYSTEM

<u>Part</u>	<u>Size</u>	<u>Material</u>	<u>Co. Name</u>
Wire	.030 dia	TBD	
Screw	.375 thread	CRES	
Screw Plate	.25 Thk	AL	

MOUNT BLOCK

Dewar Support Tube to Vent Manifold	.25 Thk	CRES	
-------------------------------------	---------	------	--

TUBES INTO DEWAR

.50 OD x .065 wall	CRES		
--------------------	------	--	--

Flanges - Same as other Varian Flanges

Bellows - TBD

LINE INTERCONNECTS BETWEEN SHIELDS

Cajon VCR Vacuum Coupling

Female Nut	Part No. SS-4-VCR-1	CRES	
Male Nut	Part No. SS-4-VCR-1	CRES	
Gland	Part No. SS-4-VCR-3	CRES	
Gasket	Part No. CU-4-VCR-2	CRES	

Cajon Co.
32550 Old South Miles Rd
Solon, OH 44139

(Above parts, except gasket, to be modified)

II. Cryostat Development

1. Cryostat Pressure Drops

The final design for the cryostat was obtained and evaluated with respect to the expected pressure drop for flow rates typical of that to be employed for the IRT experiment. The procedure used to calculate the pressure drop is the same as employed in the past. (See report for May 12 - June 11, 1978). The results for 5 mg/sec and 10 mg/sec are given in the table.

TABLE OF PREDICTED PRESSURE IN FINAL CRYOSTAT
HEAT EXCHANGER DESIGN

Cryostat Heat Exchange Section	Assumed Average Temperatures K	Hydraulic Diameter Inches	Length L Feet	$\dot{m} = 5$ mg/sec		$\dot{m} = 10$ mg/sec	
				ΔP Torr	P Average Torr	ΔP Torr	P Average Torr
Inlet to CF	2.55	.22	1.5	3.25-3	6	6.505-3	6
CF to 8K	5.75	.25	.35	1.92-3	5.9967	3.840-3	5.9935
8K	8	.3073	4.2	2.035-2	5.9948	4.069-2	5.9896
8K to 60K	34	.25	1.5	1.861-1	5.9745	3.734-1	5.9489
60K Ring	60	.375	4.46	2.849-1	5.788	5.91-1	5.5755
60K to 120K	90	.25	.42	2.679-1	5.5034	5.909-1	4.984
120K Ring	120	.5185	4.58	.2766	5.2355	.6585	4.393
120K to 230K	175	.44	.25	.0553	4.9588	.1467	3.735
230K Ring	230	.747	4.65	.204	4.9034	.5571	3.588
230K to 300K	265	.44	416	.198	4.699	.6138	3.031
300K					4.501		2.4176

2. Flow conditions in cryostat.

Due to changes in requirements in the nominal mass flow rates for the IRT, the flow conditions at critical points in the cryostat were re-examined. From past reports it has been established that the line between the transfer assembly (TA) and the cold finger is the most critical since the tube size of the helix is 1/8" and is the smallest diameter tube in the complete system. Concern had been expressed over the pressure drop calculations performed in the past which have assumed laminar flow in this region. Due to the increased flow rate requirement, the assumption of laminar flow must be investigated. Consider a 5×10^{-3} gm/sec flow rate requirement. The mass flow rate is given by

$$\dot{m} = \rho VA$$

where ρ is the density, V is the velocity, and A is the cross section area of the tube. Using the perfect gas law

$$P = \rho RT$$

where R is the gas constant given by

$$R = R/M$$

where M is the molecular weight of the gas, the mass flow rate expression becomes

$$\dot{m} = \frac{P}{RT} VA$$

Solving for velocity we obtain

$$V = \frac{\dot{m}R/MT}{PA}$$

Take as an example, the case for

$$\dot{m} = 5 \times 10^{-3} \text{ gm/sec}$$

$$M = 4$$

$$T = 1.6K$$

$$P = 16 \text{ ton}$$

$$\text{Diameter} = .105 \text{ in}$$

the result is

$$V = 1.39 \text{ m/sec}$$

the speed of sound, a , is given by

$$a = \sqrt{\gamma RT} = \sqrt{1.67 \frac{83.4}{4} 1.6} = 74.5 \text{ m/sec}$$

so that the Mach number becomes

$$M = \frac{V}{a} = .0186$$

The Reynolds number is given by

$$R_e = \frac{\rho V d}{\mu} = \frac{\dot{m}}{\mu} \frac{d}{A} = \frac{\dot{m} d}{\mu \pi d} = 4510$$

Thus, we find that the flow is turbulent and not laminar as assumed. The pressure drop is now calculated for the case of turbulent flow given by

$$\frac{\Delta P}{L} = \frac{\lambda}{d} \frac{1}{2} \rho V^2$$

where for turbulent flow

$$\lambda = .3164 (R_e)^{-1/4}$$

Substitution of the appropriate numbers and using

$$L = 2\text{m}$$

we obtain

$$(\Delta P)_{\text{turbulent}} = .148 \text{ torr}$$

The same calculation assuming laminar flow gives a value of

$$(\Delta P)_{\text{laminar}} = .06 \text{ torr}$$

This we conclude that the assumption of turbulent flow should be made and that the pressure drop should be taken as .15 instead of .06.

3. Cryostat Thermal Performance Testing

After successfully cooling the cryostat to 80K with the LN₂ during the night of February 11, transfer of liquid helium was begun on February 12. During a change in dewars on February 13, air or other gases entered the system which resulted in an ice build up which eventually prevented any transfer of helium. The system was then allowed to warm up to over 100K during the night of February 13 and started LHe transfer at 9 a.m. The cool down, however, was not successful in getting the cryostat temperatures into acceptable ranges. The T.A. substitute thermometer was indicating rather high temperatures in the 10-20K range.

The apparent lack of performance of the T.A. substitute was thought due to heat leak to the cold region down the pressure tap tube and/or lack of good thermal contact of the diode thermometer. The system was therefore allowed to warm up and the vacuum spoiled to allow for the removal of the pressure tap and to allow for soldering of the diode to the cold region. This work was done on February 15. Cool down with helium began on February 19 at 9 a.m. By 2 p.m. February 20, the cryostat had reached 20K but progress thereafter was very slow. The test was terminated on February 21 due to lack of progress in cooling in the cryostat.

The thermometers in the T.A. substitute indicated 9.9K inlet temperature, the NASA installed thermometer on the lower dummy indicated 10.2K while the thermometer on the 8K ring indicated 4.45K. The 60K ring was at 33K and the 120K ring was at 99K.

The T.A. substitute was again removed to provide for repair of a damaged thermometer and to replace the wiring with low thermal conductivity wires. Additional MLI was also installed.

Problems in the cryostat thermometry were also noted. The germanium thermometers that had been installed by the manufacturer were not operating well. A thermometer at the 8K cold ring which had been installed by the manufacturer was found to indicate a colder temperature than the indicated inlet temperatures at the T.A. substitute and the NASA installed thermometer on the lower dummy telescope tube.

The Mod II version of the T.A. substitute was delivered in mid-February and testing began while the T.A. was removed from the cryostat. Leaks were found which required some reworking.

On March 6, another cool down was attempted with the original version of the T.A. substitute with the improvements noted above. The cryostat had reached a temperature of 165K by March 11.

The cooldown test using T.A. sub Mod I was terminated on March 14 after it became apparent that the performance of the cryostat and the T.A. sub had not improved. On March 26, another cooldown of the cryostat began using Mod II which had been installed into the T.A. sub earlier. A solder blockage of the transfer line in Mod II had been discovered

and cleared prior to the March 26 test. By March 28, the indicated inlet temperatures in the T.A. sub were near 8K and the lower dummy indicated 11.7K while the thermometer on the 8K ring was out of range but below 5K.

The above discrepancies in temperature readings and a review of our past experience with the various sensors leads to one of the following two conclusions:

- (a) The 8K ring thermometer is bad and the T.A. sub is limited to delivery of helium at only 7K, or
- (b) The 8K ring thermometer is the only thermometer which is working correctly and the other cold region thermometers are reading much too high.

To help answer which of the above conclusions were correct, the system was allowed to warm up and the thermometers were checked for calibration by dipping into liquid helium. All thermometers were carefully heat sunk so that some confidence could be obtained from the future tests. The T.A. sub performance factors were reviewed which uncovered a possible heat leak due to a rather high density of MLI in the ferrofluidic seal region. This was corrected. In addition, it was concluded that the poor performance of Mod II was likely because the radiation shields of the T.A. sub were not actively cooled as they had been in the Mod I design. However, rather than returning to the original Mod I concept which required cooling room temperature helium, Mod I was modified so that the cold helium from the Helitran was split into two flows, (a) one path which leads to the cryostat and (b) a second path which cools the radiation shields. The necessary modifications were completed on April 2.

The cryogenic testing of the cryostat with modified Mod I T.A. sub began on April 7 with a precooling using liquid nitrogen. On April 8, the coldest temperature obtained corresponded to 3.7K at the T.A. inlet and 2.45K at the 8K cold ring while the cryostat vent line was being pumped on. The fact that the cryostat was colder than the inlet gas can be explained since the pumping causes the T.A. side to be at a higher pressure than the cryostat side. The recorded pressures on the two sides, when referred to the liquid-vapor equilibrium temperature, seemed to confirm the lower temperature on the cryostat side.

The thermometer question was answered in these tests since the newly installed and carefully heat sunk thermometers seemed to agree quite well with the 8K cold ring thermometer. Thus, the tests led us to choose conclusion (b) above which means that the T.A. subs were likely performing adequately all along and that many of our earlier tests resulted in cryostat temperatures at lower than those required. The major problem has been accurate and reliable themometry instead of T.A. substitute design.

III. IRT Flow Meters

1. Flow Meter Design Considerations

The two helium vent lines are to have flow meters so the performance of the dewar and cryostats can be monitored. The flow rates are of the order of 1 to 10×10^{-3} gm/sec in the two lines which are nominally 1 inch in diameter. Assuming that the temperature is about 300 K, the Reynolds number, R_e , will be given by

$$R_e = \frac{\rho v d}{\mu} = \begin{cases} 2.5 & \text{for } 10^{-3} \text{ gm/sec} \\ 25.0 & \text{for } 10^{-2} \text{ gm/sec} \end{cases}$$

The velocity in the one inch lines will be

$$v = \frac{\dot{m}}{\rho A} = \begin{cases} 9.23 \text{ m/sec} & \text{for } 10^{-3} \text{ gm/sec at 1 torr pressure} \\ 92.3 \text{ m/sec} & \text{for } 10^{-2} \text{ gm/sec at 1 torr pressure} \end{cases}$$

The Mach number will be

$$M = \frac{v}{\sqrt{\gamma RT}} = \begin{cases} 9 \times 10^{-3} & \text{for } 10^{-3} \text{ gm/sec at 1 torr pressure} \\ 9 \times 10^{-2} & \text{for } 10^{-2} \text{ gm/sec and 300 K} \\ & \text{at 1 torr pressure and 300 K.} \end{cases}$$

The mean free path will be¹

$$L = \frac{\mu}{.499 \rho \frac{8}{\pi} RT} = .0148 \text{ cm for 1 torr pressure and 300 K temperature}$$

Under the above flow conditions, the flow is classified as laminar, subsonic, and continuum.

Helium gas has a density of 1.625×10^{-4} gm/cm³ at 760 torr pressure and 300°K temperature. A mass flow rate of $(1 \text{ to } 10) \times 10^{-3}$ gm/sec represents an equivalent volumetric flow at standard conditions of 6 to 60 scc/sec or 360 to 3600 scc/min, respectively.

¹Dushman & Lafferty, Scientific Foundations of Vacuum Technique, 1962, John Wiley & Sons, Inc.

The conditions described above are unusual for most flow meter applications. The low density and low Reynold's in particular make this flow non-standard for the purpose of flow meter design. Flow meters work on the basic principle that the pressure drop generated by the flow meter element is proportional to the square of the velocity of the fluid. Thus, the flow velocity is determined by measuring the pressure drop. The pressure and temperature are also measured which, coupled with the velocity measurement, provide sufficient information to determine the mass flow rate. Flow meter design considerations include the magnitude of pressure drop expected, the magnitude of the pressure, and the temperature range of interest. For the IRT application, the pressure drop will be of the order of 1 torr as will the absolute pressure. The temperature will be near 300 K.

The magnitude of the pressure drop is governed by the design of the flow meter and two designs were under consideration; (1) the venturi meter and (2) the orifice meter. Both meters can be applied to the IRT flow requirements. The venturi meter has the advantage of creating the least total resistance to the flow but has the disadvantage of being limited in range and limited in maximum measurable pressure drop of about 50% of the inlet pressure. The orifice meter can be used over a wider range and produced a larger measurable pressure drop but at the expense of severely restricting the flow.

The flow meter being developed for IRT flows is based on acceleration of a fluid stream through some form of nozzle. The ideal flowrate is related to pressure drop by applying continuity and Bernoulli equations. If we assume for now that the flow is incompressible, Bernoulli's equation becomes

$$P_1 - P_2 = \frac{\rho}{2} (V_2^2 - V_1^2) = \frac{\rho V_2^2}{2} \left[1 - \left(\frac{V_1}{V_2} \right)^2 \right] \quad (1)$$

where p_1 and p_2 are measured at points where the velocity has changed from V_1 to V_2 , respectively. Using the continuity equation for the change in velocity due to area changes from A_1 to A_2 is

$$\rho V_1 A_1 = \rho V_2 A_2 \quad (2)$$

or

$$\left(\frac{V_1}{V_2} \right)^2 = \left(\frac{A_2}{A_1} \right)^2 \quad (3)$$

Using the above, the velocity V_2 is found

$$V_2 = \sqrt{\frac{2(P_1 - P_2)}{\rho (1 - (A_2/A_1)^2)}} \quad (4)$$

Using the perfect gas law

$$p = \rho RT \quad (5)$$

the expression for velocity becomes

$$v_2 = \sqrt{\frac{2(P_1 - P_2) RT_2}{P_2 \left(1 - \frac{A_2}{A_1}\right)^2}} \quad (6)$$

The mass flow rate is given by

$$\dot{m} = \rho v_2 A_2 \quad (7)$$

$$\dot{m} = \frac{P_2}{RT_2} v_2 A_2 \quad (8)$$

Thus, the measurement of \dot{m} requires the values of ΔP , P_2 , and T_2 , in addition to the known values of A_1/A_2 and the gas constant R .

The above expressions are all derived assuming incompressible, ideal flow. In practice, corrections must be made to the above to take into account the effects of compressibility, friction, and energy changes. For the IRT experiment, it is proposed to develop the corrections to the equations from experimental studies of prototype flow meters.

One of the disadvantages of orifice or nozzle type flow meters is understood by reference to Eq. (6). The measurement of velocity is seen to be a non-linear function (square root) of the measurement of ΔP . The non-linear behavior means the range of flow measurement is limited by a factor of the square root of the range of the ΔP measurement.

2. Flow Meter Design

Flow meters of two different designs were under consideration for possible application to the IRT experimental requirements: (a) a commercial thermal type mass flow meter and (b) a standard orifice or venturi type meter using sensitive pressure meters. While both types will impose considerable total pressure loss to the flow, the orifice type meter gives the most flexibility in design and the smaller total pressure drop of the two types. Both meters are described in attachments. Attachment A gives the specifications for the Teledyne Hastings-Raydist mass flow meter. Also included in attachment A is a letter describing the performance under the conditions representative of the IRT applications.

Attachment B gives the preliminary layout of an orifice type flow meter which employs a Validyne Corporation ultra low-range-pressure-transducer, DP 103. The specifications for the transducer are attached along with the specifications for the CD16 demodulator. A preliminary layout showing two flow meters using a DP 103/CD16 assembly is shown. Also provided in attachment B is a memo to Dr. Katz concerning the transducer and the demodulator.

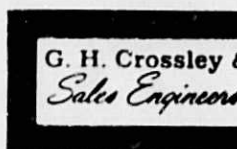
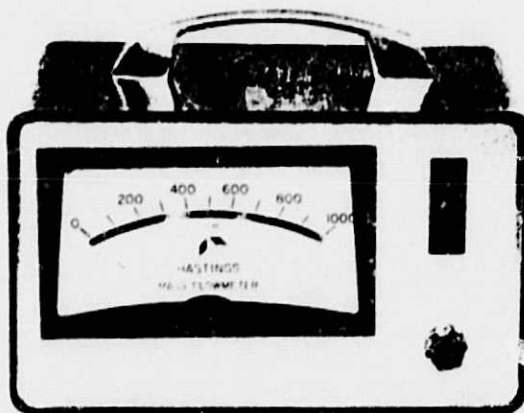
ATTACHMENT A

Teledyne Hastings - Raydist Mass Flow Meter

Hastings Linear Mass Flowmeters

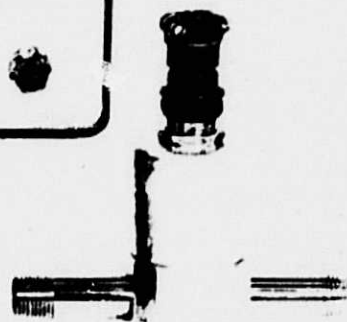
ALU-SERIES WITH LOW PRESSURE DROP TRANSDUCERS

- **PRESSURE DROP FULL SCALE ON ALL RANGES:
LESS THAN .07" H₂O @ ATM PRESSURE
LESS THAN 1 TORR @ 30 TORR PRESSURE**
- **MEASURES MASS FLOW OF GASES**
- **IDEAL UNDER VACUUM CONDITIONS
AS LOW AS 30 TORR**
- **RUGGED MONEL TRANSDUCERS**
- **RANGES FROM 0-100 SCCM TO 0-50,000 SCCM**
- **SUITABLE FOR UF₆ & OTHER CORROSIVE
GASES**
- **OUTPUT: 0-1 VDC**



G. H. Crossley & Associates, Inc.
Sales Engineers

3131 MAPLE DR. N.E.
ATLANTA, GEORGIA 30305
(404) 261 - 4278



TRANSDUCER

DESCRIPTION

The Hastings Linear Mass Flowmeters, ALU Series, are designed for applications requiring minimum pressure drop. This is particularly important in atmospheric sampling applications and vacuum applications.

The flowmeter uses the tried and proven Hastings thermal principle. Gas passes through a heated tube and in doing so causes temperature gradients in the wall of the tube proportional to mass flow of the gas and to its heat capacity. Thermoelectric elements attached to the outer wall of the heated tube sense the changing temperature gradients and produce a proportional electric signal.

The ALU Series has been used successfully for many years to measure Uranium Hexafluoride flowrate under vacuum conditions. It has also been used to measure vacuum pumping speeds

and in atmospheric sampling trains. Large diameter sensing tubes also reduce the chances of fouling when measuring contaminated gases. Transducer and Laminar Flow Element are constructed of monel.

SELECTION CHART

Range In Air	Indicator Model	Transducer Type	Laminar Flow Element Type
0-100	ALU-100	U-100M	—
0-500	ALU-500	U-500M	—
0-1000	ALU-1K	U-1KM	—
0-5000	ALU-5K	U-5KM	—
0-10,000	ALU-10K	U-10KM	—
0-20,000	ALU-20K	U-3M	LU-2M
0-50,000	ALU-50K	U-3M	LU-3M

SPECIFICATIONS:

ORIGINAL PAGE IS
OF POOR QUALITY

MODELS

CABINET ALU-(range)
NIM PANEL ALU-(range)P

POWER

115 volt 50-60 hz @ 15 watts
230 volt 50-50 hz @ 15 watts
*Add the prefix "E" to model number

TRANSDUCER CABLE

TYPE NF-8-NM 8 ft.
NF-25-NM 25 ft.
NF-50-NM 50 ft.
NF-100-NM 100 ft.

ACCURACY: ± 1% of full scale

PRESSURE LIMITS: 1 torr to ATM
TEMPERATURE LIMITS: 0 to 40° C

PRESSURE DROP

Less than .07" H₂O @ 1 ATM pressure
Less than 1 torr @ 30 torr pressure

CALIBRATION

Air calibration is standard
Calibration for other gas optional

OVERPRESSURE

Withstands 250 psig without damage

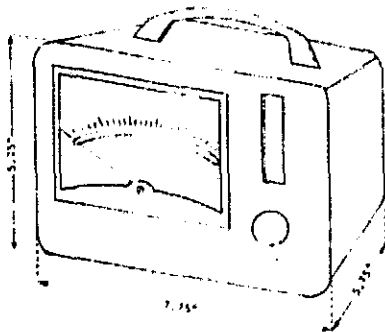
TRANSDUCER CONSTRUCTION

All parts in contact with the gas are monel family alloys

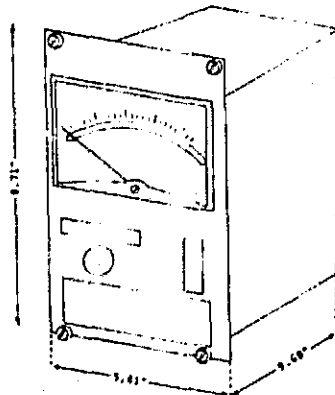
REQUEST CATALOG 500 FOR INFORMATION ON
HASTINGS AUTOMATIC FLOW CONTROLLERS,
MINI-FLO CALIBRATORS, GAS FLOW PROBES, AND
STACK GAS VELOCITY METERS.

INDICATOR OUTLINE DIMENSIONS

Cabinet
Model



NIM Panel
Model



3 NIM panel instruments can be
mounted on an 8-3/4" x 19" frame

GAS CONVERSION FACTORS FOR HASTINGS LINEAR FLOWMETERS

(Multiply Air scale by these Hastings Conversion factors)

*Empirical data; others theoretical

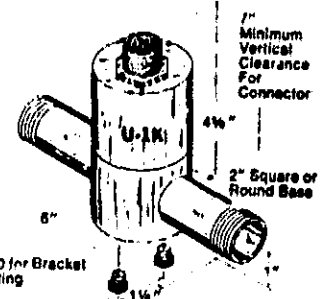
Gas	Conversion Factor	Gas	Conversion Factor
ACETYLENE	.67	HYDROGEN	*1.03
AIR	*1.00	HYDROGEN CHLORIDE	1.01
AMMONIA	.77	HYDROGEN FLUORIDE	1.00
ARGON	*1.43	HYDROGEN SULFIDE	.85
ARSINE	.76	ISOBUTANE	.31
BROMINE	.88	KRYPTON	1.39
BUTANE	.30	METHANE	*.65
BUTENE 1	.34	NEON	1.38
CARBON DIOXIDE	*.73	NITRIC OXIDE	1.00
CARBON MONOXIDE	*1.00	NITROGEN	*1.02
CHLORINE	.85	NITROUS OXIDE	.75
CHLORINE TRIFLUORIDE	*.45	OXYGEN	*.97
CYCLOPROPANE	.52	PENTABORANE	.15
DIBORANE	.50	n-PENTANE	.22
ETHANE	.56	PHOSPHINE	.79
ETHENE (ETHYLENE)	.69	PROPANE	*.32
ETHYLENE OXIDE	.60	SILANE	.68
FLUORINE	.93	SULFUR DIOXIDE	.70
FREON 11	.36	SULFUR HEXAFLUORIDE	.28
FREON 12	*.36	TUNGSTEN HEXAFLUORIDE	.23
FREON 13	.42	URANIUM HEXAFLUORIDE	2.
FREON 14	.48	WATER VAPOR	.80
FREON 22	*.43	XENON	1.37
FREON 114	*.22		
HELIUM	*1.43		

Example: Flowmeter U-1KM 0-1000 sccm in air would be
1000 x .23 = 230 sccm at full scale in UF₆.

TRANSDUCER OUTLINE DIMENSIONS

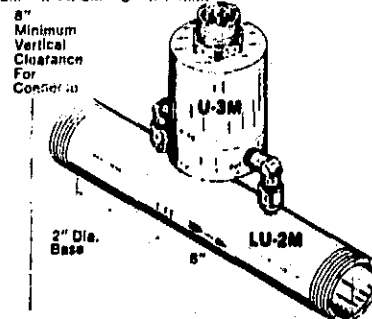
Outline for U Series Transducer

U-100M 1/4" NPT Female
U-500M 1/4" NPT Male
U-1KM 1/4" NPT Male
U-5KM 1/2" NPT Male
U-10KM 1/2" NPT Male



Outline for U JM Series Transducer
using Laminar Flow Elements

U JM w/ LU JM 2" NPT Male
U JM w/ LU JM 3" NPT Male



All U Series transducers and
Laminar Flow Elements are
constructed of Monel

G. H. Crossley & Associates, Inc.

Sales Engineers

TELEPHONE (404) 261-4278

George H. Crossley
Dennis F. Lange

October 13, 1978

Mr. Gerald R. Karr
University of Alabama
P. O. Box 1247
Huntsville, Alabama 35807

Dear Mr. Karr:

The following letter contains information pertaining to your interest in measuring a flow of helium gas at 1 Torr. The mass flow rate is 2 - 6 milligrams of helium per second.

Teledyne Hastings has a low pressure drop gas mass flowmeter that can be used at 8 Torr. The transducer has a pressure drop of 3.5 Torr.

This flowmeter has been tested at 1.4 Torr. The pressure drop across the transducer is also 1.4 Torr, causing a 50% drop in the gas flow rate.


I am including budgetary pricing for a flowmeter designed to handle the range of 2 - 6 milligrams of helium. The prices are as follows:

1. Model ALU-5KX
Range: 0 - 2,000 sccm helium
Price: \$945.00

2. Model ALU-5KGX
Range: 0 - 6 milligrams helium full scale
Price: \$1,015.00

The flowmeters are available in 4 - 5 weeks after receipt of the order. I am looking forward to working with you and your people in order to provide a flowmeter that meets your requirements for the Space Shuttle.

Sincerely,


Dennis F. Lange
/vk

Enclosure

cc: Mr. Joe Doetzer - Teledyne Hastings-Raydist

MEMORANDUM

October 25, 1978

TO: Dr. L. Katz
FROM: Gerald R. Karr
SUBJECT: Flow Meters for IRT

Attached is a copy of the preliminary ideas for the layout of the IRT flow meters. The flow will be determined from the measurement of differential pressure across a flow metering device (orifice or venturi) which will be placed in the two vent lines. The ASME standards for design of flow meters recommends that the upstream pipe have no turns or fittings for 25 diameters and the downstream pipe also be free for 5 diameters. Assuming a one inch pipe diameter, at least 30 inches of straight pipe should be available for the flow meters.

The Validyne DP 103 differential pressure transducer and the Validyne CD 16 demodulator are recommended for the flow meter application. These devices were used to form the layout and the specifications are attached.

In a phone conversation with a representative of Validyne Corporation, I learned that the current prices are:

DP 103 - \$368
CD 16 - \$341

The connectors provided with the two devices are:

DP 103 - ITT CANNON WK4-22C with Mating Connector WK4-21C
CD 16 -(Input) ITT CANNON WK-4-32S with Mating Connector WK-4-21C
(Output) ITT CANNON WK-6-32S with Mating Connector WK-6-21C

Since these connectors may not be appropriate for our purposes, I suggest that the appropriate connectors be specified so that Validyne can use them in the fabrication. This change will result in a new price which will depend upon the connector specified.

The DP 103 is stainless steel construction and is described as being rugged but there is no vibration or shock test data available. The CD 16 is completely potted and also described as being rugged.

ATTACHMENT B

Pressure drop flow meter design using Validyne transducer

Dr. Katz
Page 2

The thermal effects on the transducer are of two types: (1) zero shift and (2) sensitivity shift. The zero shift is .01%/°F and is repeatable for each transducer. The sensitivity shift is .05%/°F and is linear and repeatable. The accuracy of the meter is described as being .5% of full scale with repeatability of .1% of full scale.

The transducers output is sensitive to accelerations of magnitude 4% of full scale per g. For ease of calibration and check out, it would be best that the plane of the transducer diaphragm be mounted vertically. The mounting plate seen in the layout diagrams should be vertical.

Not shown in the layout are the two absolute pressure gauges and temperature gauges which will likely be mounted in the same temperature controlled box as the flow meters.

The tubes from the transducer are shown to be relatively short in the layout. In practice, we may want to use longer tubes with appropriate connectors for ease of mounting to the flow meters.

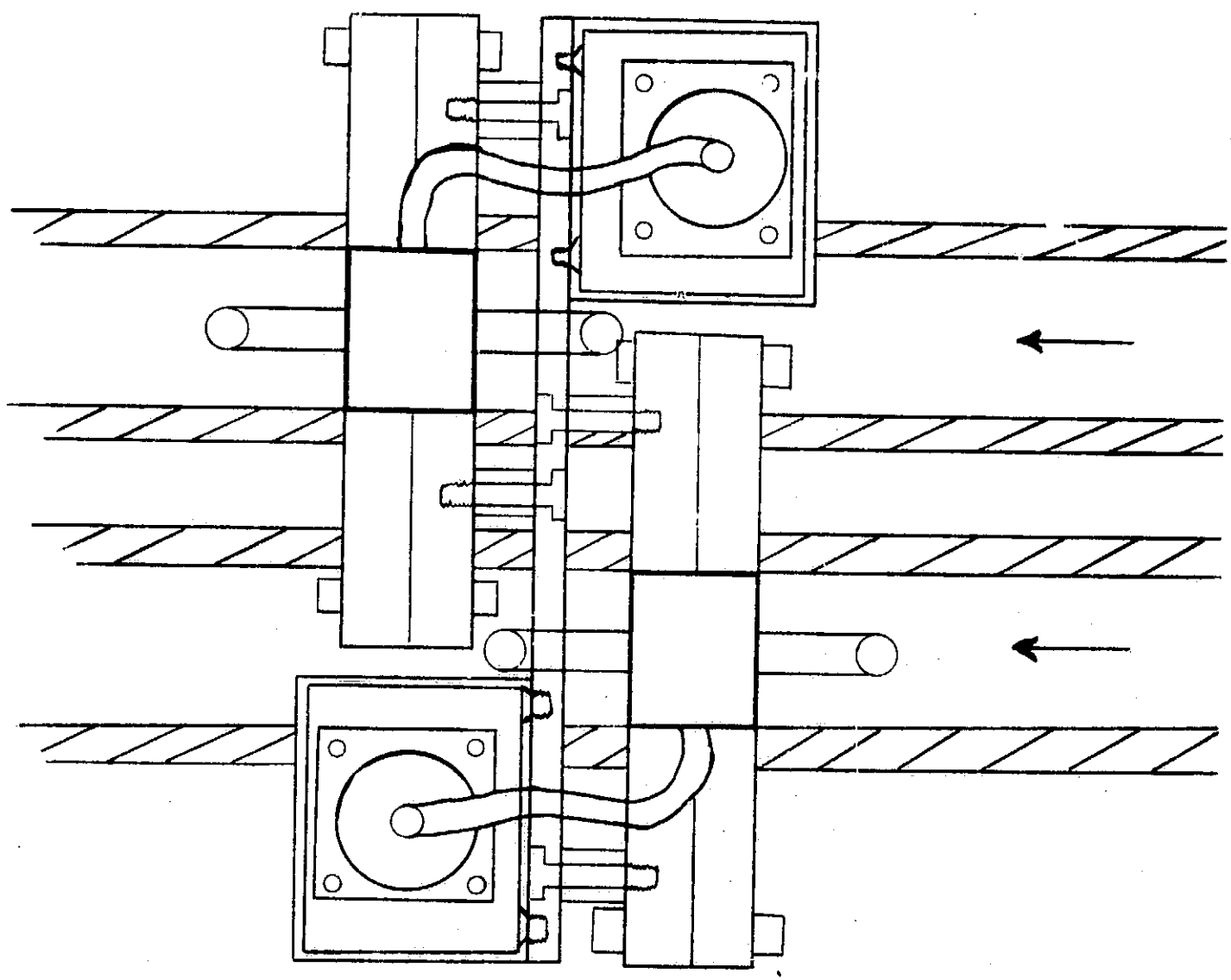
GRK/asw

Attachments

Preliminary Flowmeter Layout Using Validyne DP 103 Differential Pressure Transducer and CD 16 Demodulator

10/20/78
G. R. K.

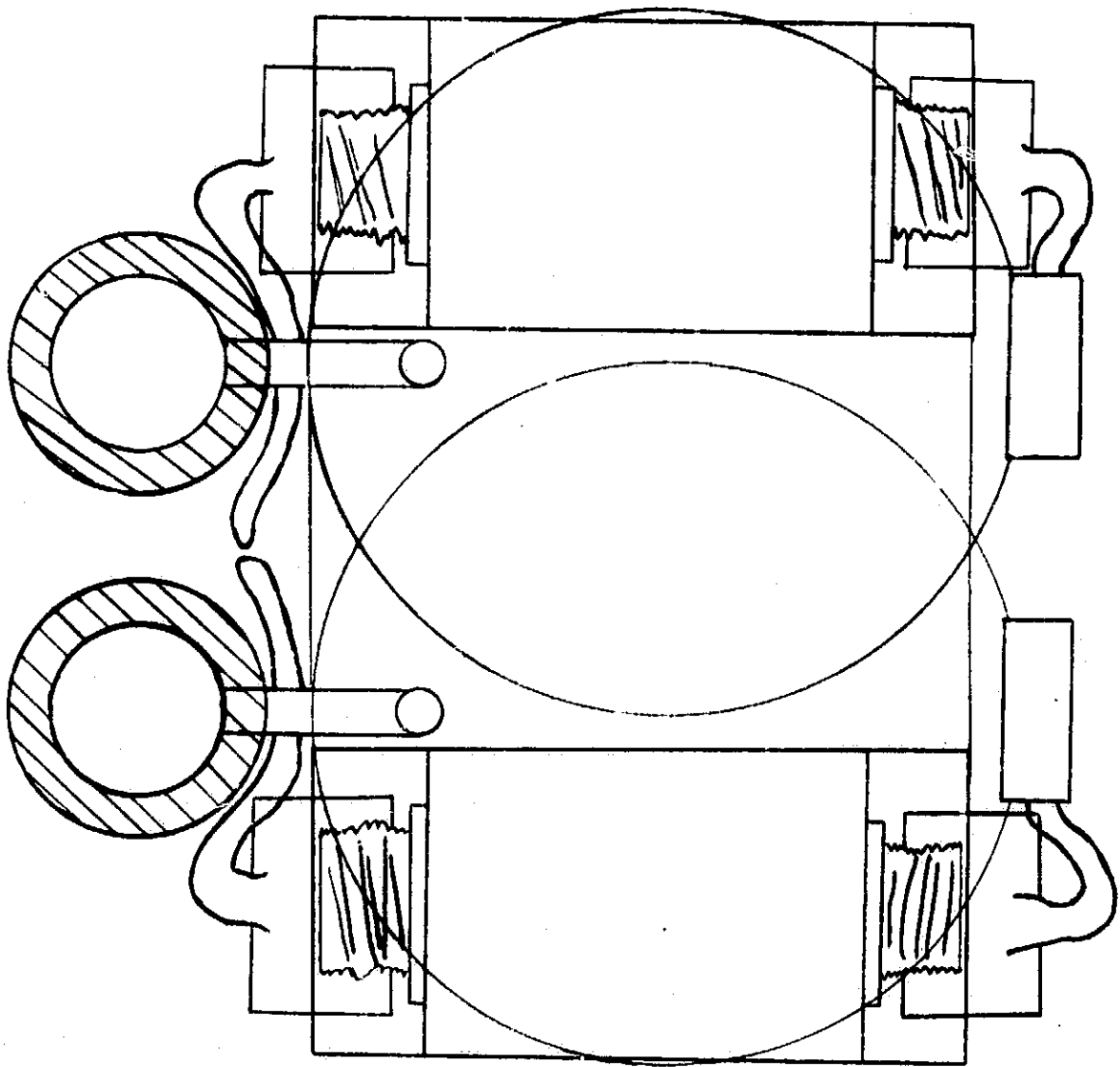
ORIGINAL PAGE IS
OF POOR QUALITY

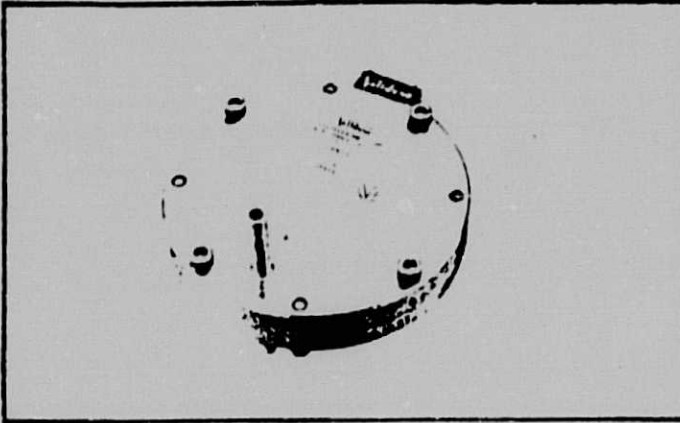


Preliminary Flowmeter Layout Using Validyne DP 103 Differential Pressure Transducer and CD 16 Demodulator

10/20/78

G. R. K.





Features

- Exceedingly Low Pressure Range
- High Overpressure Capability
- Low Acceleration Sensitivity
- Accepts Corrosive Liquids and Gases Both Sides
- Equal Pressure Inlet Volumes

Description

The DP103 is designed for exceedingly low differential pressure measurement applications where high accuracy is required under rough physical environmental conditions. With full scale ranges down to ± 0.01 psid (± 0.7 cmH₂O), this instrument is being used in the measurement of very low flow rates of gases where symmetrical pressure cavities are required for dynamic response. Also used in very small leak detection and pressure null detection systems.

Wet-wet applications involving corrosive liquids and corrosive gases are easily handled as all surfaces exposed to the media are corrosion resistant steel. Overpressures as high as 100 psid will not destroy the diaphragm and with recalibration the instrument may continue to be used. Used in conjunction with a Validyne Carrier Demodulator, a ± 10 volt DC output may be obtained for a pressure of ± 0.01 psid. The transducer may be located 1000 feet, or more from the electronics with no problem.

Specifications

- Standard Ranges:** $\pm 0.01, 0.02, 0.05, 0.1, 0.2, 0.5, 1.0, 5,$
and 10 psid
- Linearity:** $\pm 0.5\%$ FS, best straight line
- Hysteresis:** 0.1% pressure excursion
- Overpressure:** $\pm 200\%$ FS with less than 1/2% FS Zero Shift
- Overpressure Limit:** 100 psid
- Line Pressure:** 100 psig, less than 1% effect
- Inductance:** 20-mH nominal, each coil
- Zero Balance:** $\pm 10\%$ FS, calibrated excitation
- Rated Excitation:** 5-15 v rms, 5-kHz
- Excitation Limits:** 1000 to 20,000 Hz, 30 volts rms maximum at 20,000 Hz
- Sensitivity:** 20-mV/V for full scale, nominal
- Pressure Media:** Corrosive Liquids & Gases compatible with 17-7 CRES and Buna N O-rings (Optional O-ring seal compounds available)
- Operating Temperature Range:** -65 to 160 F (32° C to 71° C)
- Thermal Zero Shift:** $\pm 0.1\%$ FS
- Thermal Sensitivity Shift:** $\pm 0.05\%$ FS
- Pressure Cavity Volume:** 35×10^{-3} cubic inches (57 cc)
- Volumetric Displacement:** 3.5×10^{-3} cubic inches (0.57 cc)
- Pressure Connection:** 1/8" OD, 1/4" diam, 1/4" long
- Electrical Connection:** 1/4-22C connector (Cannon) with 18' cable. Mating connector 1/4-21C furnished
- Size:** 1.75 x 1.75 x 1.75"
- Weight:** 0.12 (1.11 kg)
- Price & Delivery:** \$100.00 - 2-4 week lead time (ARL)

Replacement Diaphragms: \$35.00 Available from Stock

ORIGINAL PAGE IS
 OF POOR QUALITY.



no vibration about date

101 psid

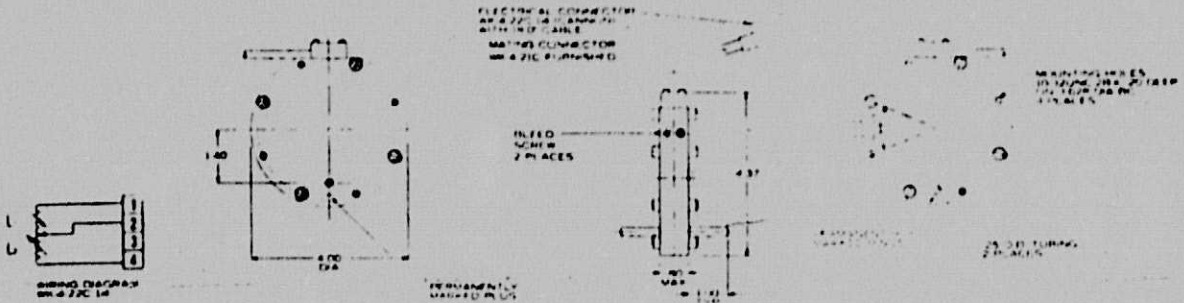
4% error

look at about same spec down to -65F to 150F

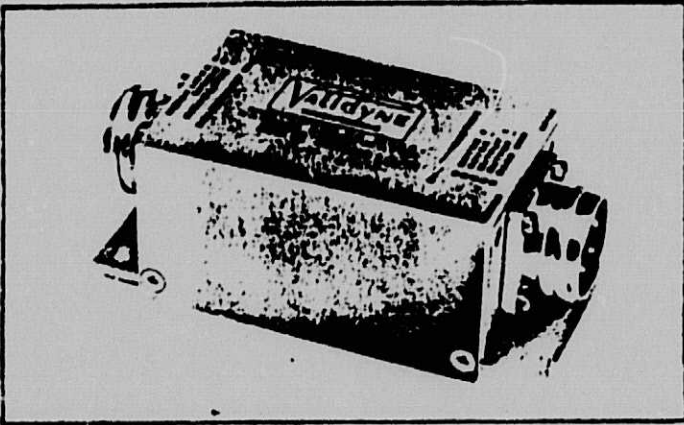
A25

INSTALLATION DRAWING

DP103 Differential Pressure Transducer Ultra Low Range



Validyne **CD16** MINIATURE CARRIER DEMODULATOR



Features

- Regulated against power variation
- Low output impedance
- Solid state reliability
- Ruggedized package
- Input/output isolation

ORIGINAL PAGE IS OF POOR QUALITY

Description

The CD16 Miniature Carrier Demodulator, designed to deliver a 0-5 or ± 5 VDC output from a Variable Reluctance Transducer and operate from an unregulated 22 to 35 VDC power. A square wave excitation of 5kHz is furnished to the transducer and the solid state integrated circuit amplifier and demodulator converts the transducer signal to analog DC output. Zero and span adjustments are made through access holes in the case.

Electrically the CD16 is a true four terminal device, the two output terminals being completely isolated from the two power input terminals. In addition neither input common or output common is connected to case ground.

*Rated in order
10% for flow*

Optional Feature

Operation from 12VDC power, specify: CD16-649

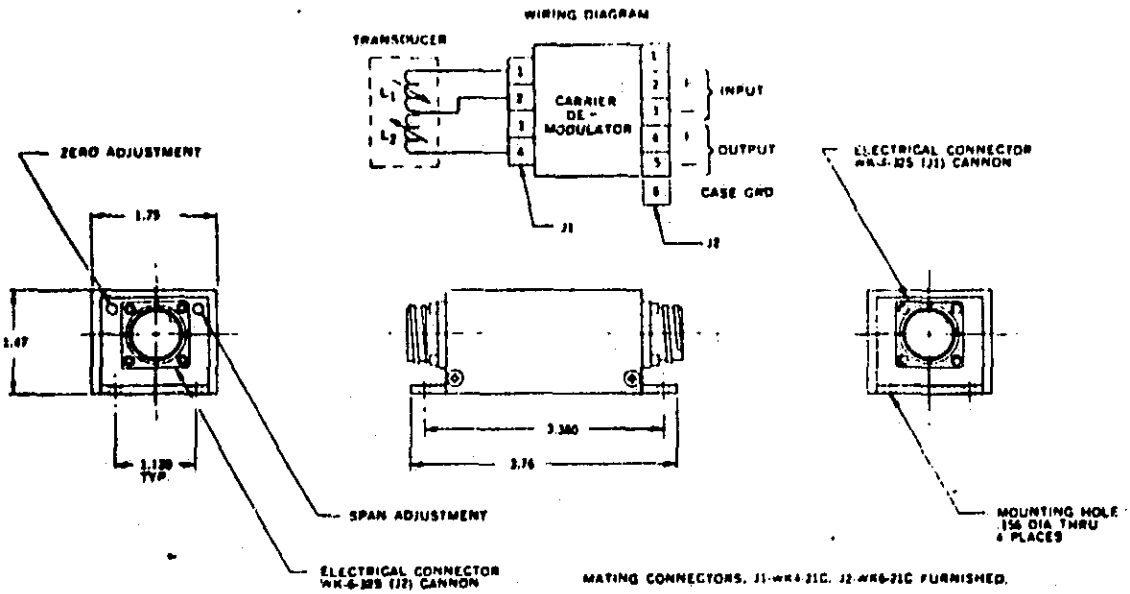
Specifications

Input Sensitivity:	15 mV/V excitation, minimum
Transducer Excitation:	15Vp, 5kHz square wave
Output Voltage:	0-5.0V or ± 5.0 VDC into 10K ohm or greater load
Output Impedance:	100 ohms, maximum
Frequency Response:	DC-1000Hz, flat $\pm 5\%$
Stability:	$\pm 0.1\%$ / supply voltage change from -22 to +35 VDC
Ripple:	10 mV peak to peak, nominal
Temperature Range:	
Ambient:	-65°F to 250°F
Compensated:	0°F to 160°F
Thermal Zero Shift:	$\pm 0.5\%$ FS / 100°F
Thermal Span Shift:	$\pm 1\%$ / 100°F
Power Requirements:	-22 to +35 VDC, 10 ma nominal

Electrical Connections

Input:	WK-4-32S (Cannon) Mating Connector WK-4-21C Furnished
Output:	WK-6-32S (Cannon) Mating Connector WK-6-21C Furnished
ght:	8 ounces avdp (227 gram)
e	S300, available from stock

INSTALLATION DRAWING CD16 Miniature Carrier Demodulator



3. Flow Meter Tests

Mr. Richard Norman of NASA/MSFC has performed calibration tests of the prototype flow meter for various orifice sizes. Data was taken for various values of inlet pressures, pressure drops, and mass flow rates. The flow meter is designed so that the measured values of P, ΔP , and temperature will provide a measure of the flow rate. Ideally, the mass flow is given by

$$\dot{m}_{\text{ideal}} = \left[\frac{2P_{\text{inlet}}(\Delta P)}{R T(1-\beta^2)} \right]^{1/2} A$$

where P_{inlet} is the inlet pressure, ΔP is the pressure drop across the orifice, R is the gas constant, T is the temperature, A is the area of the orifice, and β is the area ratio given by

$$\beta = \frac{A_2}{A}$$

where A_2 is the area of the pipe that contains the orifice. In the calibration tests, the real value of mass flow is compared to that given by the above equation in order obtain a correction parameter a given by

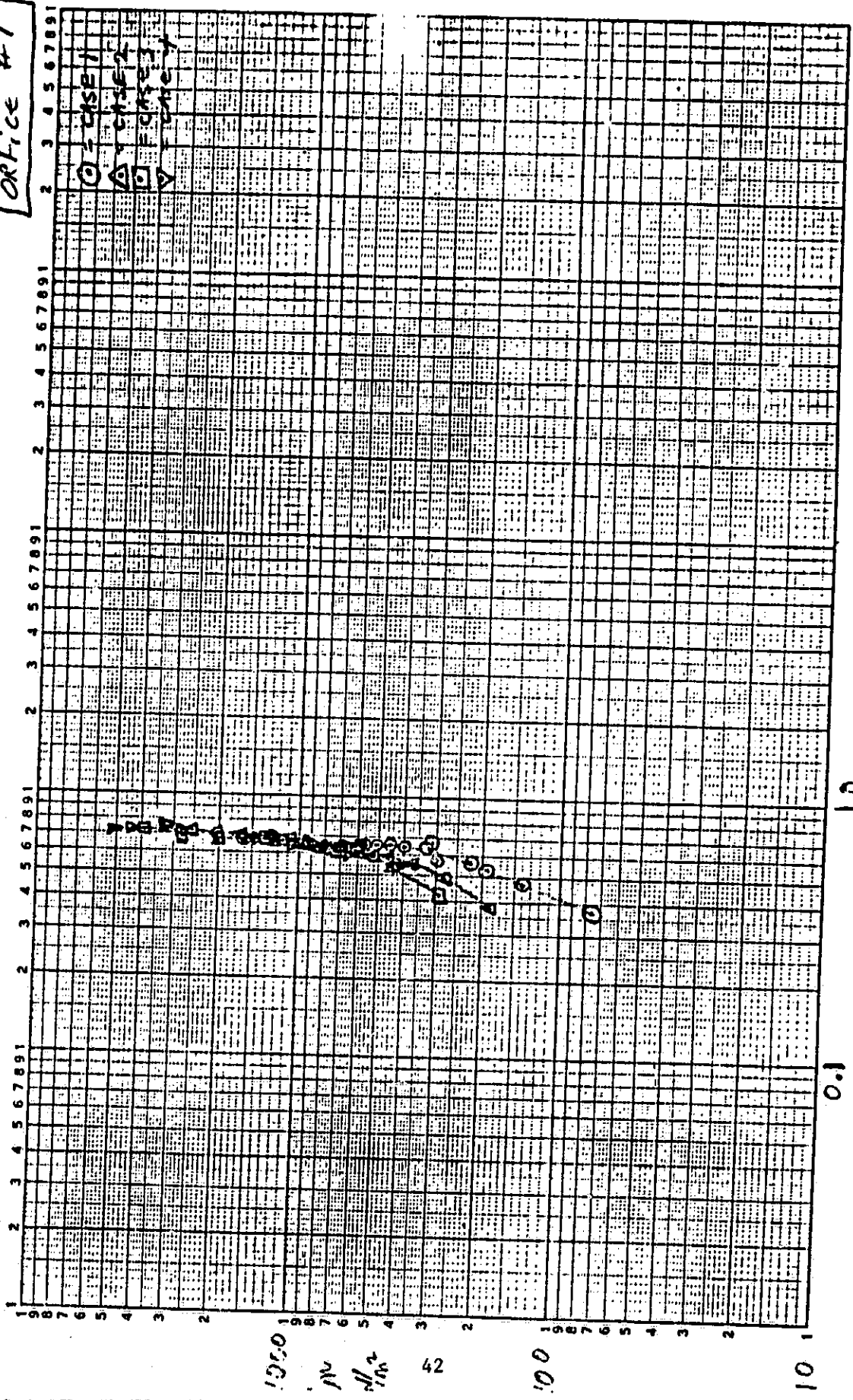
$$a = \dot{m}_{\text{real}} / \dot{m}_{\text{ideal}}$$

Results obtained from the work by R. Norman are shown in Figures 1 and 2 for two of the orifices tested. The results show that a is nearly .7 for the values of pressure and mass flow rates expected for the IRT for orifice #1 as shown in Figure 1. Figure 2 shows the results for orifice #2 which is found to have a correction of nearly 2.5.

REI.

ORIGINAL PAGE IS
OF POOR QUALITY

12-3-79
Office #1



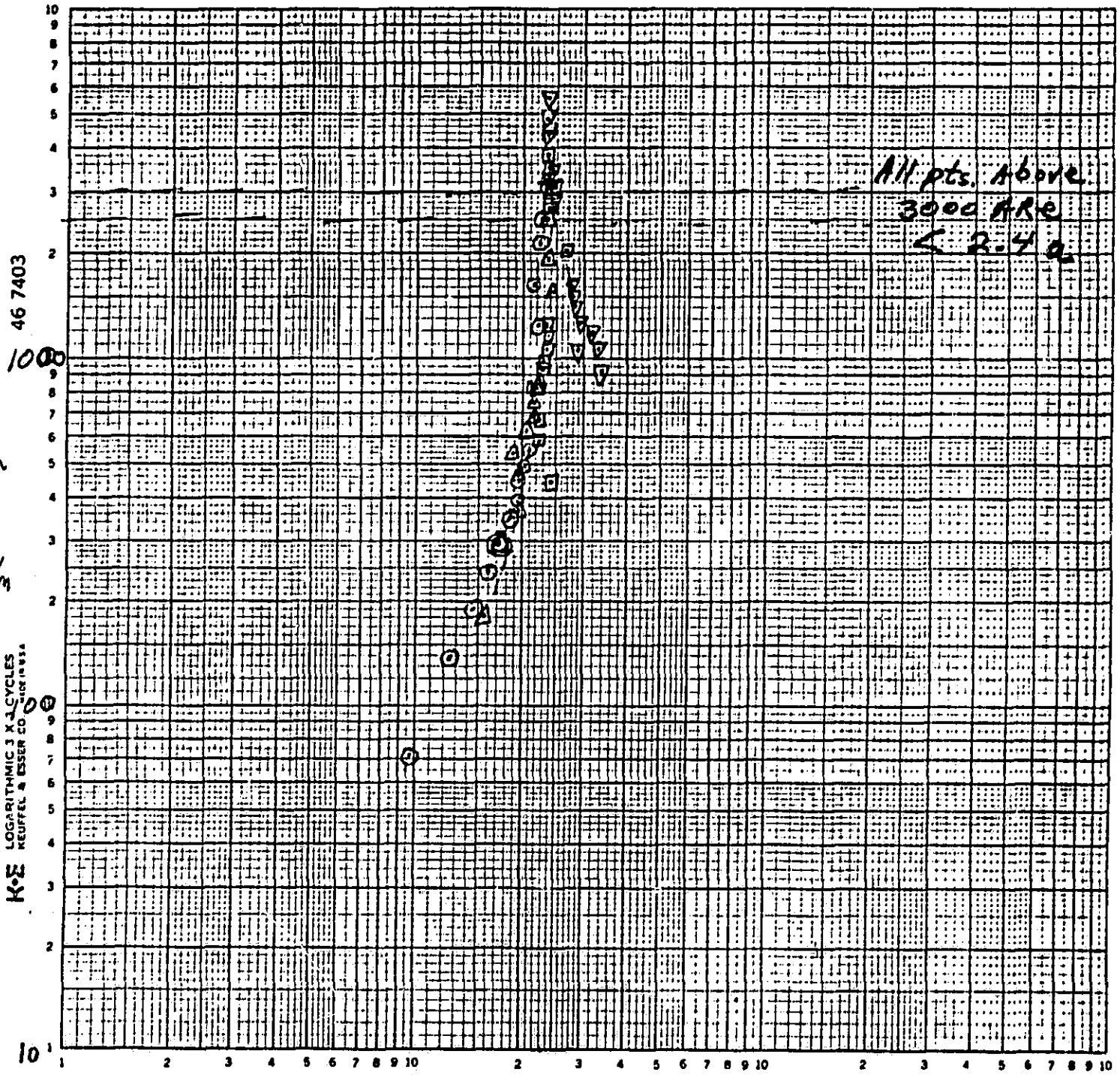
a (unitless)

Figure 1

ORIGINAL POINTS
OF POOR QUALITY

On ice #2
12-11-79 REN

CASE 1 = ○
" 2 = △
" 3 = □
" 4 = ▽



$$a = \frac{m_{real}}{m_{ideal}}$$

Figure 2

IV. Low Pressure Transfer of Liquid Helium

1. Superfluid Transfer Tests

The feasibility of transfer of superfluid helium was tested using a metering valve at the receiving Dewar. Liquid helium at near atmospheric pressure and 4.2 K was contained in a standard helium Dewar which was instrumented to monitor both liquid level and pressure. The experimental Dewar contained liquid helium at superfluid temperature and pressure below 30 torr. A transfer line was placed between the two Dewars. The transfer path into the experimental Dewar was terminated with a valve which was in the liquid helium region but could be controlled externally. While pumping on the experimental Dewar continuously, a transfer was attempted in which the warm liquid was introduced into the colder region. The expansion which takes place at the valve has the effect of vaporizing a fraction of the warm liquid and thereby also lowering the temperature of the liquid. The increased volume of vapor has the effect of increasing the pressure in the experimental Dewar for a constant pumping capability. Using the valve as a control, transfer could be realized while maintaining the experimental Dewar at approximately a constant equilibrium temperature. As the valve opening is increased, the larger vapor flow results in a higher pressure and, therefore, a higher temperature. Figures 1 and 2 show example results for two different valve settings.

Figure 1 shows the results for a relatively small valve opening. The supply Dewar liquid level fell from 28.8 to 28.05 cm during a period of 6 minutes. Since the volume of the supply Dewar is calibrated at 1.42 litres/cm of depth, the results show a loss of about one litre of liquid in the supply Dewar in the 6 minute period. The experimental Dewar shows

an increase in level from 8.35 to 9.9 cm during the same period. Since the volume of the experimental Dewar varies approximately as .324 l/cm, the 1.55 cm gain represents a volume increase of .5 litres. Thus, about one half of the liquid transferred is converted to vapor at the cold end expansion valve. These results correspond to the theoretical expectations. The temperature of the experimental Dewar is seen to rise from 2.5 to 2.75 during the transfer.

Figure 2 shows the results for a relatively large valve opening. In this experiment, the supply Dewar lost 4.3 litres of liquid in 8 minutes while the experimental Dewar gained at a correspondingly faster rate but at the expense of a higher temperature of the transferred liquid. The volume of liquid transferred into the experimental Dewar in this case cannot be determined because of the lack of an accurate calibration for the volume of the experimental Dewars as a function of depth in this range. It is assumed that approximately one half of the transferred liquid remains as liquid on the cold side.

Attempts were made to transfer liquid at below 2.1 K with no success. At very low valve settings, the experimental Dewar could be maintained at below 2.1 K but vanishingly small amounts of liquid could be collected. It is apparent that a transfer at superfluid temperature will require increased pumping capability.

The results show that transfer rates of the order of .1 litre/min. can be achieved using the valve as an expansion valve. The transfer temperature is above superfluid but considerably below 4.2. The conclusion from this work is that the helium Dewar for the IRT experiment could be topped-off with liquid that is at least below 3 K which will result in an increased superfluid volume than if 4.2 liquid were used.

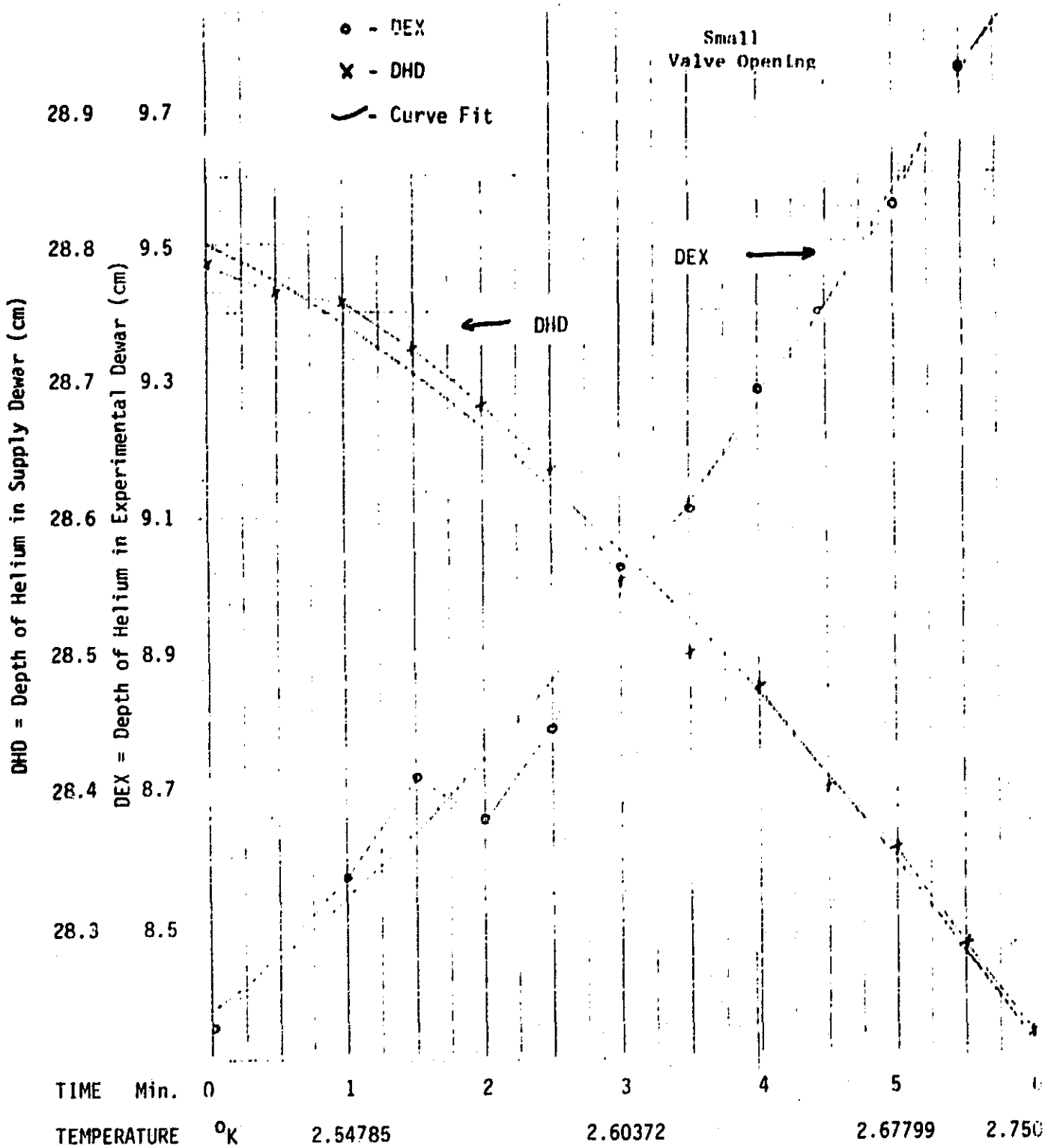
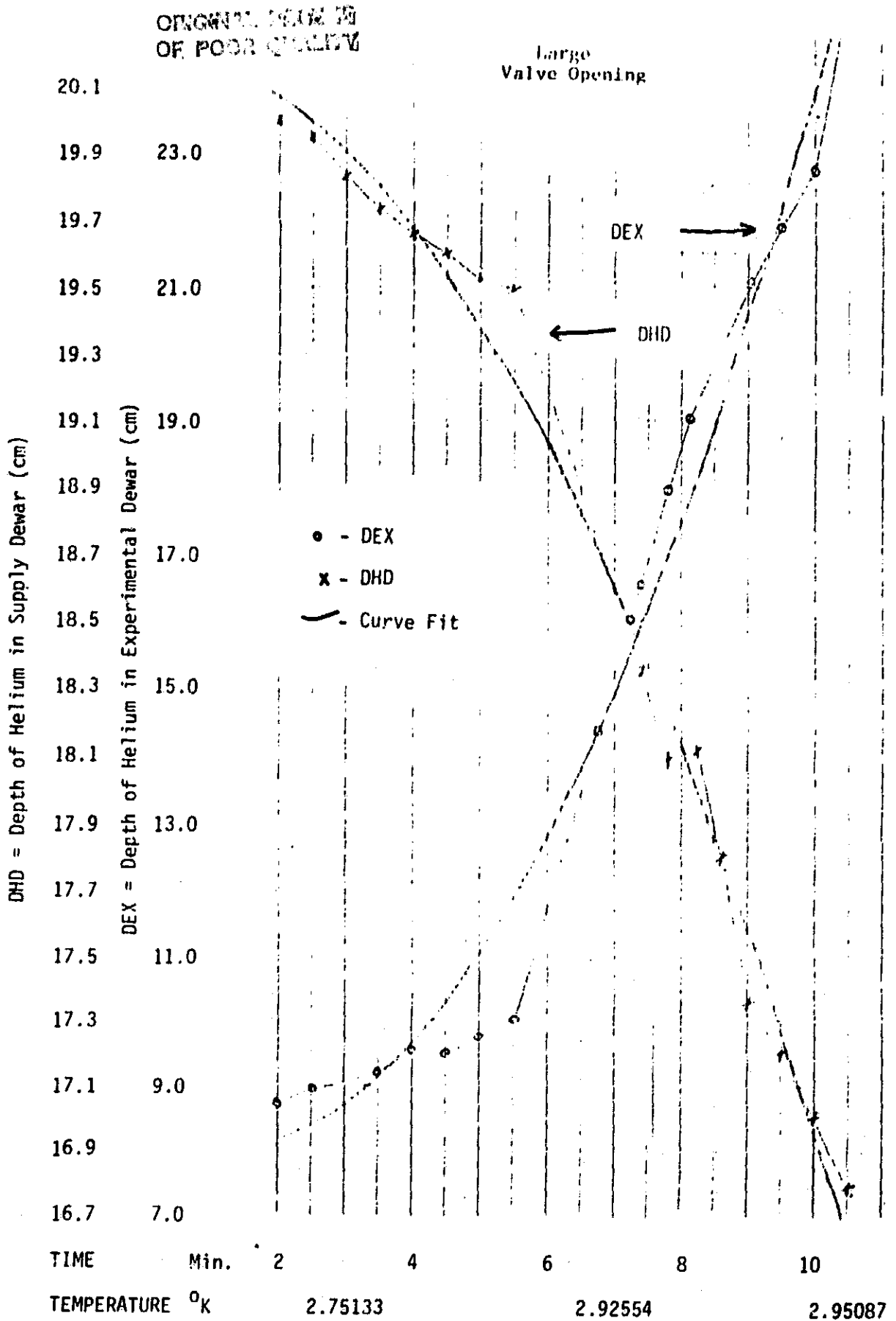


Figure 1. Liquid Helium Level in the Supply and Experimental Dewar During the Transfer as a Function of Time for a Relatively Small Valve Opening. The temperature in the experimental dewar is also listed as a function of time during the transfer.

Figure 2. Liquid Helium Level in the Supply and Experimental Dewars During the Transfer as a Function of Time for a Relatively Large Valve Opening. The temperature in the experimental dewar is also listed as a function of time during the transfer.



V. Burst Disks for IRT

1. Burst Disk Requirements

The transfer assembly requires that two burst disks be used; one to bypass the plug should the porous material become clogged and one to bypass the fill line valve should the vent line become clogged. These disks must operate at 1.6K since they will likely have liquid at that temperature on the high pressure side during orbit. The disks must also maintain vacuum tightness and operate at room temperature and high pressure such that may occur during filling operations. A disk made by Fike Metal Products Corporation of Blue Springs, Missouri, was located as a likely candidate for this application. This company has made such disks for Ball Brothers and a modification of that disk for use in the IRT experiment is under consideration.

2. Burst Disk Specifications

The burst disk under consideration is one manufactured by Fike Metal Products Corporation, Blue Springs, Missouri. This company manufactured a disk for Ball Brothers for an application similar to that of the IRT. Attachment C contains drawing number A4593-1 showing the disk. Attachment D gives a summary of the burst disk test program that was undertaken during the contract period.

ATTACHMENT C

Fike Burst Disk

FIKE METAL PRODUCTS CORP.

704 S. 10TH STREET

BLUE SPRINGS, MISSOURI 64015

PHONE: 816-229-3405

QUOTATION

To: University of Alabama
P. O. Box 1247
Huntsville, Alabama 35807

Fike P 13661
September 25, 1978

Attention: Mr. Jerry Karr

We propose, subject to final acceptance by us at Blue Springs, Missouri, of your order, to deliver the following items at prices indicated:

CONFIRMATION OF TELEPHONE QUOTATION 9/25/78

ITEM
NO.

Fike A 4593-1

Qty. of (2) \$1,450.00 ea.

Qty. of (4) \$1,306.00 ea.

Shipment: Six (6) weeks after receipt of order.

See Attachment - Rupture Disc Conditions of Sale.

All shipments F.O.B. Blue Springs, Mo., unless otherwise specified.

Terms of payment: 1/10 N/30

NOTICE:

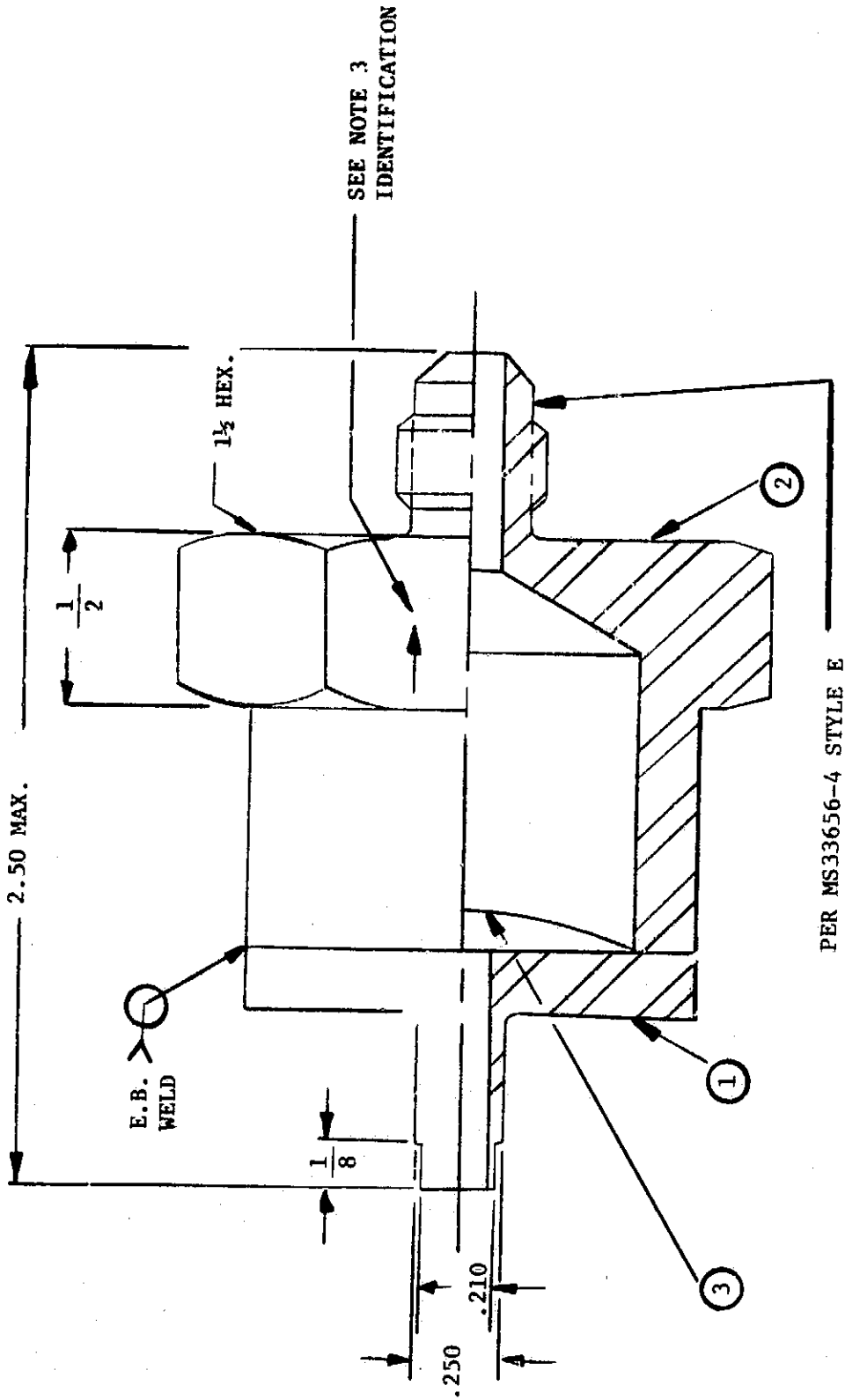
This quotation is not an offer subject to your acceptance, but is information which may be made the subject of your purchase order to Fike Metal Products Corp., and such order must be finally accepted by us at Blue Springs, Mo., to be binding upon us. Final acceptance and delivery dates are always subject to strikes, acts of God, and other circumstances beyond our control, in the event of which we do not assume liability for delays reasonably due to such occurrences.

Dated: Blue Springs, Missouri 9/25/78
Our representative in your area:
Gaines and Co.
Box 57023
Birmingham, Alabama 35209

FIKE METAL PRODUCTS CORP.

By 
Jeannie Foster, Asst. Sales Manager

1 80000 + 879-0574



PER MS33656-4 STYLE E

NOTES FOR PRECEDING DRAWING

1. Rupture Disc, Item (3) :

Material: Aluminum

Burst Pressure: 30 Psig \pm 5 Psig

@ 72°F to Withstand Full Vacuum

2. Leak Test: Leak Rate Not to Exceed

1×10^{-7} ATM. CC/SEC. Helium.

3. Identification: Etch or Steel Stamp on HEX. Flats

3.1 Fike

3.2 Flow Arrow

3.3 A4593-1

4. Supply Paper Tag Marked as Follows:

4.1 Fike

4.2 A4593-1

4.3 Lot No. XXXXXX

4.4 25 - 35 Psig @ 72°F

5. Poly Bag and Heat Seal One Assy. & Paper Tag Per Note 4.

ATTACHMENT D



The University
Of Alabama
In Huntsville

School of Science
and Engineering

January 29, 1981

MEMORANDUM

TO: Dr. Urban
FROM: G. R. Karr *G. R. Karr*
SUBJECT: Burst Disk Test Results

The experience to date with tests on burst disks prepared by Fike Metal Products is summarized in the following:

1. Four burst disk assemblies were purchased from Fike Metal Products and were labeled by Fike to have a burst pressure of 78-93 psig at 4.2°K. Two of these disks were tested at 4.2°K and found to burst at 135 psid. A third disk was burst at room temperature and found to burst at 48 psid. The ratio of 4.2°K burst to the 300K burst was then 2.8. A copy of a letter I sent to Fike Metal Products is attached and in it is a detailed description of the tests and the test setup.
2. Four replacement disks were purchased from Fike Metal Products and delivered December 19, 1980. The disks are all labeled for example as follows

Fike ↑
A4593-2
20-30 PSIG @ 72°F
lot No. 133855-1

where the last number in the lot number is 1, 2, 3 or 4.

Two burst disks (#3 and #4) were selected for use in the TA. Disk #2 was selected for a cold burst test which was run on January 9, 1981. The test setup was the same as used in the earlier tests (see letter to Fike) except that the dewar was sealed so that the helium bath could be pumped. A temperature of 2°K was obtained and the burst pressure was recorded to be 115 psid.

3. A call to Fike Metal Products was made January 22, 1981 to learn the manufacturing methods used by Fike and to determine what tests were recorded which relate to the disks to be used in the TA.

The procedure used by Fike in the disk preparation is to first perform a sufficient number of experiments with various thicknesses of formed 1100 Aluminum and/or scoring patterns until they are confident that the correct combination has been found. For our particular disks, the diameter was fixed so that only the thickness and scoring pattern were varied.

After the above experiments were concluded, seven disks were prepared for the UAH order. Three of these disks were selected at random and tested at room temperature. The burst pressure recorded were:

26 psid
26.5 psid
26.5 psid

After the above tests verified that the disk burst pressure was within the specifications, the four burst disks were assembled and shipped to UAH.

4. Taking the room temperature burst pressure as 26 psid and the 2°K burst pressure as 115 psid, the ratio of 2°K to 300°K burst pressure is 4.4 which is well above that obtained in the earlier tests.

5. An investigation of material properties of 1100 Aluminum as a function of temperature revealed that a significant increase in ultimate tensile strength can be expected as temperature is decreased. A ratio of ultimate strength at 4°K to that at 300°K can be expected to be near 4.

GRK/kpw
Attachment (1)

School of Science
And Engineering



The University
Of Alabama
In Huntsville

Department of
Mechanical Engineering

P.O. Box 1247
Huntsville, Alabama 35807

August 26, 1980

Fike Metal Products
ATTN: Stan Sigle
704 South 10th Street
P. O. Box 610
Blue Springs, Missouri 64015

Dear Mr. Sigle:

This letter concerns the four burst disks which were manufactured for UAH by Fike Metal Products. As you may recall, three disks have been burst in tests performed by me. Each of these disks is labeled as to the date of the test, the bursting pressure, and the temperature conditions. These are summarized as follows:

<u>Date</u>	<u>Burst Pressure</u>	<u>Temperature Conditions</u>
1. Test of Aug. 5, 1980	134 psid	4.2°K
2. Test of Aug. 20, 1980	137 psid	4.2°K
3. Test of Aug. 21, 1980	48 psid	Room temperature 300°K

At a temperature of 4.2°K, the burst disks were found to burst at near 135 psid which is well outside the range of 78-93 psig which is the labeled bursting pressure. Since I do not know the expected room temperature burst pressure, I am unable to tell if the test of August 21 is within specifications.

In my telephone discussion with you on August 13, 1980, you asked that I repeat the August 5 test using one of the three remaining disks. The results of the August 20 tests were then reported to you on August 21. I then burst a third disk on August 21, as per your instructions, at room temperature. The fourth disk has not been tested in any way and you asked that I return it with the other three. I understand from our conversations that Fike Metal Products will burst the fourth disk at room temperature.

The information gained from the above tests will be used by Fike Metal Products to manufacture replacement disks for the four units, all of which will then be returned to UAH at no extra cost to UAH. Since the burst disks are to become part of an assembly which UAH has contracted

Stan Sigle
Page 2
August 26, 1980

to deliver in the near future, I understand that Fike Metal Products will try to deliver the completed units within a reasonable time period of say 4 to 6 weeks. Please advise if this delivery time period is not feasible.

In view of the apparent uncertainty in burst pressure at low temperatures, I want to investigate the possibility of obtaining disks with a predicted low temperature (4K) burst pressure of 65 psid max. rather than the originally specified 93 psid max. The lower burst pressure would serve as an additional safety factor due to uncertainty concerning the maximum probable pressure on the high pressure side of the burst disk. Please advise me on the possibility of changing the burst disk specifications on those four disks that you are refabricating for us using the same holders as used in the original design. If lower burst pressure specifications will require new holders of different dimensions, please advise me on the dimension changes required and extra expenses which may be required of UAH.

In our conversation of August 21, I offered to provide you with a description of the test set-up used to test the burst disks at cold temperatures. The steps followed in both cold temperature burst tests were as follows:

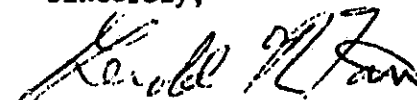
1. Mini-conflat flanges were welded to each end of the burst disk assembly.
2. Leak tests were performed at room temperature with a vacuum being pulled on the low pressure side of the disk. (The low pressure side is assumed to be the side the burst arrow points. See Figure 1).
3. A leak test was performed at a temperature of 2°K by first evacuating the low pressure side and then filling the dewar containing the burst disk to a level of nearly 50 cm. The holder used to test the disk was such that when the level was greater than 19 cm., the high pressure side of the disk would fill with liquid helium. (See Figure 2).
4. The liquid helium bath was pumped on to reduce the temperature of the bath to below 2°K. The bath level was recorded to be greater than 19 cm. when the 2°K temperatures were reached.
5. The disk holder assembly was removed from the liquid helium and allowed to warm to room temperature.
6. The high pressure supply assembly was attached to the high pressure side of the disk and the total assembly was placed in a warm dewar. The test set-up for the cold burst tests is shown in Figure 3.

Stan Sigle
Page 3
August 26, 1980

7. The low pressure side was evacuated with valves V1 and V2 open. After vacuum conditions were reached, V2 was closed and the Vacuum pressure was monitored by P1.
8. The high pressure side was evacuated with valves V4 closed and V3 open. When a vacuum was obtained, as determined by gauge P3, the valve V3 was closed.
9. The dewar was filled with liquid helium to a level of 40 cm.
10. Helium gas was allowed to enter the high pressure side by opening valves V4, V5, and the regulator valve V6. The helium gas was forced to travel through a LN₂ heat exchanger to insure any water vapor or other contaminants were removed. (The August 5 test did not use the LN₂ trap). The pressure on the high pressure side was monitored by a number of gauges. In the August 5 test, P2 which has a range of only 100 psi was the primary pressure monitor. However, after the pressure level reached above 100 psi in the August 5 test, the regulator pressure P6 was monitored instead. In the August 20 test, gauge P5 with a range of 200 psi and gauge P4 with a range of 1000 psi were added to the high pressure side. In the August 5 test, the regulator valve V6 was the primary pressure control while on August 20, the valve V5 was added and used as the primary pressure controller.
11. The liquid helium bath was not pumped on during the burst test which means that the temperature in the helium bath was at near 4.2K.
12. As warm helium is allowed into the high pressure side, liquid helium should condense in the cold region near the burst disk. Thus, during the first stages of pressurization, the warm gas flows into the cold region behind the disk and is converted to liquid. The warm helium supply was maintained at near 5 psig (20 psia or 20 psid) on the high pressure side until equilibrium conditions were reached (approximately 30 minutes).
13. The pressure was allowed to rise at about 2 psi per minute until burst was reached.

I hope the above description will be of assistance. The four burst disks have been shipped to you in a separate package.

Sincerely,



Gerald R. Karr

GRK/lpw

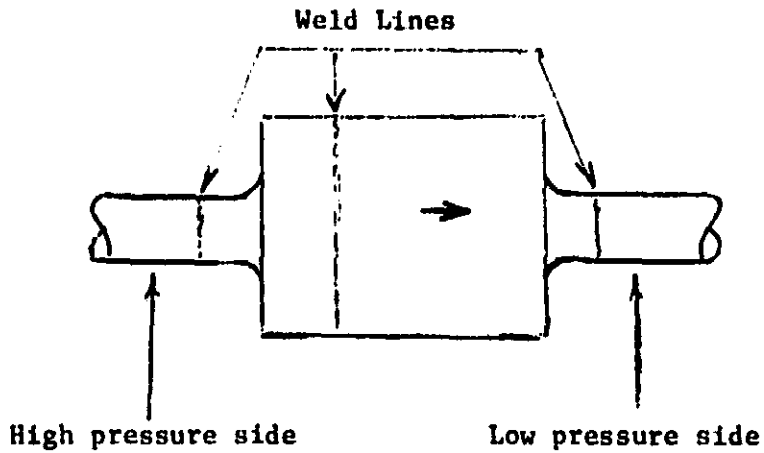


Figure 1. Assumed High and Low Pressure Sides in Relationship to the Arrow Labeled on the Disk

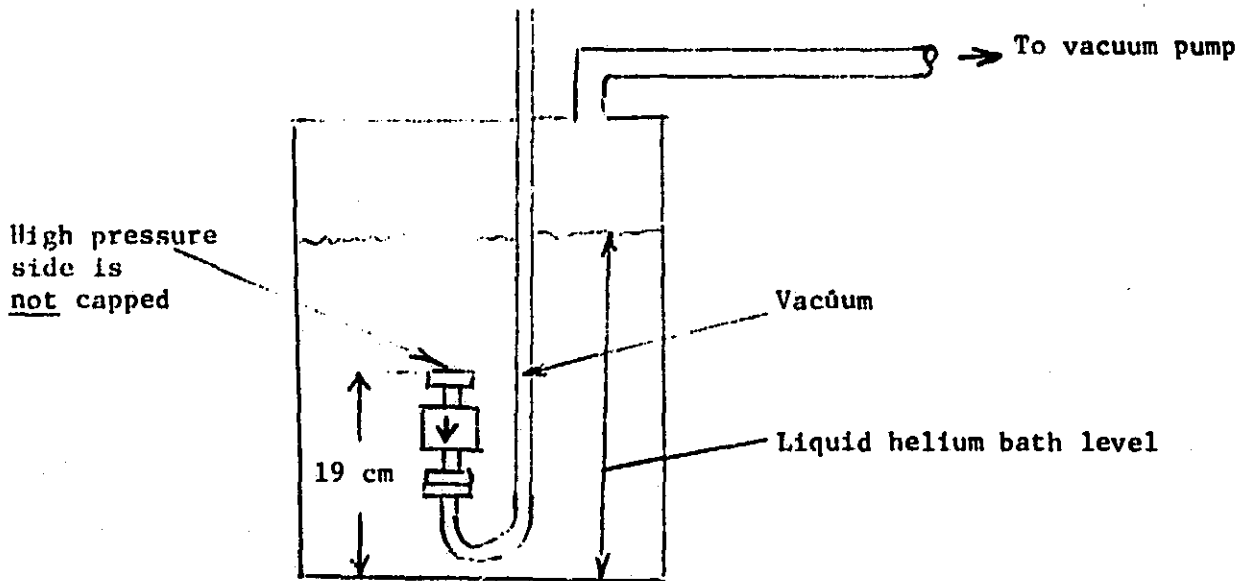


Figure 2. Experimental Set-Up to Perform Leak Test at 2°K .

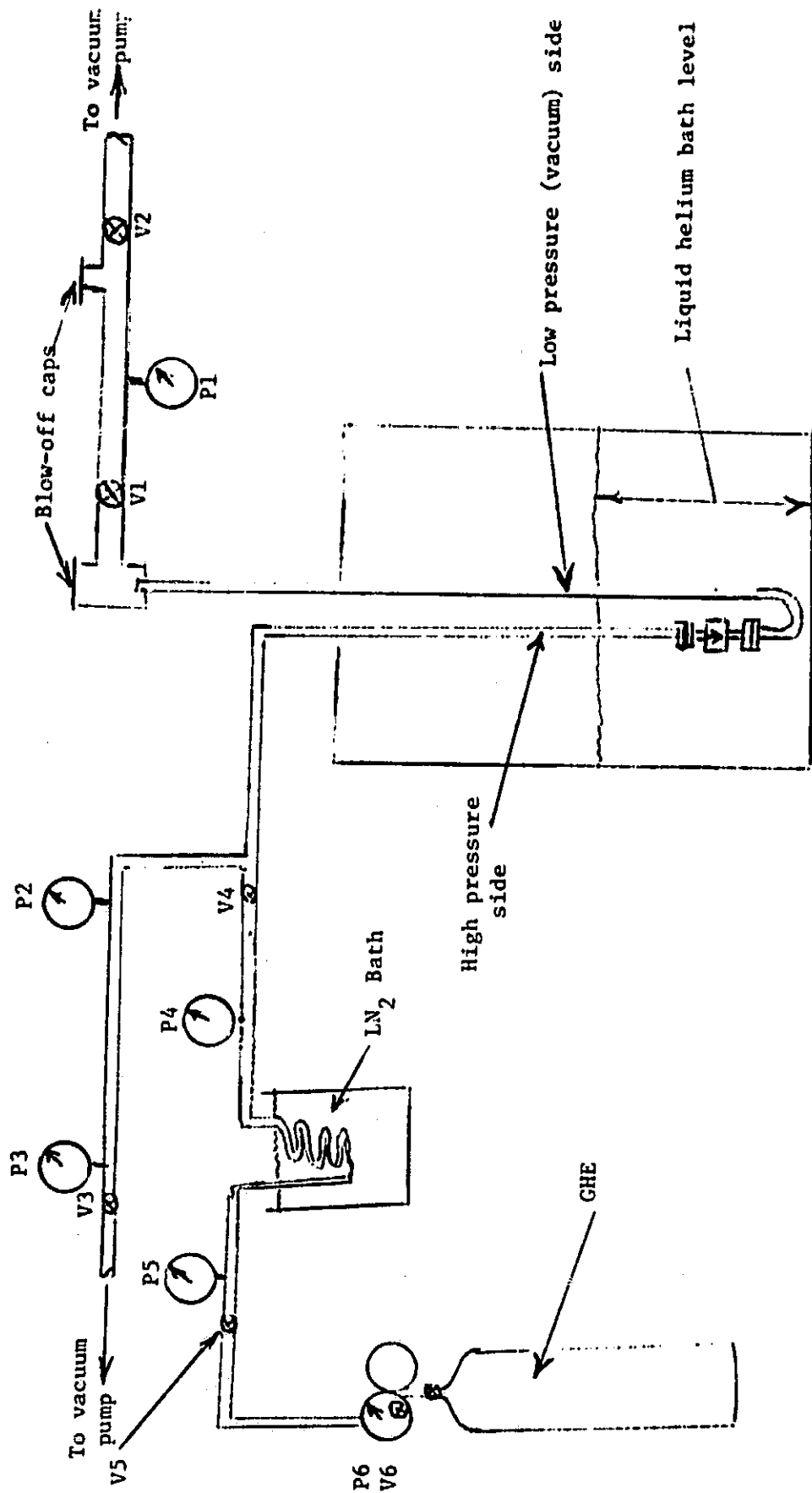


Figure 3. Test Set-Up for Cold Burst Tests

VI. Flow of Helium Gas in the IRT

1. Flow Regimes

Helium gas leaves the superfluid plug at pressures of the order 1 to 10 torr at a temperature of less than 2K. This gas absorbs heat and eventually exits the system at an assumed temperature of near 300K and a pressure of near 1 torr. It is estimated that the flow rate should be of the order of 2×10^{-3} gm/sec in order to provide cooling to the infrared telescope cold finger.

Assuming a steady flow of gas through the cold finger with an inlet temperature of 2K and an exit temperature of 3.5K, the heat absorbed by a flow of $\dot{m} = 2 \times 10^{-3}$ gm/sec is given by

$$\begin{aligned}\dot{Q} &= \dot{m} [h(3.5K) - h(2K)] \\ &= 2 \times 10^{-3} \text{ gm/s} [32 \text{ J/gm} - 23 \text{ J/gm}] \\ &= 18 \text{ mW}\end{aligned}$$

where the value of enthalpy, h , at 3.5K was obtained from NBS Technical Note 631, "Thermophysical Properties of Helium 4 from 2 to 1500K with Pressure to 1000 Atmospheres," R. D. McCarty, 1972. The value of 2K for gas was obtained by extrapolation of the values at higher temperatures given in NBS Technical Note 631.

Having established a mass flow rate, temperatures, and pressures, the flow regimes can be found. Since the pressures are low, the possibility of molecular or viscous flow is first investigated. The mean free path, L , of gas molecules is given by the equation

$$L = \frac{\mu}{.499 \rho v_a}$$

where μ is the gas viscosity, v_a is the average velocity of the molecules and ρ is the density. (See, for example, Dushman and Lafferty, Scientific Foundations of Vacuum Techniques, Wiley, 1962.) The average velocity is given by

$$v_a = \sqrt{\frac{8}{\pi} RT}$$

If the perfect gas law is used to express the density in terms of pressure and temperature, the following expression is obtained for helium gas

$$L = 57.25 \frac{\mu}{P} \sqrt{T}$$

Using this equation and values of viscosity from NBS 631, the following table is constructed

Pressure torr	Temperature K	Viscosity gm/cm-c	Mean Free Path cm
1	300	199×10^{-6}	.9148
10	300	199×10^{-6}	.00148
1	2.5	6.38×10^{-6}	4.33×10^{-5}
10	2.5	6.38×10^{-6}	4.33×10^{-6}

The table shows that the mean free path is much less than the one centimeter characteristic dimensions of pipes to be considered in this system. Therefore, the flow can be assumed to be viscous throughout the system. The next consideration is to determine if the flow is laminar or turbulent.

Laminar flow exists if the Reynolds number is less than 2000. Reynolds number is given by

$$R_e = \frac{\rho V d}{\mu}$$

where V is the velocity of the flow and d is the characteristic dimension which will be taken to be the pipe diameter. This can also be expressed in terms of the mass flow rate \dot{m} by the following

$$R_e = \frac{4\dot{m}}{\pi d \mu}$$

where we see that the largest Reynolds number will be at the region of low viscosity and small pipe diameter. Since viscosity is lowest at the low temperatures, the critical regions in the IR system are the helix and the cold finger which will have the smallest pipe diameters and are below 3K.

Using a viscosity of 6×10^{-6} gm/cm . S as representative of the values at below 3K and an $\dot{m} = 2 \times 10^{-3}$ gm/S, the following table is constructed.

Reynolds Number at Below 3K

<u>d</u>	<u>Re</u>
1 in	167
½ in	334
¼ in	668
1/8 in	1336
1/16 in	2673
1/32 in	5346

The results show that the flow can be considered laminar throughout for pipes having diameters greater than 1/16".

2. Pressure Drop for Gaseous Helium Flow

As was established in the previous section, a flow rate of 2×10^{-3} gm/sec is expected to result in laminar flow in the entire IRT flow system for pipes having diameters greater than 1/16" I. D. For laminar flow in a circular pipe, the pressure drop along the pipe is a well known relation given by¹

$$\frac{\Delta P}{L} = \frac{32 \mu V}{D^2}$$

where ΔP is the pressure drop, L is the length containing the pressure drop ΔP , μ is the viscosity, V is the velocity, and D is the inside diameter of the pipe. Since the flow rates in the IRT experiment are often quoted in terms of the mass flow rate, \dot{m} , where

¹Baumeister & Marks, "Standard Handbook for Mechanical Engineers," 7th Ed., 1967.

$$\dot{m} = \rho V A$$

and where ρ is the density and A is the cross section area, the expression for pressure drop can be rewritten as

$$\frac{\Delta P}{L} = \frac{32 \mu \dot{m}}{D^2 \rho A}$$

Since pressure and temperature are of more practical importance than density, the perfect gas law $p = \rho RT$ is used to obtain the following

$$\frac{P \Delta P}{\dot{m} L} = \frac{32 R T \mu}{\frac{\pi}{4} D^4}$$

where R is the gas constant and the equation for circular area has been used.

The results show that the pressure drop per unit length in a given pipe section is an inverse function of the diameter to the fourth power, an inverse function of the pressure, and directly proportional to the quantity $T\mu$ which is primarily a function of temperature only. At $T=2.78K$, the quantity $T\mu$ is 19.9×10^{-6} gm/cm s while at 300 K, the quantity $T\mu$ is 59.7×10^{-3} gm/cm s. Clearly, the pressure drop is a nonlinear function of temperature. The above equation has been plotted in Figure 1 as a function of temperature over the range from 1.7 K to 400 K. The values plotted are for a 1" inside diameter pipe which allows one to find the value for other diameters by dividing by the diameter (in inches) to the fourth power. By way of illustration, the following short table was constructed using the curve in Figure 1.

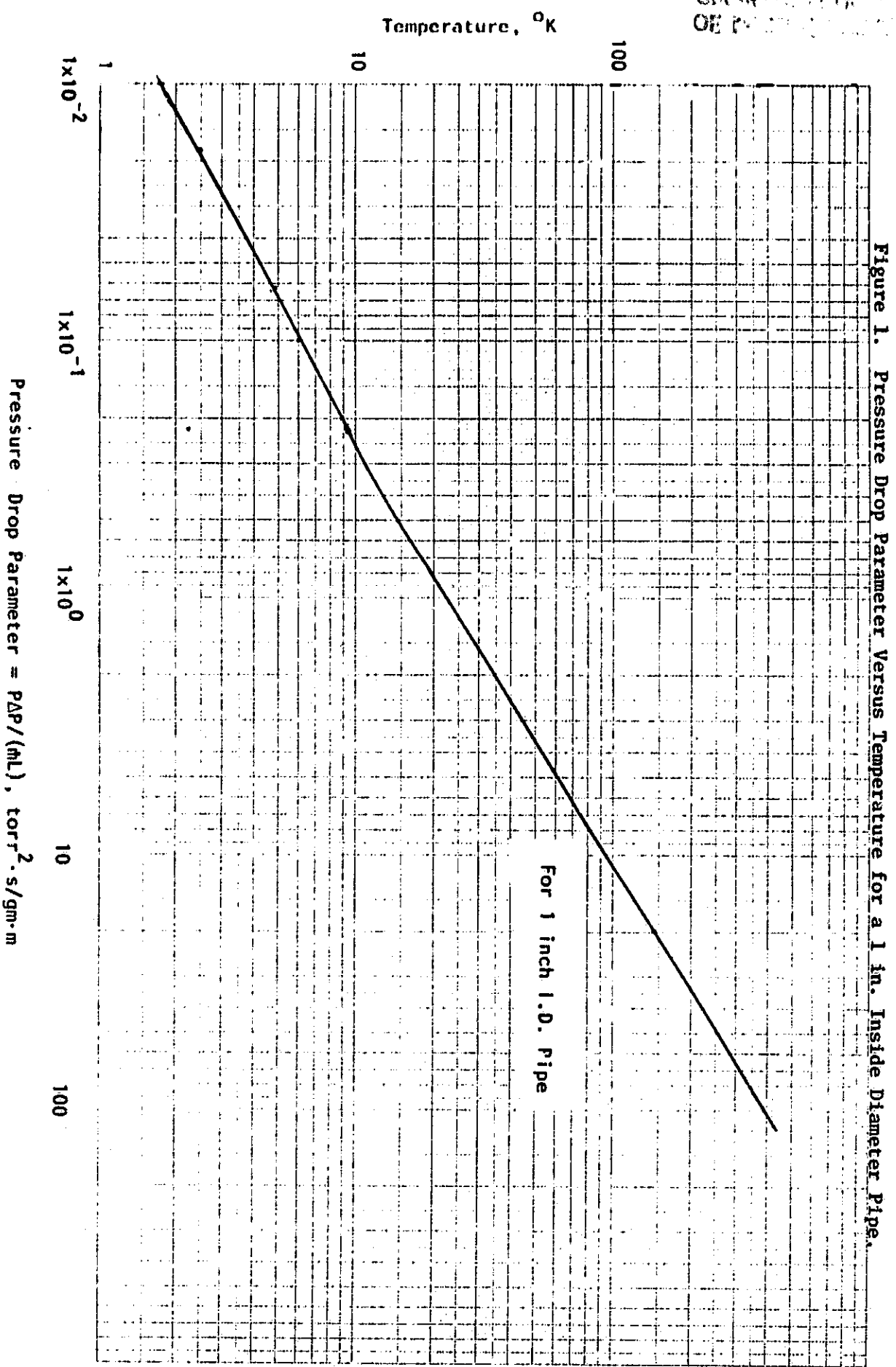
TABLE 1

Table of $\Delta P/L$ in torr/m for a Nominal Flow Rate of 2×10^{-3} gm/sec at a Pressure of 10 torr

Inside Dia. of Pipe	Temperature of Flow			
	2.5	20	100	300
1"	3.6×10^{-6}	1.6×10^{-4}	2.2×10^{-3}	1.4×10^{-2}
$\frac{1}{2}$ "	5.8×10^{-5}	2.6×10^{-3}	3.6×10^{-2}	2.2×10^{-1}
$\frac{1}{4}$ "	9.3×10^{-4}	4.2×10^{-2}	.57	3.5
1/8"	1.5×10^{-2}	.67	9.2	56.0

The results show the need to increase pipe size as the temperature increases in order to reduce the pressure drop.

ORIGINAL RECORD
OF PRESSURE



VII. Cold Finger Testing Results

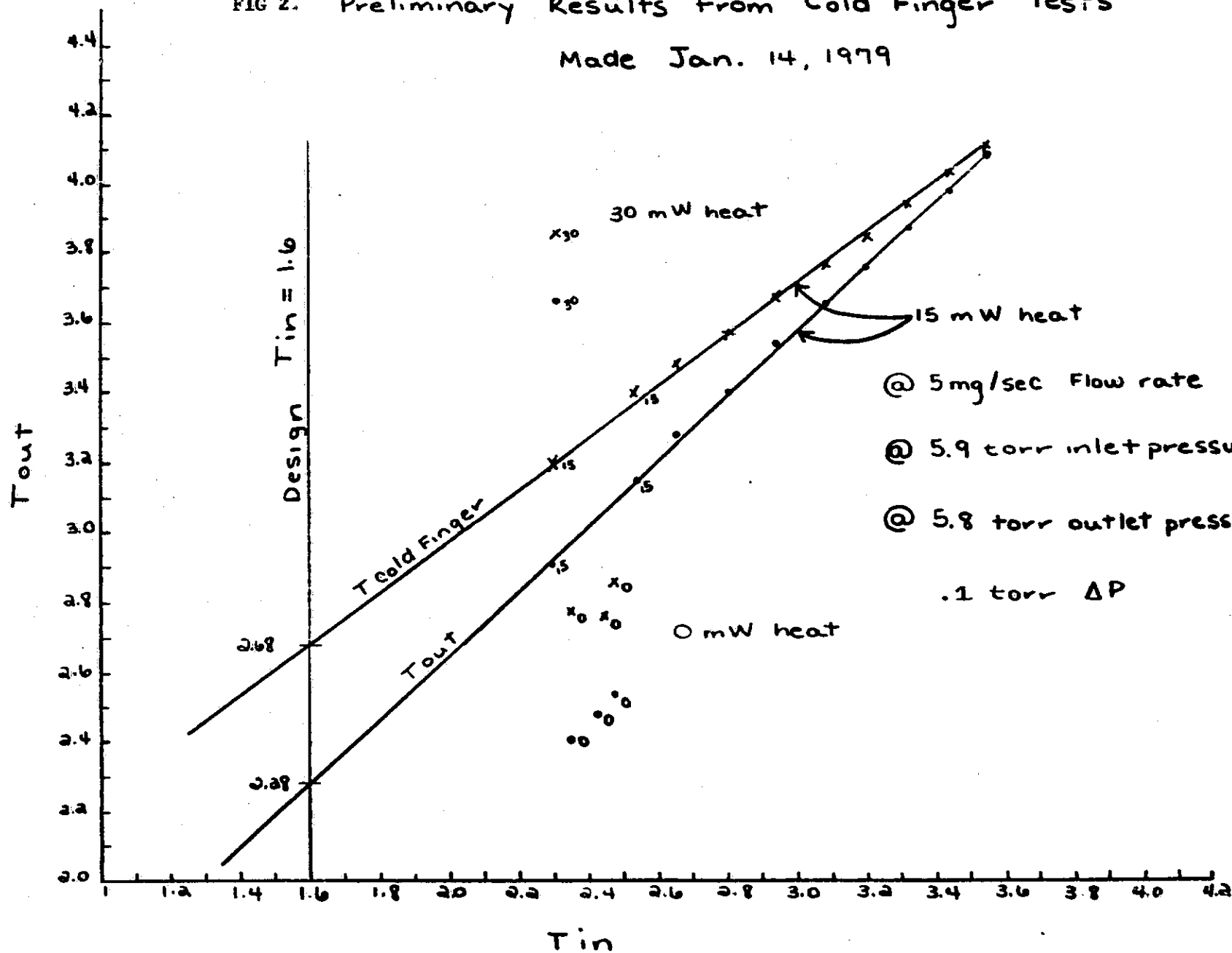
1. Cold finger test program.

Calibrated germanium thermometers were installed on the prototype cold finger with one each at the inlet, outlet, and on the cold finger body. A small heater made from resistance wire having a total resistance of 100 ohms was also installed on the cold finger. Liquid helium was transferred into the dewar on January 15, 1979 and, with pumping, a temperature of near 2.3K was obtained. Warm helium gas was passed through a long copper tube which was immersed in the helium bath. The cold gas was then introduced into the cold finger and eventually exhausted through a vacuum pump. The flow rate was monitored by a flow meter placed in the warm helium supply line.

The attached figure 2 shows the results obtained for three heater power inputs (0, 15 mw, and 30 mw). The test was run for a number of inlet temperature at a flow rate of 5×10^{-3} gram/sec. The results show that the cold finger performance can be extrapolated to the design inlet temperature of 1.6K. At 1.6K the cold finger would operate at 2.68K and the outlet would be 2.28K with a 15 mw heat load. The temperature rise of the gas can be used to measure the heat absorbed by the gas. The heat absorbed was found to be comparable to that input to the heater indicating an efficient heat exchanger. The relatively high cold finger temperature is thought to be caused by the lack of good thermal contact between the cold finger body and the heat exchanger system.

FIG 2. Preliminary Results from Cold Finger Tests

Made Jan. 14, 1979



ORIGINAL MADE IN
OF POOR QUALITY

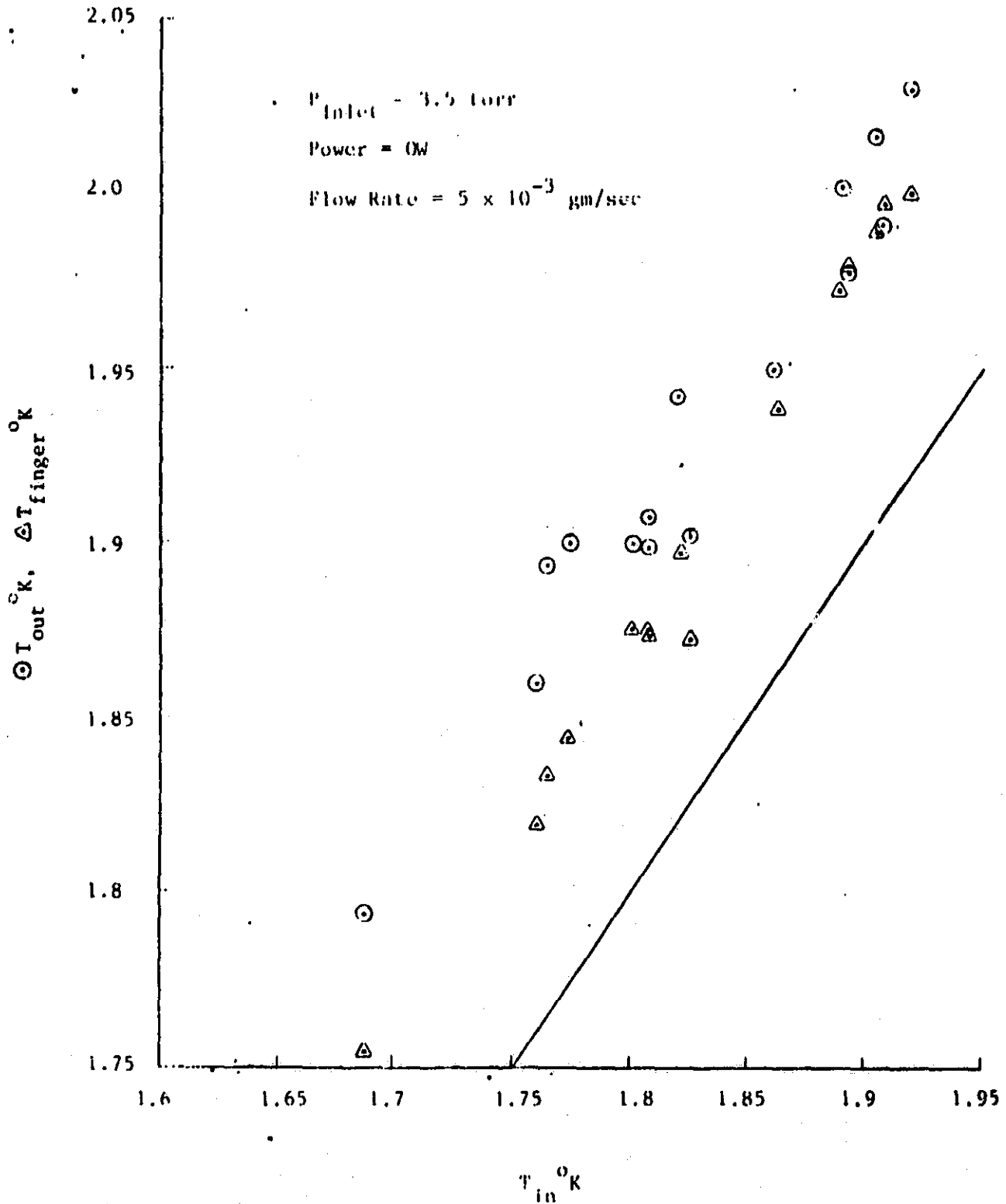
The results obtained in the cold finger tests are shown in figures 3, 4, 5 and 6. Figures 3, 4, and 5 show the temperature at the finger (on a simulated detector block) and at the outlet as a function of the inlet temperature for three different cases. For Figure 3 the inlet pressure was held at 3.5 torr, and the flow rate was 5×10^{-3} gram/sec and zero heat was applied to the detector block. The results show approximately a .1K range in the three temperatures during the cool down from 2K to 1.65K.

Figure 4 shows the results for a 6.3 torr inlet pressure, a flow rate of 5×10^{-3} gram/sec and a heat load of .0079W. As expected, the outlet gas is about .2K higher than the inlet due to the heat picked up by the gas in the heat exchanger. The detector block was forced to be .6K above the inlet temperature due to the heat transfer resistance between the detector block and the heat exchanger.

Figure 5 shows the results for an inlet pressure of 3.9 torr, a flow rate of 2.5×10^{-3} gram/sec and a power input of .0022W. The temperature differences are, as expected, much lower under these operating conditions as compared to those employed for the data of figure 4.

Figure 6 shows the results of the temperature increase of the coolant gas as a fraction of power input to the heater for the case of a constant inlet pressure of 3.9 torr and a flow rate of 2.5×10^{-3} gram/sec. The data are seen to fall on a straight line. The slope is found to be 12.63 K/mw which translates into an effective specific heat of the gas of 5.05 J/gm-K which compares favorably with a value of 5.5J/gm -K found in the literature.

Figure 3. Plot of cold finger test results of March 1979 for zero power input at 3.5 torr inlet pressure and 5×10^{-3} gram/sec flow.



$T_{out}^{\circ}K$, $T_{finger}^{\circ}K$

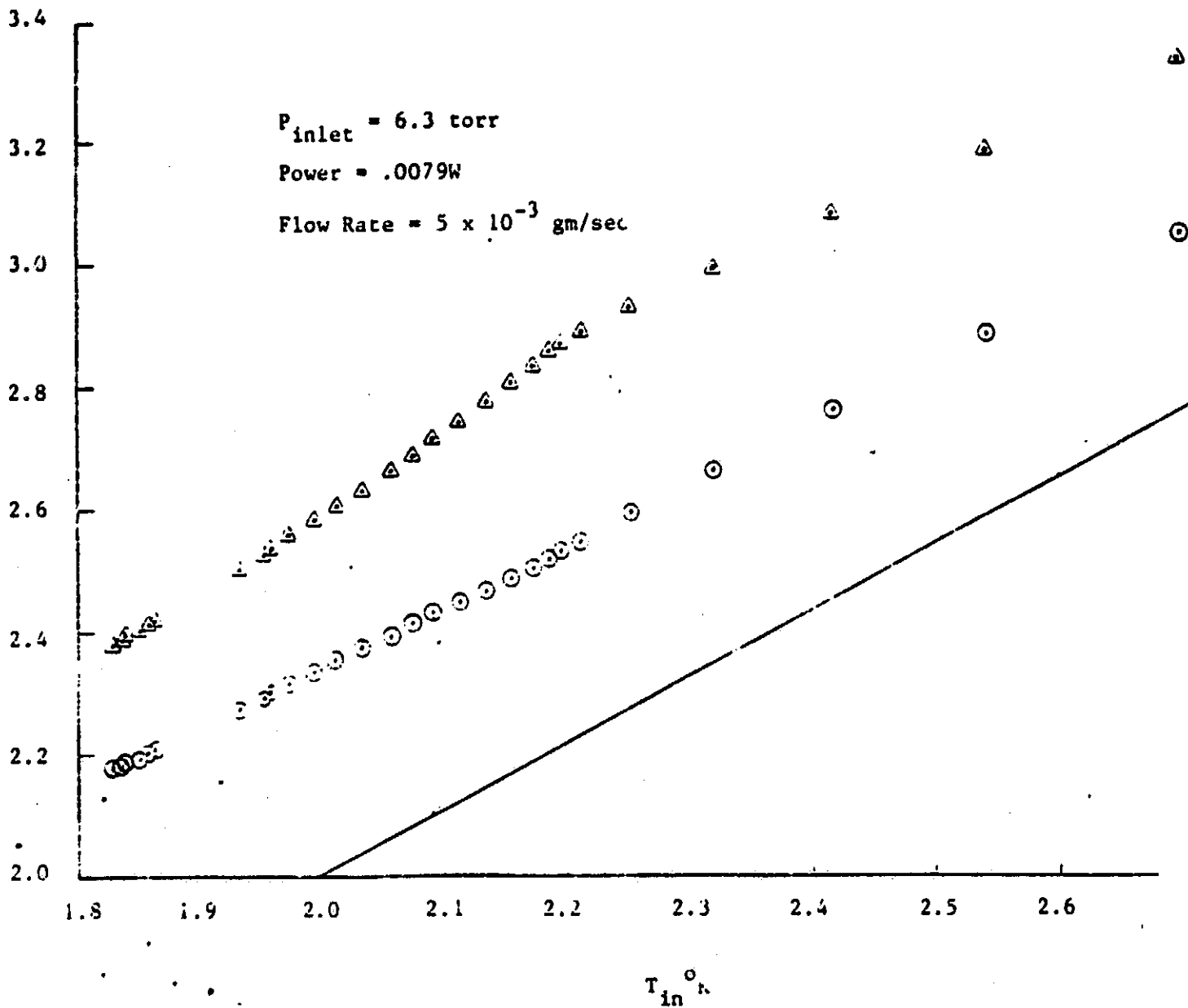
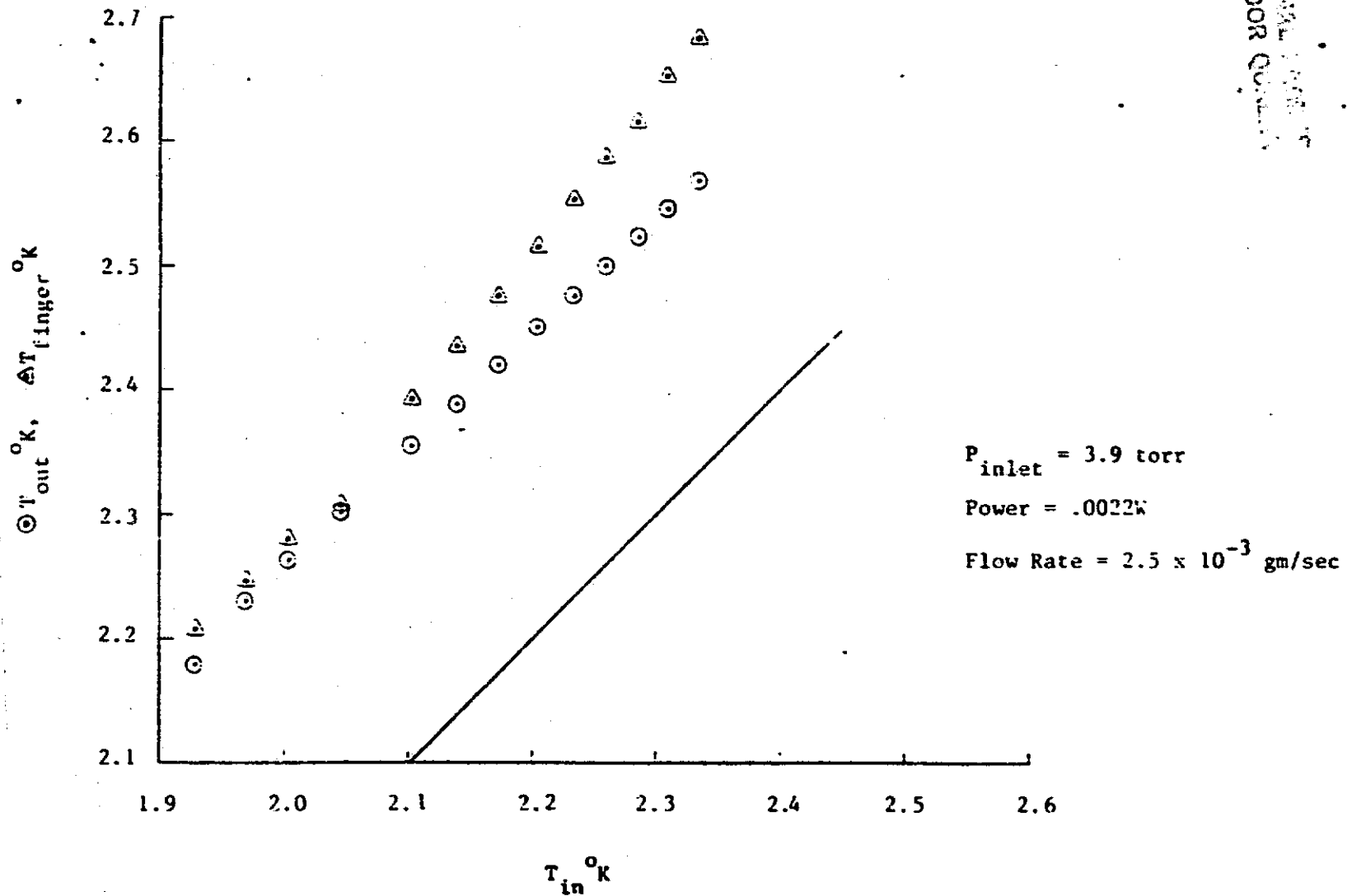


Figure 4. Plot of cold finger test results of March 1979 for .0079w power input at 6.3 torr inlet pressure and 5×10^{-3} gram/sec flow.

Figure 5. Plot of cold finger test results of March 1979 for .0022w power input at 3.9 torr inlet pressure and 2.5×10^{-3} gram/sec flow.



ORIGINAL REPORT OF POOR QUALITY

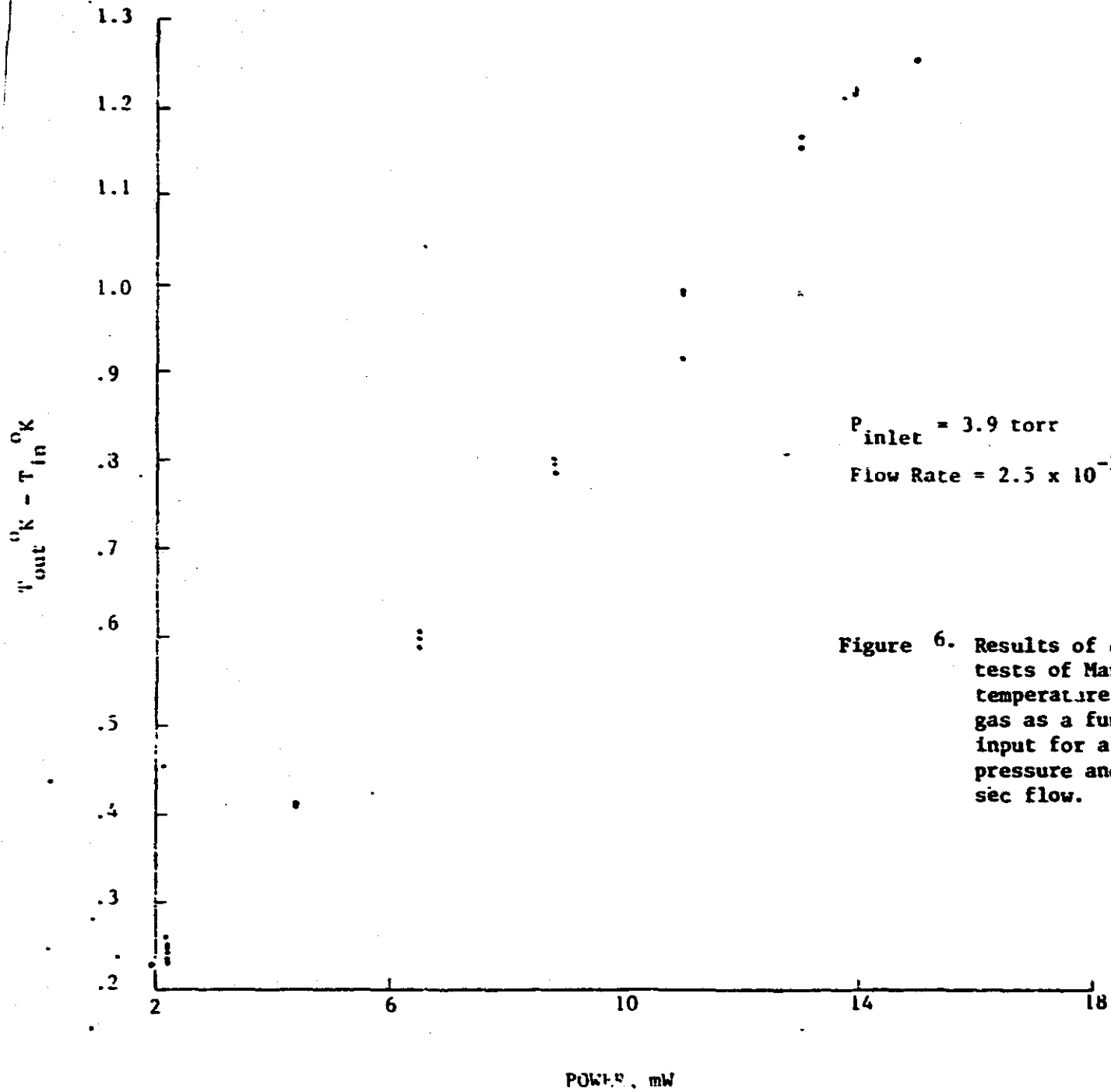


Figure 6. Results of cold finger tests of March 1979 on the temperature gain in helium gas as a function of power input for a 3.9 torr inlet pressure and 2.5×10^{-3} gram/sec flow.

VIII. Design and Testing of the Rotating Connection for IRT

1. Helix Design

Consider a helical spring made of thin-walled stainless steel such as has been proposed for the IRT experiment. This spring is designed to allow relative rotation of $\pm 45^\circ$ between the telescope and the helium Dewar while also supplying cold helium gas to the experiment. Two of the main design considerations of the helical element are (1) that the spring force produced should be small in order to reduce the possibility of leaking due to stresses in the tube material and to reduce the torque required to rotate the telescope and (2) that flow of cold helium gas should be as free of significant pressure drop as possible.

The design of cylindrical helical torsion springs of solid circular cross section or solid rectangular cross section have angular displacement, θ , for a given applied torque, T , given by¹

$$\theta/T = l/EI$$

where l is the total length of the straightened spring, E is the modulus of elasticity of the material and I is the amount of inertia of the cross section about the centroid. The applied torque produces bending stress, S , in the material given by

$$S = \frac{k T}{(I/c)}$$

where c is the distance from the neutral axis to the outer edge of the cross section which will experience the stress S . The factor k is needed for heavy, closely coiled springs and is near unity for the springs under consideration in this work. For the tubular cross section representative of the thin-walled stainless tube material,

$$I_{\text{tube}} = \frac{\pi}{64} (D^4 - d^4)$$

and

$$\left(\frac{I}{c}\right)_{\text{tube}} = \frac{\pi}{32} \frac{D^4 - d^4}{D}$$

where D is the O.D. and d is the I.D. of the tube.

Choosing a safe maximum cyclic stress of 25,000 psi and the requirement of $\pm 45^\circ$ angular displacement, the torque and total length required can be computed as

$$T = S (I/c) = S \frac{\pi}{32} \frac{D^4 - d^4}{D}$$

$$l = \frac{\theta E D}{2S}$$

Notice that the torque and length become independent of the diameter of the cylindrical coil. Table 2 is constructed using the above two equations for various candidate tube sizes.

Table 2

Table of Spring Torque and Total Tube Length for Four Nominal Tube Sizes Using 25,000 psi as the Safe Operating Stress, 30×10^6 psi for Modulus of Elasticity, and 45° as the Angular Deflection.

Tube Size (in)	D O.D. (in)	d I.D. (in)	Torque for $S=25,000\text{psi}$ (in-lbs)	Total Tube Length for $\theta = 45^\circ$		Number of Turns Req. for 2" Cyl.	Pressure Drop for $2 \times 10^{-3} \text{ gm/sec}$ at 10 torr, 1.7 K (Torr)
				(in)	(m)		
1/16	.0625	.0425	.5	29.5	.75	5	9.8×10^{-2}
1/8	.125	.105	2.4	58.9	1.5	10	1.23×10^{-2}
3/16	.187	.167	5.8	88.0	2.2	14	3.6×10^{-3}
1/4	.250	.220	15.4	117.8	3.0	20	1.5×10^{-3}

Included in Table 2 in the last column is the resulting pressure drop for a 2×10^{-3} gm/sec flow of helium gas at 1.7 K and 10 torr pressure. The pressure drop at 1.7 K for other possible flow rates or pressures is easily found from the given numbers as long as the flow remains laminar. The results show that the advantages of going to smaller tube diameter (shorter length and lower torque) is offset by the increase in pressure drop of the smaller diameter tube. The 1/8 or 3/16 inch tube appears to be the best compromise and gives an adequate flow capability in case increased flow rate is required.

2. Helix Testing

A prototype stainless steel helix was constructed by winding 1/8-inch-outside-diameter-304 seamless tubing, having 10 mil wall, about a 2 inch diameter cylinder. A helix of 20 turns was made and mated to stainless steel disks at each end. The disks contained an internal passage which allowed vacuum testing of the helix. A testing rig was made so that the helix could be submerged in liquid helium or nitrogen and twisted by an external drive mechanism. The drive was set to twist the helix at $\pm 90^\circ$ angle at a period of about 3.0 sec.

The helix was subjected to over 34,000 cycles at a temperature of 77°K at $\pm 90^\circ$ per cycle. No failure of the helix was found as determined by leak testing under vacuum conditions. The measured torque at 77°K was found to be 5 in lbs/90° which compares with 4 in lbs/90° measured at 300K. These measured values of torque compare well with that predicted by theory.

The helix tests lead to the conclusion that this design will perform as expected in the IRT experiment.

3. Ferro Fluidic Seal

A rotating, vacuum-tight seal was purchased for testing purposes from the Ferro Fluidic Corporation, 144 Middlesex Turnpike, Burlington, Mass. The seal is Ferro Fluidic Seal Model SC 1500 (special cantilevered unit with bearings out of vacuum) having a bore of 1.5 inches, outside diameter of 3.25 inches, and overall length of 3 inches. The unit was vacuum tested using a helium leak detector for both the stationary case and with rotation. No leaking was detected during these tests.

Torque required to rotate the seal was found to be approximately 2 in lbs for rates of rotation typical of the IRT requirements. The torque was measured while the seal was under vacuum conditions.

The seal uses a low vapor pressure liquid which has magnetic particles in suspension. The magnetic fluid is forced by magnets to act as a barrier between the high and low pressure regions while also allowing relative movement of the sealing surfaces. The seals are designed for rotation rates far in excess of that expected in the IRT application.

IX. Porous Plug Development

1. Porous Plug Experiments

The porous plug experimental apparatus was prepared by Dean Hart. The purpose of the tests were to confirm previous test results obtained at MSFC on the cylindrical plugs. These earlier tests were in question because of recent results reported by JPL that the cylindrical plugs could not work as phase separators. Tests were made by Dr. Karr and Dean Hart on December 6 which confirmed the JPL results. The cylindrical samples were unable to serve as phase separators at any temperatures between 1.5K and the lambda point.

A .5 micron disk shaped plug was installed in the test equipment and was found to operate successfully. Tests of the "low-end breakthrough" phenomena were attempted. The tests were designed so that small ΔP could be generated by closing the valve to the pump on the vapor side of the plug. As the valve approached nearly 100% closing, the liquid did flow through the plug as had been described by Mason and Petrac. The valve used for these tests was, however, not controllable enough to obtain good data on the exact ΔP value that the liquid flowed into the tube.

2. Porous Plug

As reported in the above, the cylindrical plugs which were originally to be used in the T.A. were found to not be acceptable. Designs have since been made to modify the plumbing to accommodate a disk type plug. Paul Clemons has determined that the maximum diameter

plug which can be accommodated without considerable redesign is about 2". Based on this diameter constraint, a study is underway to select the best plug for the IRT system. Plug material is available from Mott Metalurgy having a diameter of about 3 inches, thickness of $\frac{1}{2}$ inch, and pore sizes of $\frac{1}{2}$, 2, and 5 micron.

One of the important requirements for the porous plug for the IRT experiment is the gas flow throughput at cold temperatures. The IRT plug must have enough throughput to maintain the dewar at super fluid temperatures before launch. This requirement may be as high as 20mg/sec with the liquid at 1.6K or 6 torr pressure.

The volumetric gas flow, Q , through a porous plug is predicted to be a function of the pressure drop, ΔP , the gas viscosity, μ , the plug area, A , the plug length, l , and the plug permeability, k , given by

$$Q = \frac{kA}{\mu} \frac{\Delta P}{l}$$

The mass flow, \dot{m} , is related to the volumetric flow by the following

$$\dot{m} = \rho VA = \rho Q$$

where ρ is the density, V is the velocity. Using the perfect gas law

$$P = \rho RT$$

where R is the gas constant, an expression is obtained for the mass flow rate per unit area given by

$$\frac{\dot{m}}{A} = \frac{kP\Delta P}{\mu l RT}$$

Based on the above expression, the gas flow rate at 1.6K can be predicted based on gas flow rate data obtained at room temperature. That is, assuming that the permeability and gas constant are independent of temperature, we obtain

$$\frac{(\dot{m}/A)_{300K}}{(\dot{m}/A)_{1.6K}} = \frac{\Delta P_{300} P_{300} \mu_{1.6} T_{1.6}}{\Delta P_{1.6} P_{1.6} \mu_{300} T_{300}}$$

Previous room temperature tests of gas flow of helium through the plug have revealed the following data for four different samples

Room Temperature Gas Flow Data ($\Lambda = 15 \text{ cm}^2$)

Sample Description	$\Delta f / \Delta P$ (SCCS) psi	$\frac{\dot{m}}{\Delta P}$ (mg/sec) torr	$\frac{\dot{m}}{P \Delta P}$ (mg/sec) torr ²
½ micron Al ₂ O ₃	.448	1.54 X 10 ⁻³	2.03 X 10 ⁻⁶
3 micron Al ₂ O ₃	6.23	2.14 X 10 ⁻²	2.82 X 10 ⁻⁵
10 micron Al ₂ O ₃	18.64	6.42 X 10 ⁻²	8.45 X 10 ⁻⁵
10 micron Ni	31.45	.108	1.42 X 10 ⁻⁴

Based on the above data and the relationship developed above, we see that for the same diameter plug, the cold gas flows should be proportional to the ratio of the viscosities and temperatures given by (using published data for viscosity at 2.5K for example)

$$\frac{\left(\frac{\dot{m}}{P \Delta P}\right)_{300}}{\left(\frac{\dot{m}}{P \Delta P}\right)_{2.5K}} = \frac{\mu_{2.5} T_{2.5}}{\mu_{300} T_{300}} = \frac{6.38(2.5)}{200(300)} = 2.66 \times 10^{-4}$$

Based on the above relationship the following table is generated using the warm gas flow data.

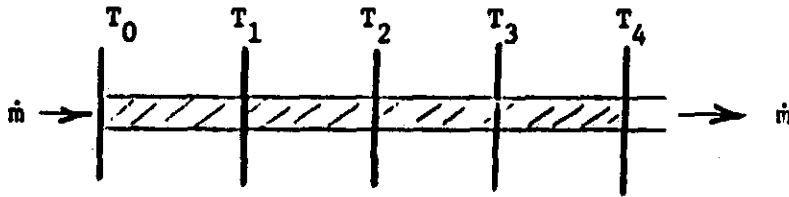
Predicted Cold Gas Flow ($\Lambda = 15 \text{ cm}^2$) at 2.5K

Sample Description	\dot{m} (P = 6 torr, $\Delta P = 4$ torr) mg/sec
½ micron Al ₂ O ₃	.183
3 micron Al ₂ O ₃	2.55
10 micron Al ₂ O ₃	7.63
10 micron Ni	12.82

X. Thermal Modelling and Heat Exchanger Design

1. Thermal model of typical dewar system.

Consider a typical dewar system in which cold vapor is used to remove heat at various shields as shown in the figure



If the vapor reaches a steady state equilibrium at each station, the amount of heat absorbed by the vapor is given by the increase in temperature which results. Therefore, at each of the 4 stations, assuming constant specific heat, the heats absorbed are

$$Q_1 = \dot{m} C_p (T_1 - T_0)$$

$$Q_2 = \dot{m} C_p (T_2 - T_1)$$

$$Q_3 = \dot{m} C_p (T_3 - T_2)$$

At the liquid, the amount of heat is Q_0 and is balanced by the heat of vaporization

$$Q_0 = \dot{m} L(T_0)$$

The heat which reaches a given stage is the result of conduction and radiation. A given shield will radiate and conduct energy to a lower temperature shield and will gain energy by the same means for the shield at a higher temperature. Denoting heat conduction coefficients by K and radiation coefficients by R , the following relationships are obtained for the heat loads.

$$\begin{aligned}
Q_0 &= K_{01} (T_1 - T_0) + R_{01} (T_1^4 - T_0^4) \\
Q_1 &= K_{12} (T_2 - T_1) + R_{12} (T_2^4 - T_1^4) \\
&\quad - K_{01} (T_1 - T_0) - R_{01} (T_1^4 - T_0^4) \\
Q_2 &= K_{23} (T_3 - T_2) + R_{23} (T_3^4 - T_2^4) \\
&\quad - K_{12} (T_2 - T_1) - R_{12} (T_2^4 - T_1^4) \\
Q_3 &= K_{34} (T_4 - T_3) + R_{34} (T_4^4 - T_3^4) \\
&\quad - K_{23} (T_3 - T_2) - R_{23} (T_3^4 - T_2^4)
\end{aligned}$$

The above equations for Q_0 , Q_1 , Q_2 , and Q_3 may be combined with those given before for the energy gained by the vapor.

Four equations result in which the quantities T_0 , T_1 , T_2 , T_3 , T_4 and \dot{m} appear as unknowns, assuming the conductivity coefficients, radiation coefficients, specific heat and heat of vaporization are known. Clearly there are more unknowns than equations. If two of the unknowns are specified, the system may then have a unique solution.

For application to the IRT experiment, the dewar variables to be specified would be the value of T_4 , T_0 , and a certain fraction of the total mass flow which is devoted to the dewar shields. The remaining mass flow is sent to the cryostat which will have a set of equations similar to the above but without the heat of vaporization term.

2. Thermal Performance Prediction

The necessary equations were developed which will be employed to predict the thermal performance of the IRT. The equations are heat balance relationships for each heat station in the system. For example, for the i heat station which has a temperature T_i , the heat balance is

$$\dot{m}_k C_p (T_i - T_{i-1}) = k_j (T_j - T_i) + R_j (T_j^4 - T_i^4)$$

where \dot{m}_k is the flow rate (\dot{m}_1 = dewar flow rate, \dot{m}_2 = cryostat flow rate),

C_p is the specific heat of the helium, k_j is the coefficient for heat conduction between the j heat station at a temperature T_j , and R_j is a coefficient for the radiative heat transfer from the j heat station.

The heat station is seen to be modeled so that the gas which enters the heat exchanger from the previous heat station at temperature T_{i-1} is warmed to the temperature T_i . The heat required to warm the gas is equal to that supplied by the conduction and radiation terms. The equations are written using the convention that the repeated subscript implies the summation. Thus, the equations are designed to simulate conductive and radiative paths to heat stations that are not necessarily the nearest.

The heat balance for the liquid container has the left hand side replaced by $\dot{m}_k L$ where L is the latent heat of vaporization.

The equations which result from the above are clearly non-linear which requires that iterative solution procedures be employed. A Newton-Raphson type method is to be employed which is given by

$$J_{\alpha\beta}^{(n)} \Delta Y_{\alpha}^{(n+1)} = -f_{\beta}^{(n)}$$

where $f_{\beta}^{(n)}$ are the residuals of the equations to be solved, $\Delta Y_{\alpha}^{(n+1)}$ is the correction to the unknown Y_{α} at the $n+1$ iterative step, and $J_{\alpha\beta}^{(n)}$ is the Jacobian given by

$$J_{\alpha\beta}^{(n)} = \frac{\partial f_{\beta}^{(n)}}{\partial Y_{\alpha}}$$

where the superscript (n) means that the information available at the n iterative step is used in the evaluation.

3. Heat Exchanger Design Considerations

The IRT experiment employs a number of heat exchangers in the cryogenic system. Typically, cold helium gas enters a tube which is in good thermal contact with a surface which is to be cooled. The gas picks up the heat resulting in a gain of energy of the gas. The gas, being a compressible fluid in motion, reacts with increases in temperature, pressure, and velocity. Thus, heat transfer is strongly coupled to the fluid mechanics of the helium coolant and the entire gas system of the IRT experiment.

The mechanisms of friction and heat transfer are basically the same so that pressure drop and heat transfer become closely coupled in a fluid system. This is illustrated by the following equation¹

$$dM^2 = F_{T_o} \frac{dT_o}{T_o} + F_f 4f \frac{dx}{D}$$

which relates the change in flow Mach number to the change in total temperature of the gas and the effect of friction over the distance dx . The values of F_{T_o} and F_f are given as a function of the local Mach number (see Ref. 1). Since previous reports have treated the effect of friction on the gas flow, this report will consider the effect of heat transfer.

Considering the case of constant wall temperature T_w , the equation which gives the temperature of the gas as a function of position x along the tube is given by

¹Shapiro, A. H., Compressible Fluid Flow, Vol. I, page 243.

$$T_o(x) = T_w - (T_w - T_{o_1}) e^{-2 f \frac{L}{D} \left(\frac{x}{L}\right)}$$

where T_{o_1} is the entering gas temperature, f is the friction factor, L is the characteristic length and D is the hydraulic diameter of the tube. The friction factor f has been described in previous reports and is a function of Reynolds number. For the case of laminar flow,

$$f = \frac{16}{R_e} = \frac{16\mu}{\rho V D}$$

Consider, as an example, the case of $\frac{1}{2}$ " ID tube with a wall temperature of $3K = T_w$, an inlet temperature of $2K = T_{o_1}$, a flow rate of 1000 scc/min, and take $L = 1m$. The following table is constructed for these conditions.

$T_o(x), ^\circ K$	x/L
2.44	.1
2.69	.2
2.94	.5
2.997	1

The results show that the gas temperature approaches the temperature of the wall in a distance of about 1 meter for the conditions given. The pressure drop for the above example was calculated to be of the order of 1×10^{-4} torr over the 1 meter length.

XI. Results and Conclusions

The major results and conclusions of this effort have been adequately reported in the open literature and through drawings which can be obtained from MSFC.

The first major paper concerning this effort was given at the 7th ICEC in 1978. This paper is included as Appendix A. In 1979 we reported on the early design of the IRT at a SPIE Conference. This paper is included as Appendix B.

In 1980 we reported on the cryostat thermal testing at the 8th ICEC. This paper is included as Appendix C. In 1982 we reported on the thermal testing of the dewar at the 9th ICEC. This paper is included as Appendix D. In 1983 we reported on the thermal testing of complete IRT system. This paper is included as Appendix E. In 1984, two papers were given which concluded the reporting by the UAH group. One paper was a report on the Transfer Assembly design and performance and the second was a report on the overall performance of the IRT. These papers are included as Appendix F and G respectively.

A CRYOGENIC HELIUM II SYSTEM FOR SPACELAB

APPENDIX A

E. W. Urban and L. Katz

J. B. Hendricks and G. R. Karr

NASA/MSFC, Huntsville, Alabama, USA

University of Alabama in Huntsville, USA

The large number of missions planned for Spacelab aboard the Space Shuttle Orbiter will provide many opportunities for experiments on cryogenic fluid properties or space science experiments requiring cooling of apparatus to cryogenic temperatures. The total cryogenic lifetime is only required to be a few weeks. We are developing such a helium II system to refrigerate a scanning infrared telescope experiment for the Spacelab 2 mission in early 1981. A 250 liter dewar will store adequate liquid for pre-launch and on-orbit operations. The versatile cryogen control and delivery system will be able to cool other types of experiments on later missions. This paper describes the special problems we have had to address and the resulting technical approach to the system.

INTRODUCTION

We are developing a helium II storage and gas delivery system to provide refrigeration to a scanning infrared telescope (IRT) experiment which will be flown in space in 1981 aboard the Spacelab 2 mission. Instead of submerging the infrared apparatus within a large, specially constructed helium dewar, which has been the usual approach to space cryogenics, we have elected to separate the cooled infrared optical system from the storage dewar. This decision resulted from a number of factors, partly technical and partly economic, and has led to a number of new technical problems, as well as a cryogenic supply system which will be able to deliver gaseous or liquid helium cooling to other types of experiments on later Spacelab missions.

Some of the factors which influenced our approach included: (1) several specific requirements of the infrared experiment itself; (2) very limited time (2½ years) for design, development and delivery of the complete experiment for flight; (3) limited funding; (4) a relaxed, higher risk approach to Spacelab experiment qualification and reliability, except where it affects crew and Shuttle safety; (5) the availability of some hardware design, fabrication, and testing support from the NASA Marshall Space Flight Center; and (6) experience within our own team on helium II systems for ground and space applications.

EXPERIMENT SYSTEM

The IRT experiment is shown schematically in Figs. 1 and 2. It consists of five major subsystems: (1) a dewar subsystem, which includes a 250 liter liquid helium dewar, a transfer assembly (TA) containing the porous plug flow control and fill and vent plumbing; (2) a cryostat subsystem, which includes a gas-cooled, evacuated vessel, a vacuum cover and a sunshade, and which contains; (3) the infrared telescope itself consisting of an upper baffle section, and a lower section with baffles, mirror, and detector array; (4) a mechanical subsystem including scan drive components, warm plumbing and valves, and a support structure which interfaces with the Spacelab pallet; and (5) an electronic subsystem to control all infrared science and electro-mechanical activities and to interface with the Spacelab power, data and command systems.

An important infrared science goal is to generate a map of faint diffuse infrared objects over a large area of the sky in several wavelength bands out to 120 μm . Therefore the infrared detectors must be cooled to about 3K, the two telescope sections must be cooled to 8K and 60K respectively, and the entire cold optical system must be scanned.

The experiment will be mounted toward the aft end of the Space Shuttle Orbiter payload bay. In its latched position the cryostat/telescope will point directly out of the bay (+ Z axis) and the scan drive motor will be oriented forward. The telescope consists of a highly baffled Herschelian system with an off-axis parabolic 15 cm-diameter, f/4 primary mirror, and a detector array positioned on the scan axis. The 3° field-of-view telescope will be scanned back and forth perpendicular to the direction of flight at a rate of $6^\circ/\text{second}$, generating 3° wide maps which extend over 90° centered on the + Z axis. With a Shuttle orbital motion of $4^\circ/\text{minute}$ each map band overlaps its neighbors by 67%.

We were concerned about two problems which could arise if we attempted to rapidly scan a large liquid helium dewar containing the telescope. First, there was a potential vibrational interaction between the very sensitive infrared detectors and the liquid helium which would be disturbed every 15 seconds at each end of the scan by an unknown amount and for an indefinite time. Second, electrical power and particularly total energy are quite limited on the SL-2 mission and we wished to minimize the moment of inertia of the scanning part of the apparatus. Rotating only the gas cooled cryostat and telescope will permit the use of a reasonably sized scanning motor and allow rapid (1.5 second) scan reversals without consuming excessive power.

Dewar

Having decided to separate the experiment from the storage dewar, we first addressed the dewar design. We will employ a modified conventional storage dewar similar to the type used to transport liquid helium by ground or air freight for laboratory supply. This will insure the availability of a well established fabrication technology in several potential vendors, including basically rugged design, good thermal efficiency, and, hopefully, a considerably lower cost than for a special aerospace type dewar design. For reasons to be discussed below we have chosen a 250 liter dewar. It will be loaded and topped-off before launch with superfluid helium at a nominal temperature of 1.6K and vapor pressure of 6 torr.

Modifications are required chiefly in the dewar neck tube to permit fluid control and to mate with the transfer assembly (TA). The neck tube is closed at the bottom to prevent liquid helium from flowing into it in the low gravity orbital environment. Fill and outlet tubes pass into the liquid vessel from the TA. A third tube returns cold helium gas from the porous plug in the TA to the base of the neck tube to provide the essential cooling to the dewar thermal shield heat exchanger. The dewar gas vents at the top of the neck tube at ambient temperature as in a standard dewar.

To insure good thermal efficiency three nested vapor cooled shields will be used in the TA. The heat they intercept will also be delivered to the dewar neck tube heat exchange gas. The dewar neck tube diameter will be somewhat greater than that of a standard dewar in order to provide space for the three helium tubes and the three TA shield terminations. Delivering the TA heat to the dewar neck tube heat exchanger has the effect of increasing the surface area of the dewar heat shield system by about 60%, thus increasing the steady state boiloff rate by the same factor.

Transfer Assembly

We will build up the transfer assembly onto the dewar after its delivery. In addition to the heat shields mentioned above, the TA contains several essential components which operate at helium temperature. The porous plug, discussed later, is the

primary helium flow control device. A manual fill valve prevents liquid helium from flowing to the warm end of the fill line. A manual bypass valve in parallel with the porous plug permits high gas flows during dewar fill and pumpdown. Both valves are Nupro bellows sealed valves modified for superfluid service, and both have retractable stem operators to reduce heat leak.

Helium (liquid or vapor) leaving the dewar through the outlet tube flows to the upstream side of the porous plug. Cold helium gas drawn from the downstream side of the plug is divided into two vent flow paths, one returning gas to the dewar neck heat exchanger, and the second delivering refrigeration to the cryostat and the infrared telescope. Division of the flow between the two vents is controlled by external warm valves.

The connection between the stationary TA and the scanning cryostat/telescope must satisfy two important functions. First, it must maintain the high vacuum integrity of the interior of the TA and cryostat whenever atmospheric pressure exists around the apparatus, including tests on the ground and the first few minutes of the Shuttle launch. We will employ a commercially available rotary high-vacuum seal with magnetically retained sealing fluid. Second, the cryostat gas delivery tube must cross over within the internal vacuum. A small diameter helical tube with a low spring constant within the TA takes up the rotation. A relatively short section of the gas tube passes through the fluid-sealed rotary joint and is not protected within the thermal shields of the TA.

Pressure relief of the dewar if accidental overpressurization should occur has been of great concern in the design of this cryogenic system, since manual valves will usually be inaccessible and the Spacelab command and data system will not be activated until several hours after launch. We will mount two enclosed burst diaphragms within the TA. One will be in parallel with the cold fill valve and the second in parallel with the porous plug assembly and its bypass valve. Any leakage through the fill line burst diaphragm will be contained within the fill tube and will at worst cause increased gas conduction heat leak from the warm end of the fill tube. Leakage through the bypass burst diaphragm will be in parallel with the porous plug and therefore will probably be negligible. The plug requires a bypass relief in the event that it becomes clogged by debris and cannot vent normally. Venting of the burst diaphragms is provided by external relief valves.

Dewar Subsystem

The dewar and transfer assembly together comprise the dewar subsystem, which is almost a stand-alone cryogenic system for space. All that would be required to make the subsystem fully independent is a vacuum termination in place of the rotary seal. We will, in fact, test the dewar subsystem as an independent unit by use of a "cryostat substitute," while the cryostat subsystem is being separately assembled and tested. This parallel development of the two cryogenic subsystems is necessitated by the short development time available to us, but our testing method points out the potential of the dewar subsystem to deliver cooling to other types of experiments.

Cryostat

The cryostat will be a rather special modification of an open neck laboratory dewar. The essential special features include mounting flanges for the two sections of the infrared telescope, an access port for telescope alignment, a side extension on the cryostat rotation axis through which the cold gas from the TA enters, and a gas heat exchanger tube within the thermal shield system. A vacuum cover insures that a high vacuum can be maintained within the cryostat and telescope. The cold gas from the TA is first delivered to a cold finger, designed to maintain a temperature of about 3K, to which the IR detector block will be clamped, and then to the heat shield system. The lower and upper telescope sections are designed to operate at maximum temperatures of 8K and 60K, respectively. They will be cooled by conduction to their mounting flanges. The two telescope mount flange

to be maintained. If less gas is returned to the neck tube, the boiloff rate will increase, decreasing storage lifetime and producing an excess of cold gas for use in the cryostat. We have estimated that a cold gas input to the cryostat of 2.5 mg/s will be required to achieve the previously stated operating temperatures. This represents an additional boiloff rate of 1.5 l/day. Total boiloff rate will thus be about 5.5 l/day.

Adjustment of dewar and cryostat vent flows will be possible during the mission by means of warm valves in the respective vent lines when measured temperature, pressures and flow rates indicate the need. The system, and particularly the telescope and liquid helium temperatures will respond rather slowly to changes in these valve settings. We anticipate the occasional need to rapidly deliver additional cooling to the cryostat as, for example, when closure of the vacuum cover induces a burst of heat onto the cold optics. This rapid delivery of extra cooling can be achieved by small heaters on the porous plug, as described below.

Porous Plug

The use of a porous material as a superfluid helium flow control device is discussed in detail elsewhere. [1, 2, 3] Briefly, superfluid helium attempts to flow through the very small plug pores driven by the vapor pressure within the liquid vessel. Evaporation on the vent line (downstream) side causes cooling and a small temperature gradient across the plug. This results in a thermomechanical or fountain pressure gradient directed upstream, which restrains fluid flow. The cooling due to evaporation is communicated back to the fluid bath by the high thermal conductivity of the liquid in the pores.

When superfluid helium is in contact with the upstream side of the plug, as when the IR experiment is either horizontal (Orbiter vertical) or in low gravity, the evaporation takes place at the downstream plug surface, and helium flows through the plug as relatively high density liquid. When the experiment is vertical (Orbiter or Spacelab horizontal), the liquid free surface at which evaporation takes place will be within the dewar. The porous plug will be required to pass the same mass flow rate, but in the form of lower density cold gas. The plug surface area must be chosen large enough to permit the gas flow with an acceptably low pressure drop. We will probably select a plug with 5-10 μm diameter pores, and an estimated surface area of about 35 cm^2 .

In order to permit a rapid increase in cold fluid flow to the cryostat to counter an increased thermal load on the telescope, we mount a small heater on the downstream side of the porous plug. Heat at this location will reduce or reverse the fountain pressure, permit increased gas evolution or even liquid withdrawal, and slowly heat the main bath. When the heat is removed the system will return toward the original state.

Prelaunch Cryogenic Support Functions

Cryogenic servicing of the IRT experiment before launch presents a number of unusual and challenging requirements which are shared with a second Spacelab 2 experiment whose objective is to measure certain properties of superfluid helium in low gravity. We will coordinate our ground servicing functions and apparatus with the superfluid physics experiment. Spacelab 2 will be fully assembled into a single structural entity in the Operations and Checkout (O&C) facility at Kennedy Space Center. During the O&C operations we will evacuate, purge and initially fill the experiment with LHe at 4.2K by means of conventional ground support equipment (GSE). Late in the O&C cycle (at about 15 days before launch) the helium will be converted to superfluid by pumping through the vent lines with a large GSE pump. From this time on until the flight mission is completed the superfluid must be maintained at a pressure below 38 torr, by active pumping. If pumping is stopped, as when pump power is interrupted, the superfluid will rapidly warm. We have estimated that pumping can be stopped once for about 4 hours duration or for a number of shorter periods, before the helium will warm to the lambda temperature

and the porous plug will no longer operate properly. We are providing at the vent tube outlet of the experiment a direct drive rotary vane vacuum pump. During pre-launch operations the pump will operate as continuously as possible. On orbit the experiment will, of course, be pumped by the vacuum of space.

When the O&C assembly and tests are completed, the Spacelab 2 payload will be transported in a special enclosed carrier to the Orbiter Processing Facility (OPF) where it will be installed into the Orbiter vehicle. Throughout these operations electrical power must be provided for the on-board vacuum pump by an auxiliary power cable and power supply. The experiment will be connected to two special Orbiter services: (1) a 28 VDC electrical connection for the pump via the aft T-O umbilical plug which disconnects at launch; and (2) a vent pipe which conducts the venting helium overboard through a midbody panel. Even in space, pumping will be via this pipe to prevent the helium from disturbing any of the astronomical instruments. The vent pipe will be shared with the superfluid physics experiment.

In the OPF at about ten days before launch we will top-off the dewar with superfluid. When Orbiter checkout is completed, the payload bay doors will be closed, and the Orbiter will be moved to the Vehicle Assembly Building. There it will be rotated nose up and mated to the External Tank and two Solid Rocket Boosters of the launch platform. The ground side of the T-O umbilical connection will then be attached to the Orbiter. Through most of these activities DC power is to be maintained and the pump will operate. Only during power changeover, while the Orbiter is being rotated to the vertical, and while explosive devices are being installed, must the pump be turned off.

The Orbiter will be rolled to the launch pad, again with the pump powered through the T-O umbilical and vented through the midbody umbilical panel. On the launch pad the pump and valve operation is controlled from the launch control center. A few minutes before launch the vacuum pump will be stopped, isolated, and not used again. When the Orbiter reaches an altitude at which the atmospheric pressure is below five torr, a barostatic switch will open a valve between the experiment vent tube and the overboard vent. This will permit pumping on the superfluid to resume several hours before the Spacelab is activated.

We will monitor and control the cryogenics during the mission from the ground in the Spacelab Payload Operations Control Center (POCC). Emergency monitoring and control will also be possible by the on-board Payload Specialist (scientist). Shortly before landing the experiment will be stowed, the vacuum cover sealed, and the vent valves closed. Relief valves on the vent lines will permit the experiment to warm up safely and untended.

CONCLUSION

The cryogenic system for the Spacelab 2 Infrared Telescope Experiment has been designed to fit within the many technical and programmatic constraints and capabilities of the Spacelab program. The result is a system which will satisfy the cooling requirements of the IRT and also be capable of furnishing cooling to a variety of follow on Spacelab experiments.

REFERENCES

- 1 Selzer, P.M. et al 'A Superfluid Plug for Space.' Adv. Cryo. Eng., vol. 16 (1971), pp. 277-281.
- 2 Urban, E.W. et al 'Helium II Flow Through and Vapor Separation by Porous Plugs.' Proc. 14th Internat. Conf. Low Temp. Physics, vol. 4 (1975), pp. 37-40.
- 3 Karr, G.R. and Urban, E. 'Super Fluid Plug as a Control Device for Helium Coolant.' 71st Annual Meeting, American Institute of Chemical Engineers, Miami, Florida, November 12-16, 1978.

ORIGINAL DRAWING IS
OF POOR QUALITY

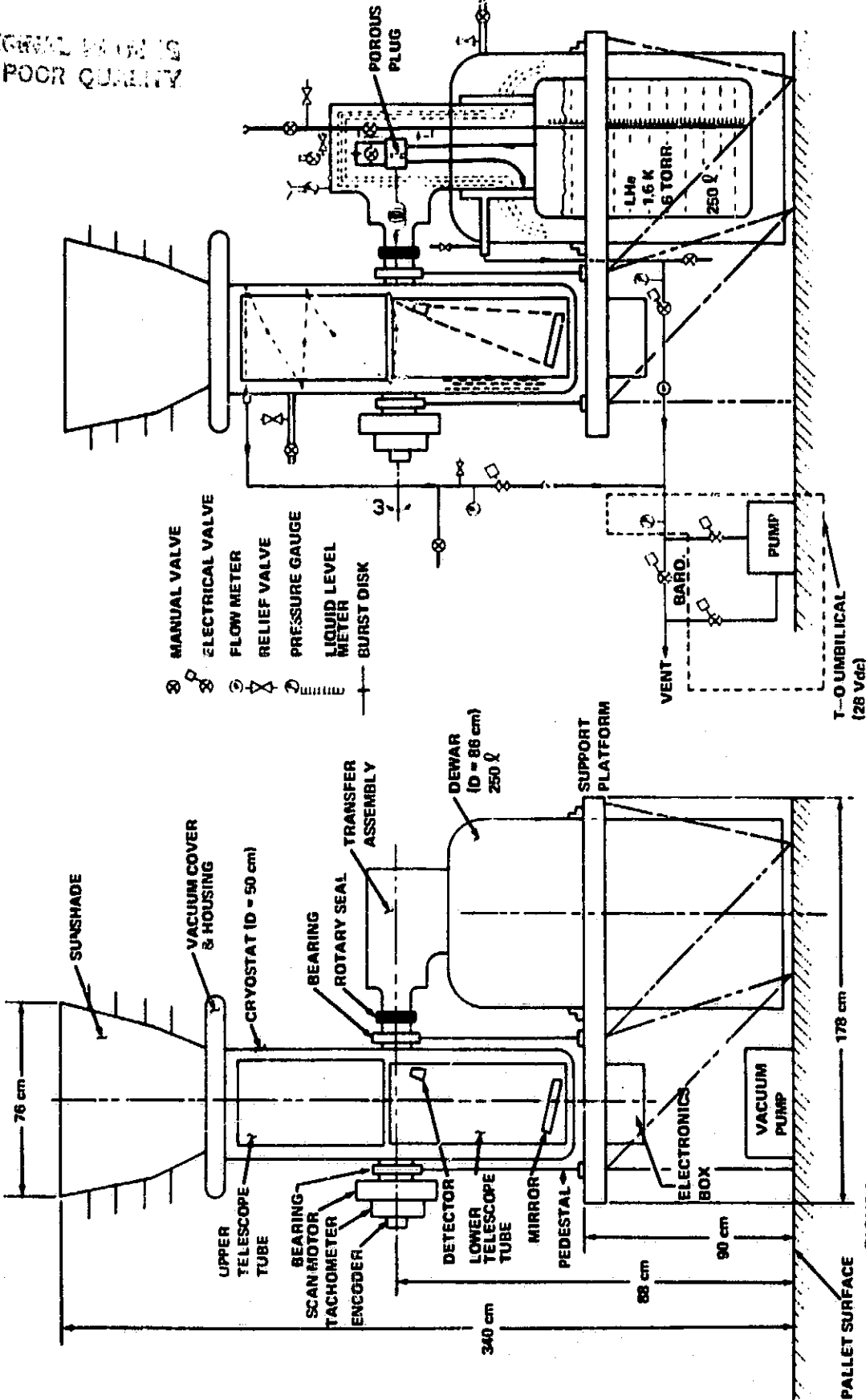


FIGURE 2. IRT PLUMBING SCHEMATIC

FIGURE 1. IRT SYSTEM OVERALL LAYOUT

Spacelab 2 infrared telescope cryogenic systemE. W. Urban and L. Ketz
NASA/MSFC (Huntsville, AL)J. B. Hendricks and G. R. Kerr
University of Alabama in HuntsvilleAbstract

We are developing a cryogenic helium system to provide cooling to a scanning infrared telescope for the Spacelab 2 mission in 1982. The infrared optical/detector system and related electronics are being developed by the Smithsonian Astrophysical Observatory and the University of Arizona. A superfluid helium dewar and porous plug phase separator permit gas cooling of the infrared focal plane assembly to about 2.5K, and of the two telescope sections to 8K and 60K respectively. In this paper the design of the cryogenic system, including a commandable vacuum cover, and the prelaunch liquid helium servicing and maintenance approach will be discussed. The system can be readily adapted to other types of cryogenic experiments on later Spacelab missions.

Introduction

The Infrared Telescope (IRT) Experiment to be flown on Spacelab 2 in early 1982 is a joint project of the Smithsonian Astrophysical Observatory (SAO), the University of Arizona (UA), and the NASA Marshall Space Flight Center (MSFC). Our responsibility at MSFC is the development of the cryogenic and mechanical systems of the IRT. The University of Alabama in Huntsville is collaborating on the cryogenic design, fabrication of special cryogenic apparatus, and cryogenic performance testing. UA and SAO are responsible for the infrared instrument and data analysis. The NASA Ames Research Center is collaborating in the analysis of contamination and zodiacal light data. This paper describes the cryogenic apparatus, its control and operation, and prelaunch cryogenic support activities at the launch site. The infrared instrument is described in another paper in this conference (183-03).

Experiment System

The IRT experiment is shown schematically in Figure 1. It consists of four major subsystems; (1) a dewar subsystem, which includes a 250 liter liquid helium dewar, and a transfer assembly (TA) containing the porous plug, flow control and fill and vent plumbing; (2) a cryostat subsystem, which includes a gas-cooled, evacuated cryostat, a vacuum cover and a sunshade, which contains the infrared telescope and detector array; (3) a mechanical subsystem including scan drive components, plumbing, valves, control instrumentation and a support structure which interfaces with the Spacelab pallet; and (4) an electronic subsystem (not shown) to control all infrared science and electro-mechanical activities and to interface with the Spacelab power, data and command systems.

The IRT will be mounted toward the aft end of the Space Shuttle Orbiter payload bay on a Spacelab pallet. The top of the sunshade will be 3.4 m above the pallet floor; the experiment is 2.0 m long and 0.4 m wide. The total mass of the experiment at liftoff will be 690 kg, including liquid helium and separately mounted electronics boxes. In its latched position the cryostat and sunshade will point directly out of the bay; the scan drive motor will be oriented forward.

On orbit when the external environment is suitable (low contamination, and sun, moon and earth out of view), the vacuum cover will be opened and the cryostat scanned from side to side (145°) at an angular rate of 6°/second to generate an infrared map of the sky. The primary function of the cryogenic system is to provide adequate continuous cooling to the infrared instrument within the cryostat to permit the scientific observations to be made during the planned 9 day mission. A secondary objective is to obtain data on the performance of the large superfluid helium storage system in space.

The requirement to scan the infrared telescope resulted in the choice of a helium gas-cooled cryostat which could move about one axis independently of the fixed liquid helium storage dewar. The limited funding available and the short flight mission time led us to adapt commercially available helium apparatus and fabrication techniques to this new application, rather than develop a high performance and high cost system with long storage time. The lack of firm information on prelaunch ground hold time and our inability to predict actual cryogenic system performance early in the program, dictated the selection of a 250 liter liquid helium dewar. In the following we describe in detail the Dewar Subsystem, the Cryostat, the plumbing and control, and the prelaunch ground servicing operations.

SPACELAB 2 INFRARED TELESCOPE CRYOGENIC SYSTEM

Dewar Subsystem

The superfluid liquid helium (LHe) dewar subsystem shown schematically in Figure 2 consists of two major parts - the 250 liter storage Dewar and the Transfer Assembly (TA). The dewar is to be fabricated by a commercial vendor to our designs, after which the TA will be assembled into it at MSFC. The closely integrated thermal design of the dewar and TA results in a dewar subsystem which is essentially a single complex superfluid helium dewar with the liquid containment vessel at one end of a neck structure and a number of cold flow control components at the other; all are surrounded by a common thermal protection system, discussed below.

Dewar

In a conventional storage dewar the liquid vessel is surrounded by a system of nested metal surfaces, separated by superinsulation and mounted within a high vacuum space. They serve to intercept heat being radiated and conducted in toward the cold liquid from the outer shell. The intercepted heat is then conducted up to the dewar neck where it warms the venting helium gas and is carried out of the dewar by the gas. Thus the metal surfaces act as vapor cooled shields (VCS), and the dewar neck is a heat exchanger as well as a support structure. The source of the venting gas in the neck is the slow evaporation of the stored liquid by the unavoidable parasitic heat conducted down the neck tube and radiated in from the coldest VCS. A typical unmodified conventional 250 liter dewar achieves a steady state boiloff rate of 1% per day or 2.5 liters of liquid per day corresponding to a heat input to the liquid of 75 mW.

In order to retain the stored LHe in space, it is necessary to close off the dewar neck at the liquid vessel entrance. Liquid is filled and withdrawn through tubes which pass down the neck from the TA, and valving and flow control is accomplished by the cold components in the TA. These components must also be insulated from the outside world by a VCS system. We have chosen to connect the dewar and TA VCS systems together within the flight dewar neck, thus complicating the neck design and assembly. As a result the TA and the inside of the dewar neck share a common vacuum. We have avoided the further complication of the heat exchange function of the neck tube by constructing the heat exchanger in the TA. Thus the dewar provided by the vendor will have a structural neck supporting the closed liquid vessel; the liquid fill and withdrawal tubes; and three concentric VCS extension tubes within the neck. These components can be seen in Figure 2.

During prelaunch activities the dewar will be filled with superfluid helium at a temperature of about 1.6K and a vapor pressure of 800 N/m² (6 torr). At a density of 0.145 kg/liter a full dewar will contain about 35 kg of liquid. We hope to launch with at least 100 liters (14.5 kg) of liquid.

Transfer Assembly

After the dewar is delivered the TA will be built up onto it. The internal components will operate in space at the liquid helium temperature (1.6K). A cold fill valve prevents liquid helium from flowing out the fill line to the warm outer shell when the experiment is in space. A bypass burst disk permits controlled venting through the fill line in the event of accidental overpressurization. In space, liquid flows into the TA through the withdrawal line and is restrained by the porous plug. The principle and operation of porous plugs, which are essentially liquid/vapor phase separators for superfluid helium, are described elsewhere. In the event of plug blockage and overpressurization a second bypass burst disk provides relief to the vent lines. When a dewar is being initially filled or when normal helium (4.2K, 1 atmosphere vapor pressure) is being converted to superfluid, large gas flow rates must be vented. A bypass valve is provided in parallel with the porous plug to permit high flow rates and avoid possible contamination of the plug pores.

The cold fill and bypass valves are operated by vacuum-tight, retractable operator shafts having low thermal conductivity and low thermal mass. When retracted, the operator shafts will become warm. When inserted into the valves they will introduce pulses of heat into the cold environment. To minimize this problem the valves will be opened at the beginning of cryogenic operations and will not be closed except when the dewar subsystem must be turned on its side (launch attitude) for testing or just before the actual launch.

The cold helium vapor evaporates from the porous plug at about 1.6K and is divided into two vent lines. The first line forms the heat exchanger which removes heat from the VCS system of the entire dewar subsystem. The second line delivers refrigeration to the cryostat and the infrared telescope. The division of flow in the two lines is controlled by external valves which will be discussed below.

The vapor in the dewar vent line flows first to the innermost VCS which will operate at a goal temperature of about 20K. We anticipate a total heat load on this shield of about 770 mW.

URBAN, KATZ, HINDRICKS, KAHL

The gas will then pass successively to the middle VCS at a temperature of roughly 60K and heat load of about 1.7W, then to the outer VCS at approximately 120K and 2.6W, and finally out of the TA. The cold helium gas flow rate to remove these expected heat loads at the goal temperatures is 8.4×10^{-3} g/s or 5.0 liter/day corresponding to a net heat input to the 1.6K region of the dewar subsystem of 150 mW. The actual steady state temperatures and heat loads will undoubtedly be somewhat different from the goal values mentioned above. The chief concern is, of course, that the system boiloff rate be low enough that the experiment gets to orbit with enough liquid to permit cooling and operation of the infrared telescope.

The dewar is filled with liquid helium, and high flow rates of cold gas are vented through vacuum jacketed bayonets and valves on the TA shell. When the filling and superfluid conversion operations have been completed, special inserts with relief valves will be fastened into the two bayonets. The jacketed valves will then be opened, providing a relief path for the two cold burst disks. The steady state (low flow) venting is via an unjacketed line to one set of flow control valves.

The second vent line from the porous plug will deliver cold helium gas to the cryostat. Both the gas line and the outer shell of the apparatus must permit the rotation of the cryostat, and the outer shell must in addition maintain the high vacuum integrity of the TA and cryostat whenever the atmospheric pressure exists around the apparatus. The gas line is wrapped into a helical coil which flexes easily with the cryostat motion. At the exit from the TA a straight section of the tube passes through a commercially available rotary vacuum seal which employs magnetically retained sealing fluid to maintain the vacuum integrity of the TA and the cryostat. A short section of metal bellows permits minor misalignment of the TA and the cryostat when they are assembled together.

It will be possible and it is our plan to test the dewar subsystem by itself. This will require a special termination on the cryostat gas line and the rotary joint so that the TA and dewar neck can be evacuated. The dewar will be filled with normal liquid helium, the liquid converted to superfluid, and the thermal performance of the system measured with the apparatus both upright and rotated 90° into the launch attitude. It is anticipated that the boiloff rate will be somewhat greater in launch attitude than upright. The performance of the porous plug can only be tested in the complete tipped system, since in the upright position superfluid will not reach the porous plug. This subsystem test will demonstrate the fact that the unit can operate as a stand-alone superfluid dewar which could be employed to cool a variety of experiments on later Spacelab flights. Note that a performance test of the dewar by itself is not practical, since the VCS system is not operative until the TA is fully assembled to the dewar to complete the subsystem.

Cryostat

The cryostat shown schematically in Figure 3 will be a rather special modification of an open neck laboratory dewar. The essential special features include mounting flanges for the two sections of the infrared telescope, an access port for telescope alignment, a side extension on the cryostat rotation axis through which the cold gas from the TA enters, and a gas heat exchanger and VCS system. A vacuum cover insures that a high vacuum can be maintained within the cryostat and telescope before the experiment is in space. The cold gas from the TA is first delivered at a temperature of about 2K to a cold finger, designed to maintain a temperature of about 2.5K, to which the IR detector block will be clamped, and then to the heat shield system. The lower and upper telescope sections are designed to operate at maximum temperatures of 8K and 60K, respectively. They will be cooled by conduction to their mounting flanges. The two telescope mount flange rings, and two additional rings which are at temperatures of approximately 120K and 200K are suspended from the top of the cryostat on fiberglass-epoxy tubes. Each ring carries a VCS and each delivers its collected heat to the cold venting helium gas. The vent tube, after leaving the cold finger, is fastened to the four rings in turn and then exits the cryostat at ambient temperatures.

The heat load on the cold finger at 2.5K will be about 10 mW from the infrared detectors including absorbed radiation, and heat conducted in along the IR signal leads. The estimated 230 mW heat load on the 8K ring will include the heat radiated into the lower telescope tube from the upper telescope tube, heat from the cold infrared electronics, plus the parasitic heat onto the 8K VCS from the warmer parts of the cryostat. The estimated 2 watt heat load on the 60K ring will include heat radiated onto the upper telescope tube from the sunshade, or from the closed vacuum cover, plus the parasitic heat onto the 60K VCS. Finally the heat input to the "120K" and "200K" rings will only be the parasitic heat from the warmer outer parts of the cryostat.

The locations and temperatures of the 8K and 60K mounting/thermal flanges are dictated by the infrared telescope design. The cryostat fabricator will determine the location and actual temperature of the thermal rings of the "120K" and "200K" shields in order to optimize the thermal performance of the cryostat. The tentative helium mass flow rate into the cryostat at 2K will be of the order of 7.5×10^{-3} g/s or 4.4 liters per day. This flow rate can be

varied, as discussed below, to increase or decrease cooling as necessary.

The vacuum cover can be commanded open and closed; it will be quickly closed, but not fully sealed, if gas or particulate contamination levels become too high, if a hot object (sun, moon, earth) accidentally approaches the field of view, or when the experiment is not mapping the sky. Before landing the cover will be sealed. When the cover first closes, the inner cover surface will be at ambient temperature. It will be thermally isolated from the warm outer cover surface and will have a low emissivity and a low thermal inertia. Upon closure the inner surface will cool by radiation into the cryostat and telescope until it reaches some equilibrium temperature, perhaps 150K. Thus the radiative heat load onto the cold optics will be as small and of as short a duration as possible.

The access port is located on the side of the cryostat to permit mounting and alignment of the infrared detector block to the cold finger after the lower telescope section is installed through the top of the cryostat. The access port therefore penetrates all of the thermal shields and multilayer insulation blankets. Up to 100 low-conductivity infrared signal and control leads from the detectors will be brought out of the cryostat through the access port with heat stations at each shield.

Cryogenic Operations

Correct operation of the infrared experiment and achievement of adequate helium storage lifetime is paramount. As discussed above, the cold helium gas evolving from the porous plug refrigerates the dewar/TA heat shields and the cryostat/telescope. The only source of cold gas is vaporization of superfluid liquid by either parasitic or electrically produced heat in the dewar/transfer assembly. For a given rate of heat input and a given pumping rate, the liquid temperature and vapor pressure will come to some equilibrium value. More heat and/or slower pumping results in higher equilibrium temperature and pressure.

We have indicated above that the expected steady state helium boiloff of the dewar subsystem at optimum efficiency will be about 5 liters/day and the flow rate into the cryostat to maintain full cooling is about 4.4 liters per day. Starting with the 250 liter dewar full, the total flow rate of 9.4 liters/day could be maintained for about 26 days; with 200 liters, lifetime would be 21 days. The Spacelab 2 mission duration is planned to be 9 days, thus permitting 17 days and 12 days respectively, from final dewar fill operations until launch with the above initial fill conditions.

We anticipate that it will not be necessary to keep the cryostat fully cooled until the experiment is in space. Consequently, on the ground, gas flow through the cryostat can be somewhat reduced to conserve liquid helium. When the experiment is in space any reasonable extra cooling requirements for the cryostat can be met by reducing vent gas flow in the dewar subsystem. This will increase the heat input to the liquid helium and the boiloff, more of which will be directed to the cryostat. Alternatively, a reduction in refrigeration to the cryostat can be achieved by increasing vent gas flow from the dewar subsystem and reducing flow from the cryostat vent.

This adjustment of dewar and cryostat vent flows will be possible during the mission by operating sets of three commandable warm valves in each of the vent lines as shown in Figure 1. The three on/off valves in each vent are sized with orifices allowing 14%, 29% and 57% of full flow in the vent line. Thus, particular combinations of 0, 14, 29, 43, 57, 71, 86 or 100% of full flow can be selected for each vent line with the setting of three valves. The system, and particularly the telescope and liquid helium temperatures will respond rather slowly to changes in these valve settings. We anticipate the occasional need to rapidly deliver additional cooling to the cryostat as, for example, when closure of the vacuum cover indicates a burst of heat onto the cold optics. This rapid delivery of extra cooling can be achieved by a small heater on the porous plug which makes use of the well-known superfluid helium "fountain-effect."

Porous Plug

The use of a porous material as a superfluid helium flow control device is discussed in detail elsewhere. (1,2,3) Briefly, superfluid helium attempts to flow through the very small plug pores driven by the vapor pressure within the liquid vessel. Evaporation on the vent line (downstream) side causes cooling and a small temperature gradient across the plug. This results in a thermo-mechanical or fountain pressure gradient directed upstream, which restrains fluid flow. The cooling due to evaporation is communicated back to the fluid bath by the high thermal conductivity of the liquid in the pores.

When superfluid helium is in contact with the upstream side of the plug, as when the IR experiment is either horizontal (Orbiter vertical) or in low gravity, the evaporation takes place at the downstream plug surface, and helium flows through the plug as relatively high density liquid. When the experiment is vertical (Orbiter or Spacelab horizontal), the liquid-

free surface at which evaporation takes place will be within the dewar. The porous plug will be required to pass the same mass flow rate, but in the form of lower density cold gas. The plug surface area must be chosen large enough to permit the gas flow with an acceptably low pressure drop. We will select a plug with 5-10 μ m diameter pores, and an estimated surface area of about 35 cm².

Prelaunch Cryogenic Support Functions

Cryogenic servicing of the IRT experiment before launch presents a number of unusual and challenging requirements which are shared with a second Spacelab 2 experiment whose objective is to measure certain properties of superfluid helium in low gravity. We will coordinate our ground servicing functions and apparatus with the superfluid physics experiment. Spacelab 2 will be fully assembled into a single structural entity in the Operations and Checkout (O&C) Facility at Kennedy Space Center. During the O&C operations we will evacuate, purge and initially fill the experiment with He at 4.2K by means of conventional ground support equipment (GSE). Late in the O&C cycle (at about 15 days before launch) the helium will be converted to superfluid by pumping through the vent lines with a large GSE pump. From this time on until the flight mission is completed the superfluid must be maintained at a pressure below 38 torr, by active pumping. If pumping is stopped, as when pump power is interrupted, the superfluid will rapidly warm. We have estimated that pumping can be stopped once for about 4 hours duration or for a number of shorter periods, before the helium will warm to the lambda temperature and the porous plug will no longer operate properly. A direct drive rotary vane vacuum pump will be provided at the vent tube outlet of the experiment. During prelaunch operations the pump will operate with as few interruptions as possible. On orbit the experiment will, of course, be pumped by the vacuum of space.

When the O&C assembly and tests are completed, the Spacelab 2 payload will be transported in a special enclosed carrier to the Orbiter Processing Facility (OPF) where it will be installed into the Orbiter vehicle. Throughout these operations electrical power must be provided for the on-board vacuum pump by an auxiliary power cable and power supply. The experiment will be connected to two special Orbiter services: (1) a 115 VAC electrical connection for the pump via the aft T-0 umbilical plug which disconnects at launch; and (2) a vent pipe which conducts the venting helium overboard through a midbody panel. Even in space, pumping will be via this pipe to prevent the helium from disturbing any of the astronomical instruments. The vent pipe will be shared with the superfluid physics experiment.

In the OPF at about ten days before launch we will top-off the dewar with superfluid. When Orbiter checkout is completed, the payload bay doors will be closed, and the Orbiter will be moved to the Vehicle Assembly Building. There it will be rotated nose up and mated to the External Tank and two Solid Rocket Boosters on the launch platform. The ground side of the T-0 umbilical connection will then be attached to the Orbiter. Through most of these activities AC power is to be maintained and the pump will operate. Only during power change-over, while the Orbiter is being rotated to the vertical, and while explosive devices are being installed must the pump be turned off.

The Orbiter will be rolled to the launch pad, again with the pump powered through the T-0 umbilical and vented through the midbody umbilical panel. On the launch pad the pump and valve operation is controlled from the launch control center. A few minutes before launch the vacuum pump will be stopped, isolated by valves, and not used again. When the Orbiter reaches an altitude at which the atmospheric pressure is below five torr, a barostatic switch will open a valve between the experiment vent tube and the overboard vent. This will permit pumping on the superfluid to resume several hours before the Spacelab is activated.

We will monitor and control the cryogenics during the mission from the ground in the Spacelab Payload Operations Control Center (POCC). Emergency monitoring and control will also be possible by the on-board Payload Specialists (scientists). Shortly before loading, the experiment will be stowed, the vacuum cover sealed, and the vent valves closed. The relief valves on the vent lines will permit the experiment to warm up safely and unattended.

Conclusion

The cryogenic system for the Spacelab 2 Infrared Telescope Experiment has been designed as a low-cost approach to the storage of liquid helium during the preparation of a Spacelab payload for launch and the supply of adequate cooling to a separate Infrared Telescope for the duration of a typical Spacelab mission. The result is a system which will satisfy the requirements of the IRT and also be capable of furnishing cooling to a variety of follow-on Spacelab experiments. It is expected that as the Spacelab and Space Transportation System flight program matures, flight durations will increase and prelaunch preparation times will decrease. The superfluid helium system described herein should be capable of satisfying experiment helium cooled refrigeration requirements for the next several years.

References

1. Seltzer, P.M. et al "A Superfluid Plug for Space." *Adv. Cryo. Eng.*, vol. 16 (1971), pp. 277-281.
2. Urban, E.W. et al "Helium II Flow Through and Vapor Separation by Porous Plugs." *Proc. 14th Internat. Conf. Low Temp. Physics*, vol. 4 (1975), pp. 37-40.
3. Karr, G.R. and Urban, E. "Super Fluid Plug as a Control Device for Helium Coolant " 71st Annual Meeting American Institute of Chemical Engineers, Miami, Florida, November 12-16, 1978.

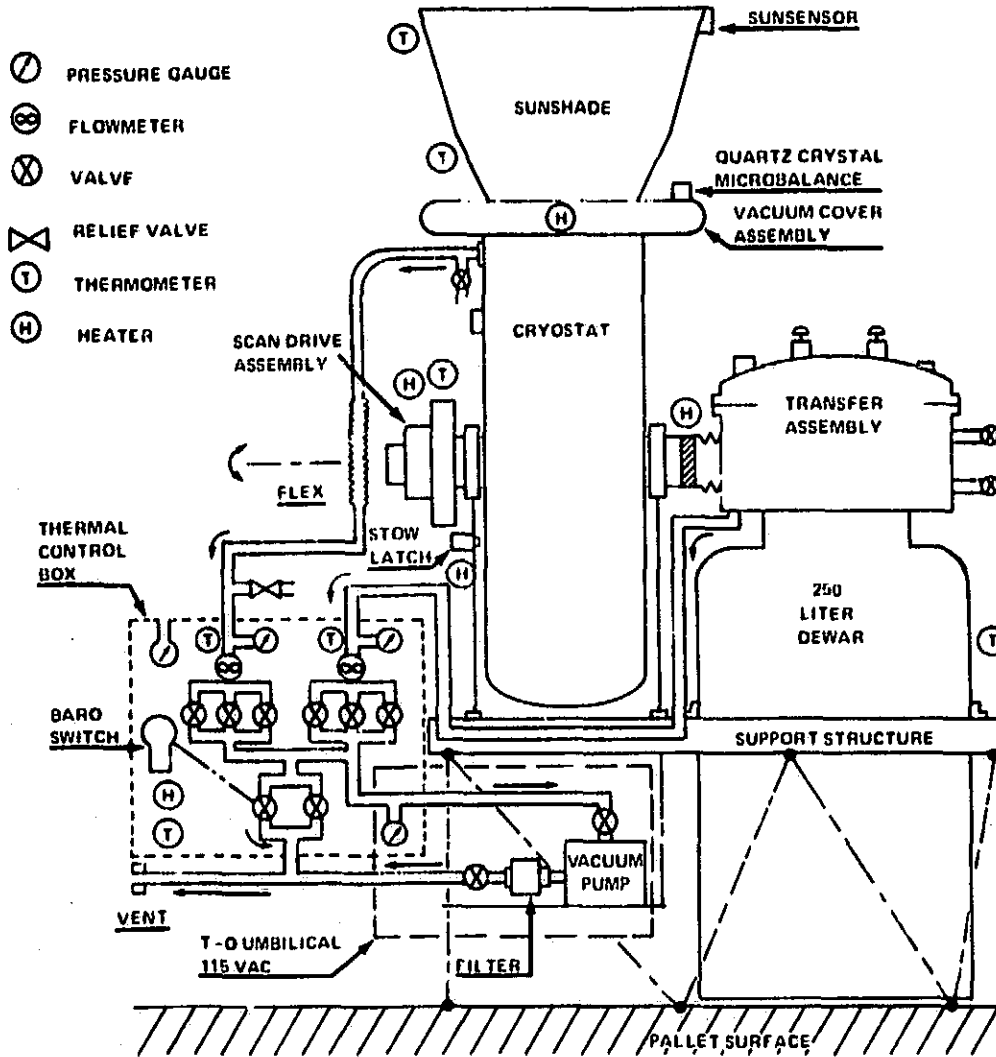


FIG. 1 INFRARED TELESCOPE
ENVELOPE AND PLUMBING

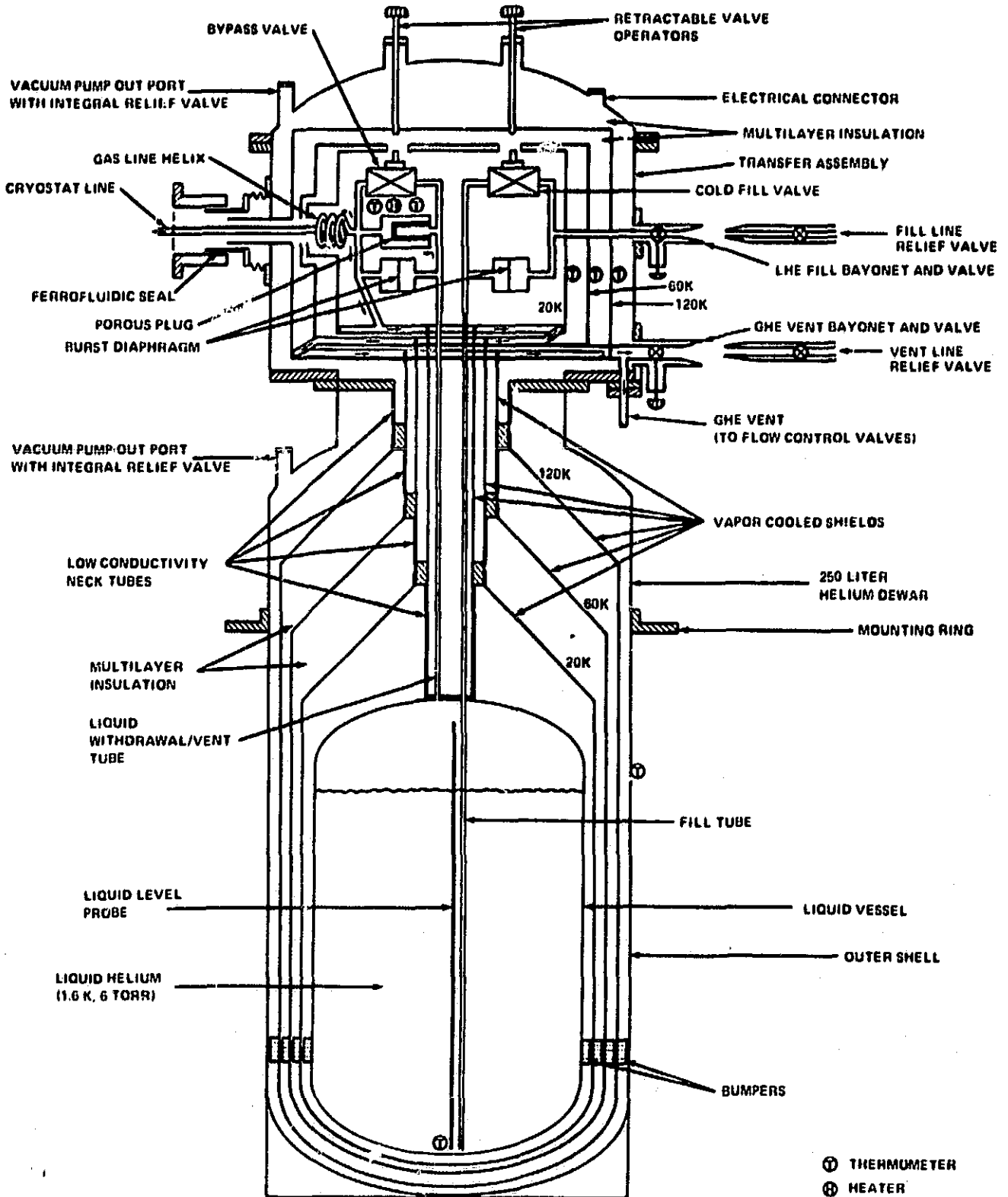


FIG. 2 DEWAR SUBSYSTEM

SPACELAB PREPARED TELESCOPE CRYOGENIC SYSTEM

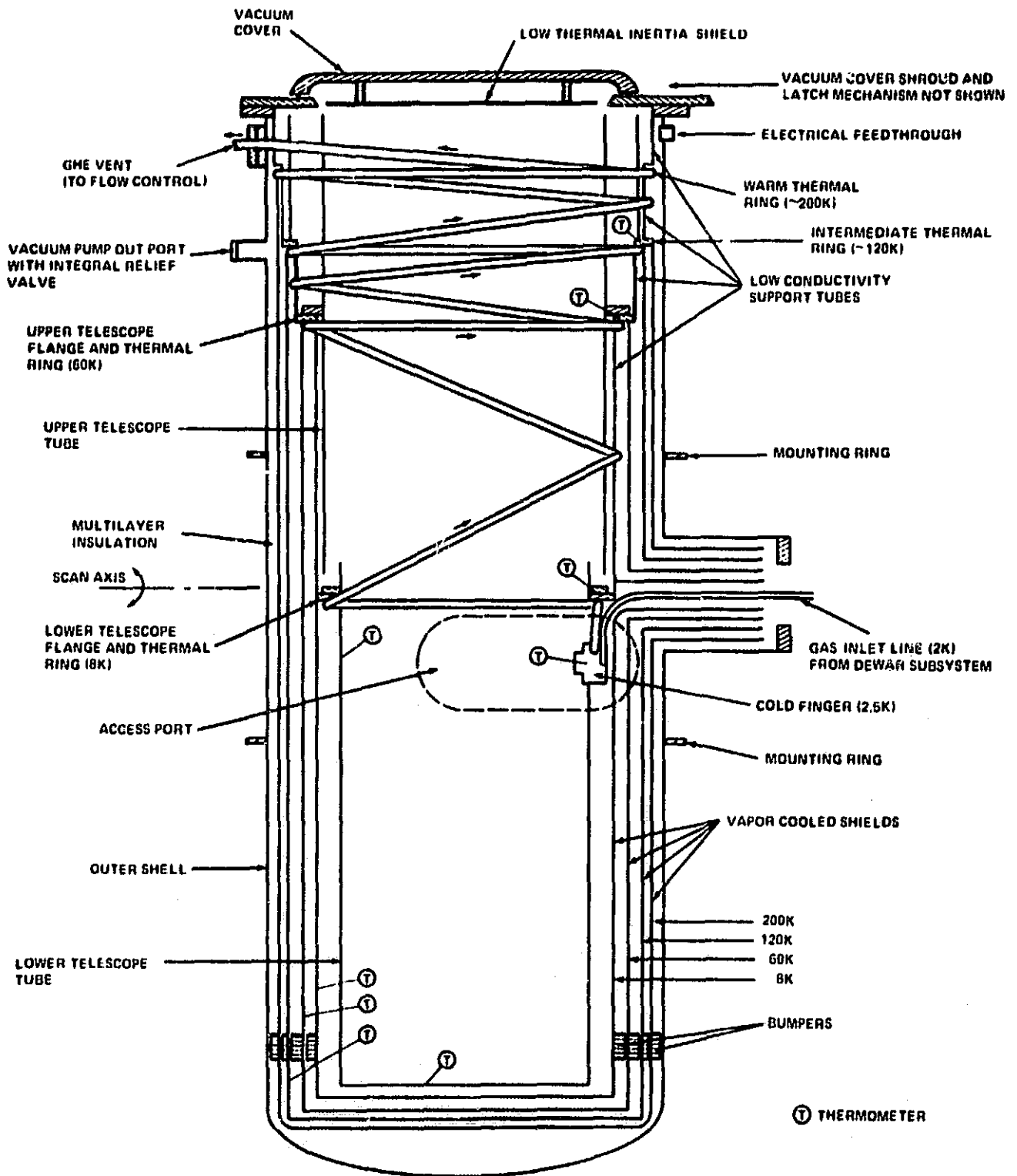


FIG. 3 CRYOSTAT

APPENDIX C

CRYOGENIC SUB-SYSTEM PERFORMANCE OF THE INFRARED TELESCOPE FOR SPACELAB 2

G. R. Karr and J. B. Hendricks
University of Alabama in Huntsville, USA

E. W. Urban, L. Katz, and D. Ladner
NASA/MSFC, Huntsville, Alabama, USA

Paper to be presented at the Eighth International Cryogenic Engineering Conference
3-6 June 1980 Genova, Italy

CRYOGENIC SUB-SYSTEM PERFORMANCE OF THE INFRARED TELESCOPE FOR SPACELAB 2

G. R. Karr and J. B. Hendricks
University of Alabama in Huntsville, USA

E. W. Urban, L. Katz, and D. Ladner
NASA/MSFC, Huntsville, Alabama, USA

The development of a scanning Infrared Telescope (IRT) experiment which will be flown on the Shuttle Spacelab 2 mission has progressed to the point that the major cryogenic sub-systems have been designed and manufactured. Thermal performance tests have been completed on the cryostat sub-system which will house the optics and infrared detectors. The dewar sub-system has been manufactured and the thermal performance tests will be made in mid 1980 after the transfer assembly sub-system has been assembled onto the dewar sub-system. This paper reports on (1) the present development of the cryogenic sub-systems, (2) the results from the analytic model which predicts the thermal performance of the sub-system, and (3) the results of the thermal performance tests of the cryostat sub-system.

INTRODUCTION

The infrared telescope (IRT) experiment is to be flown on the Shuttle Spacelab 2 flight with the major science goal of mapping the infrared sources over a large area of the sky in several wavelength bands out to 120 μm . Another major goal of the experiment is to prove the technological capability of providing 2K cryogenic support for the periods of time associated with shuttle flights. The cryogenic system which has been designed for this experiment is one which has the capability to provide coolant at near 2K to the IRT experimental sub-system and to also provide the necessary thermal stations to cool the optics to 8K and the telescope baffle tube to 60K. The cryogenic system is designed to accept the infrared telescope sub-system as a separate complete unit which simply bolts onto the necessary heat stations. Another feature of the cryogenic system is the capability of providing varying amounts of coolant to accommodate a wide range of heat load requirements. This capability also means that future experiments could readily be accommodated even though they may require levels of coolant flow different than that of the present science package. A third important feature of the cryogenic system is the capability of providing coolant through a flexible joint which was required for the IRT science package because of the need to scan the IRT optics $\pm 45^\circ$ with respect to the shuttle platform. The flexible coolant joint has the advantage of allowing the large helium storage dewar to remain stationary, while the smaller science package is scanned, thus reducing the mass which must be scanned.

This paper reports on the present development of the IRT cryogenic system, the predicted performance of the system, and the results of thermal performance tests that have been completed on the cryostat sub-system.

PRESENT DEVELOPMENT OF THE CRYOGENIC SYSTEM FOR IRT EXPERIMENT

As reported in earlier papers [1,2], the IRT cryogenic system consists of three major components (see Figure 1): 1) the 250 liter storage dewar which contains liquid helium II (superfluid helium) at approximately 1.6K in equilibrium with its vapor at a pressure of approximately 6 torr, 2) the Transfer Assembly (TA) which provides for the phase separation of the liquid helium via a porous plug device, provides for the rotating joint, provides the necessary valving for filling and venting the dewar,

and also provides heat exchangers for cooling the dewar, and 3) the cryostat which contains various thermal stations to which the science package is attached. Since the final design of these components differ little from the preliminary design reported previously [1,2], this paper will report on the predicted performance of the cryogenic system and the results obtained in early cryogenic tests on the cryostat sub-system. The present status of the experiment development is that (1) the dewar has been designed, manufactured and delivered to NASA/MSFC; (2) the cryostat has been designed, manufactured, tested cryogenically at NASA/MSFC, and delivered to the University of Arizona where the optics and detectors will be inserted and tested (see reference [3] for details on the IRT experiment package); (3) the Transfer Assembly has been designed, is being manufactured, will be assembled onto the dewar in mid 1980, and will undergo thermal testing soon after installation.

PREDICTED PERFORMANCE OF THE IRT CRYOGENIC SYSTEM

A computer program has been prepared to simulate the performance of the cryogenic system for a wide range of possible operating conditions. The program is based on the heat balance at each of the system heat exchangers. The dewar-TA system has three heat exchangers while the cryostat has four. The heat balance on a given heat exchanger is given by

$$\dot{m}_k c_p (T_n - T_{n-1}) = \sum_i C_{i,n} (T_i - T_n) + \sum_i R_{i,n} (T_i^4 - T_n^4) \quad (1)$$

where \dot{m}_k represents either the dewar flow (\dot{m}_1) or the cryostat flow (\dot{m}_2), c_p is the specific heat of the helium gas, $C_{i,n}$ represents the conduction heat transfer coefficient between the heat station at T_i and the heat station at T_n , and $R_{i,n}$ represents the radiative heat transfer coefficient between the i th and n th heat station. The primary conduction and radiation paths for each heat exchanger is between those heat stations directly above and below in temperature. Notable exceptions to this pattern is the radiation onto the lower telescope tube during times that the vacuum cover is closed and certain support strapes that have conduction paths through neighboring heat shields. The total mass flow rate ($\dot{m} = \dot{m}_1 + \dot{m}_2$) is governed by the heat balance for the dewar liquid vessel given by

$$\dot{m}L = \sum_i C_{1,i} (T_i - T_1) + \sum_i R_{1,i} (T_i^4 - T_1^4) \quad (2)$$

where L is the latent heat of vaporization of liquid helium at temperature T_1 . A set of equations can then be developed for the dewar system given by Equation 2 for the inner vessel and three equations of the type given in Equation 1 to represent the heat balance of the three heat exchangers. Equation 1 applied to the dewar will have $\dot{m}_1 = s\dot{m}$ where s represents the fraction of total helium boil off sent to the dewar heat exchangers. Assuming that the outer case temperature is given and the liquid helium temperature T_1 is given, we obtain, for the dewar, a set of four equations in four unknowns of the form

$$R_i (\dot{m}, T_2, T_3, T_4) = 0, \quad i = 1, 4 \quad (3)$$

where $T_2, T_3,$ and T_4 are the unknown temperature of the three dewar heat exchangers.

The cryostat will receive a mass flow of $\dot{m}_2 = (1-s)\dot{m}$ where \dot{m} is determined from the solution to Equation 3. Thus, the cryostat has a set of type 1 equations representing the heat balance of the four heat exchangers given by

$$R_i (T_6, T_7, T_8, T_9) = 0, \quad i = 5, 6, 7, 8 \quad (4)$$

where $T_6, T_7, T_8,$ and T_9 are the unknown temperatures for the four cryostat heat exchangers.

The dewar and cryostat sets of equations can be solved separately and in a similar fashion. The equations are found to be algebraic and non-linear which requires that

an iterative technique be used for numerical solution. A Newton-Raphson method was chosen in which the residuals given in Equations 3 and 4 are differentiated with respect to the given unknowns to form, for each R_i , the following equation

$$\frac{\partial R_i}{\partial Y_1} (\delta Y_1) + \frac{\partial R_i}{\partial Y_2} (\delta Y_2) \dots = -R_i \quad (5)$$

where Y_i represents the unknowns. This set of equations is solved for the corrections, δY_i , to be used to provide a new value of Y_i at the n^{th} iteration, given by,

$$Y_i^{(n)} = Y_i^{(n-1)} + (\delta Y_i)^{(n)} \quad (6)$$

The above procedure was found to converge rapidly.

The results from the computer program applied to the dewar are as shown in Figure 2 which shows the heat station temperatures for various values of s , the fraction of helium boil off which is directed back to the dewar heat exchangers. Figure 3 shows how the total helium boil off is effected by the value of s and illustrates one of the primary controls of total mass flow rate for the system. As the dewar heat exchanger flow is reduced, the total boil off is increased resulting in an even greater amount of coolant to the experiment package.

Figure 4 shows the results obtained from the computer program applied to the cryostat system. The results show how the cryostat system responds to increased coolant flow with the expected effect of lower temperatures for the upper and lower tubes. The results in Figure 4 are for the case of constant inlet temperature of 2.5K.

THERMAL PERFORMANCE TESTING OF THE CRYOSTAT

The cryostat was tested as a separate unit by use of a transfer-assembly substitute which allowed helium to be supplied from an ordinary helium dewar. The substitute allowed for early testing of the cryostat sub-system, independent of the dewar-transfer-assembly development. The inlet temperature and mass flow rate were monitored as were the temperatures of the vapor cooled shields and the temperature number of steady state conditions. The results show that the cryostat is running a little hotter than expected which will require that some modifications to the computer program will have to be made.

CONCLUSION AND DISCUSSION

The results shown in the above indicate that the computer simulation is a tool which can be used to predict the dewar-transfer-assembly performance. The results of the thermal performance tests on the dewar-transfer-assembly will be used to adjust certain system parameters within the program. The final computer program will be used to predict the performance of the cryogenic system for the complete experiment history which consists of the following major phases:

1. The horizontal prelaunch phase after filling with superfluid and while the porous plug is not in contact with the liquid.
2. The vertical prelaunch phase when the shuttle is erected just prior to launch. The superfluid plug is then in contact with the liquid. The cryostat vacuum cover is still in place.
3. The open-cover space phase when the cryostat vacuum cover is removed.
4. The closed-cover space phase when the cover has to be closed periodically to protect the optics from hot objects or contamination.

All of the above phases result in different rates of helium usage and temperature distribution in the system. The test program described above and the computer

simulation will provide information on this helium usage and will be used in the development of ground support and prelaunch operations requirements.

REFERENCES

- 1 Urban, E.W., Katz, L., Hendricks, J.B. and Karr, G.R. 'A Cryogenic Helium II System for Spacelab'. Proceedings of Seventh International Cryogenic Engineering Conference, 1978, pp 113-119
- 2 Urban, E.W., Katz, L., Hendricks, J.B. and Karr, G.R. 'Spacelab 2 Infrared Telescope Cryogenic System'. Proceedings of Space Optics, SPIE Vol. 183, 1979, pp 40-47.
3. Koch, D. 'The Infrared Telescope on Spacelab 2'. Proceedings of Space Optics, SPIE, Vol. 183, 1979, pp 16-23.

ACKNOWLEDGMENTS

This work was supported in part under National Aeronautics and Space Administration contract number NAS8-32818.

ORIGINAL FIGURE
OF POOR QUALITY

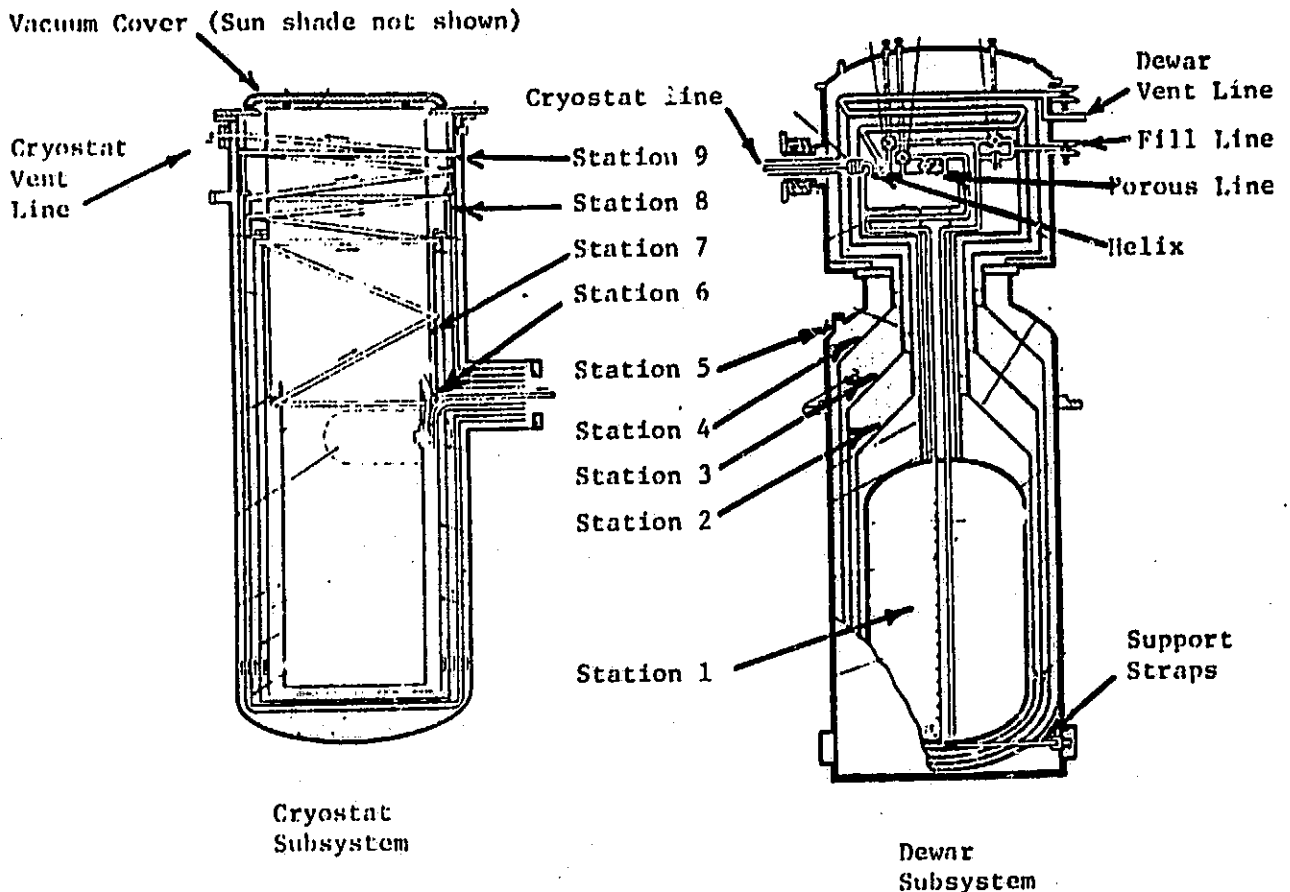


Fig. 1 Schematic of the cryostat and dewar-TA subsystems

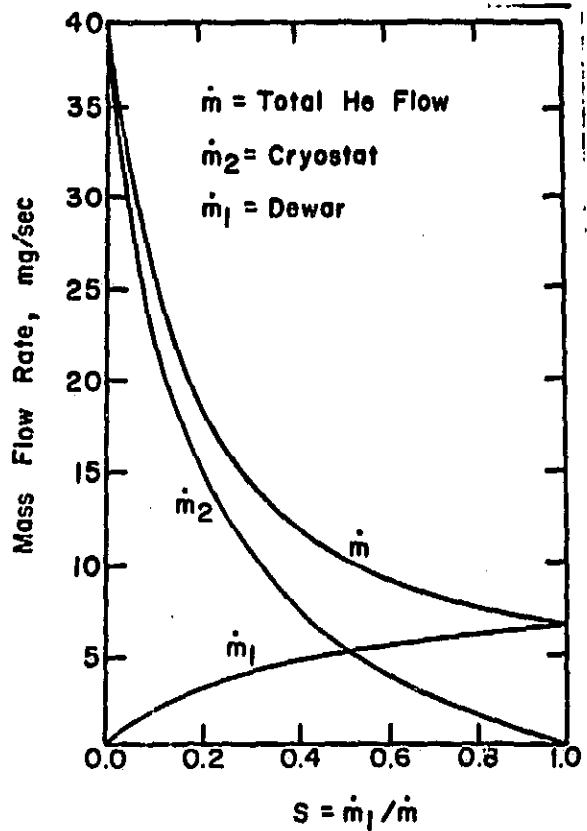
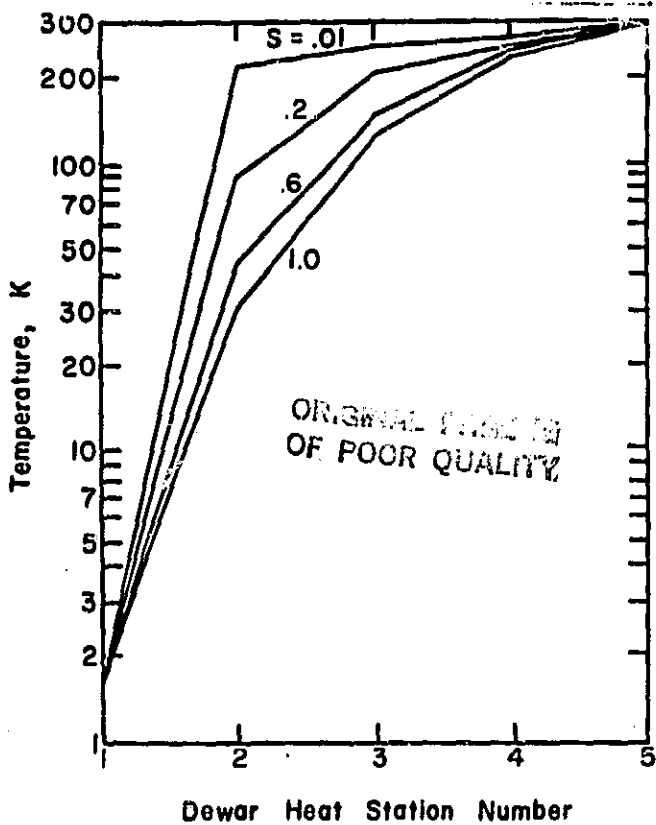


Fig. 2 Predicted dewar heat station temperatures for values of s

Fig. 3 Total helium flow and cryostat and dewar flows as a function of s based on computer simulation

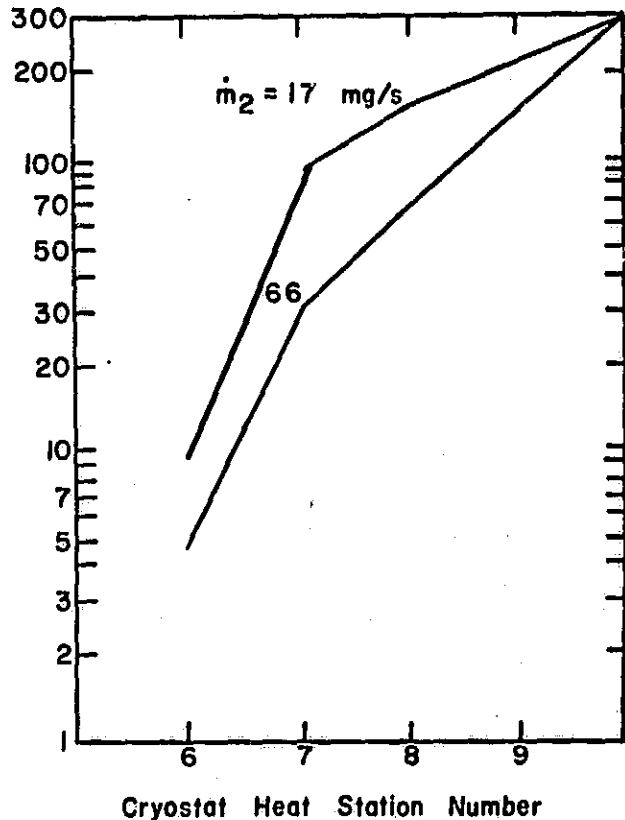
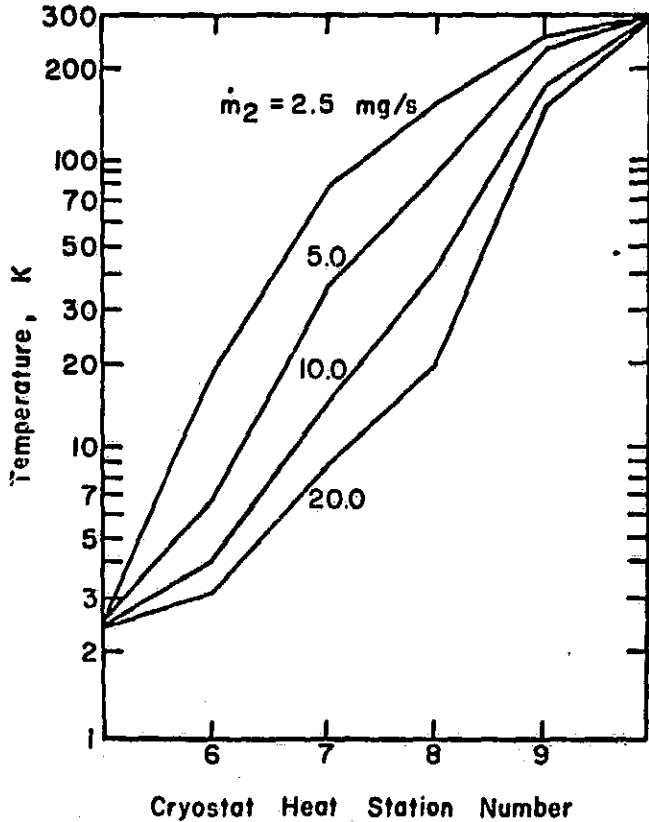


Fig. 4 Predicted cryostat heat station temperatures for various values of cryostat flow

Fig. 5 Measured values of heat station temperatures for various values of cryostat flow

**PERFORMANCE OF THE HELIUM II DEWAR SUBSYSTEM FOR THE SPACELAB 2
INFRARED TELESCOPE**

Gerald R. Karr and John B. Hendricks
University of Alabama in Huntsville, Huntsville, Alabama 35899, U.S.A.

Eugene W. Urban and Dan R. Lidner
NASA/Marshall Space Flight Center, Alabama 35812, U.S.A.

The 250 liter flight Dewar of the scanning Infrared Telescope (IRT) for Spacelab 2 shuttle flight has undergone cryogenic testing with helium II under thermal conditions simulating flight operation. The thermal performance tests show that lifetime is more than adequate to provide the 2K environment required by the infrared detectors. This paper presents data obtained during the thermal performance testing. Data was taken on helium flow rates and vapor cooled shield temperatures as a function of time. The data shows the approach to equilibrium after filling and conversion operations.

INTRODUCTION

The Spacelab 2 infrared telescope (IRT) is a Space Shuttle payload with the major science goals of mapping diffuse, low surface brightness infrared sources over a large area of the sky in several wavelength bands out to 120 μm and measuring the infrared contamination environment of the Shuttle [1,2]. A second major goal of the first flight of the IRT experiment will be to prove the technological capability of providing 2K cryogen in zero gravity for the duration of a typical shuttle flight. The design of the cryogenic system for IRT is unique in that the 250 liter Dewar containing the liquid helium is a separate unit from the cryostat which contains the IRT optics and detectors. The system design was described in detail at ICEC7 [3]. Since the experiment consists of these two separate units (Dewar subsystem and cryostat subsystem) the development of the units could be separated. The cryostat was developed first, and cryogenic testing, completed in 1980, was reported at ICEC8 [4]. The cryostat was then delivered to have the telescope and detectors installed and tested. During the telescope installation and testing, the Dewar subsystem was developed and tested. This paper reports on the results of the initial cryogenic tests performed on the Dewar subsystem.

TESTING OF IRT DEWAR SUBSYSTEM

The purpose of the cryogenic testing of the IRT Dewar subsystem has been to measure the performance under conditions simulating those of the actual flight and also simulating the procedures required to service the experiment prior to flight. The typical shuttle flight will involve about seven days in space. Prior to launch, the Dewar must be filled with superfluid helium and maintained for a period of perhaps seven to fourteen days. The superfluid state is maintained during these ground operations by a vacuum pump which will fly with the experiment [1]. The testing programs of the Dewar has involved filling with normal liquid helium, conversion of the liquid helium to

superfluid, and topping off of the Dewar. The performance of the Dewar was monitored during the various operations and during the approach to steady state. Data taken included the flow rate of the helium, volume and temperature of the liquid helium vapor cooled shields (Figure 1). Since in flight a fraction of the Dewar exhaust gas is sent to the cryostat, while the remaining flow cools the vapor cooled shields, tests were performed in which a fraction of the helium boil-off was diverted through the fill line (Figure 1).

RESULTS

The temperatures and flow rate data versus time immediately after filling the Dewar with normal liquid helium are shown in figure 2. The shield temperatures show an approach to steady state that requires about 12 days. The vent flow rate at steady state was measured to be 12 mg/sec. The corresponding evaporation rate and heat input were 14.1 mg/sec. and 296 mW, respectively. There is evidence that thermo acoustic oscillations (TAO) are present, increasing the boil off rate somewhat. Figure 3 shows the temperatures and flow data versus time immediately after pumping was initiated to convert the liquid to superfluid. During the pumping, the shield temperatures drop to very low values which then take the order of a week to stabilize. The conversion requires about 6 hours. At 1.6K the Dewar steady state performance was found to correspond to 8.3 mg/sec. boil-off and 191 mW heat input. If the Dewar were operated by itself, the boil-off rate gives a 50 day lifetime for an initially full Dewar. Figure 4 shows the temperatures and flow data for a divided flow simulation. When flow is diverted from the Dewar shields, the performance naturally degrades, resulting in an increased boil-off rate.

Our data were complicated by the development of a small superfluid helium leak in the Dewar plumbing which decreased the efficiency of part of the Dewar guard vacuum and contributed to the higher total boil-off. Figure 4 shows, for example, that when half the total flow was diverted from the Dewar shields, the total flow rate was 22.0 mg/sec., corresponding to a heat leak of 462 mW and a full Dewar lifetime of 19 days.

CONCLUSIONS AND FUTURE PLANS

The Dewar subsystem of the IRT operates essentially as predicted. When the superfluid leak is repaired, the cryogenic performance will be adequate to supply the 2K cryogenic requirements of the shuttle flight.

When the leak is repaired and certain other modifications are complete, a Dewar subsystem reverification will be performed in mid 1982. Then the cryostat containing the infrared telescope will be assembled to the Dewar and full system tests conducted in late 1982. Extensive cryogenic testing will then be made for various cryostat flows. The numerical simulation will be modified to reflect the measured performance of the Dewar and cryostat.

ACKNOWLEDGEMENT

This work was supported in part under contract NAS8-32818, NASA, Marshall Space Flight Center, Huntsville, Alabama.

REFERENCES

1. Urban, E.W., Katz, L., Hendricks, J.B., and Karr, G.R. "Spacelab 2 Infrared Telescope Cryogenic System" Proceedings of Space Optics, SPIE 183, 1979, 40-47.
2. Koch, D. "The Infrared Telescope on Spacelab 2" Proceedings of Space Optics, SPIE, 183, 1979, 16-23.
3. Urban, E.W., Katz, L., Hendricks, J.B., and Karr, G.R., "A Cryogenic Helium II System for Spacelab" Proceedings of Seventh International Cryogenic Engineering Conference, 1978, 113-119.
4. Karr, G.R., Hendricks, J.B., Urban, E.W., Katz, L., and Ladner, D. "Cryogenic sub-system Performance of the Infrared Telescope for Spacelab 2." Proceedings of the Eighth International Cryogenic Engineering Conference, 1980, 38-42.

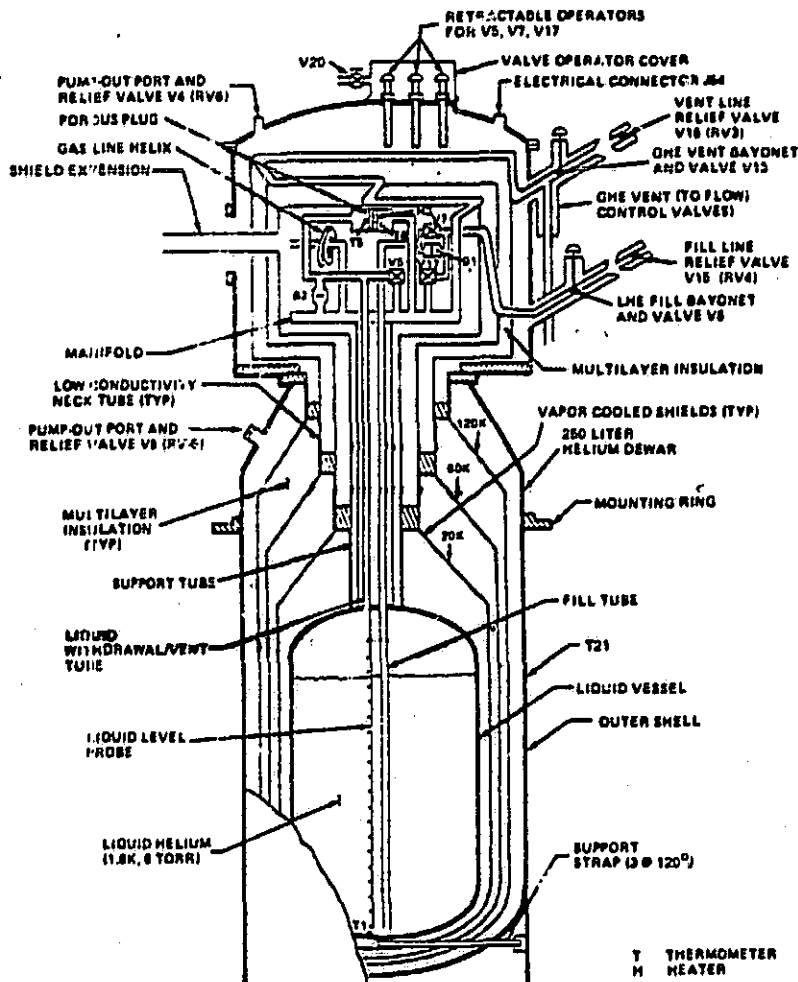


FIGURE 1. DEWAR SUBSYSTEM

ORIGINAL PAGE IS
OF POOR QUALITY

ORIGINAL PAGE IS
OF POOR QUALITY

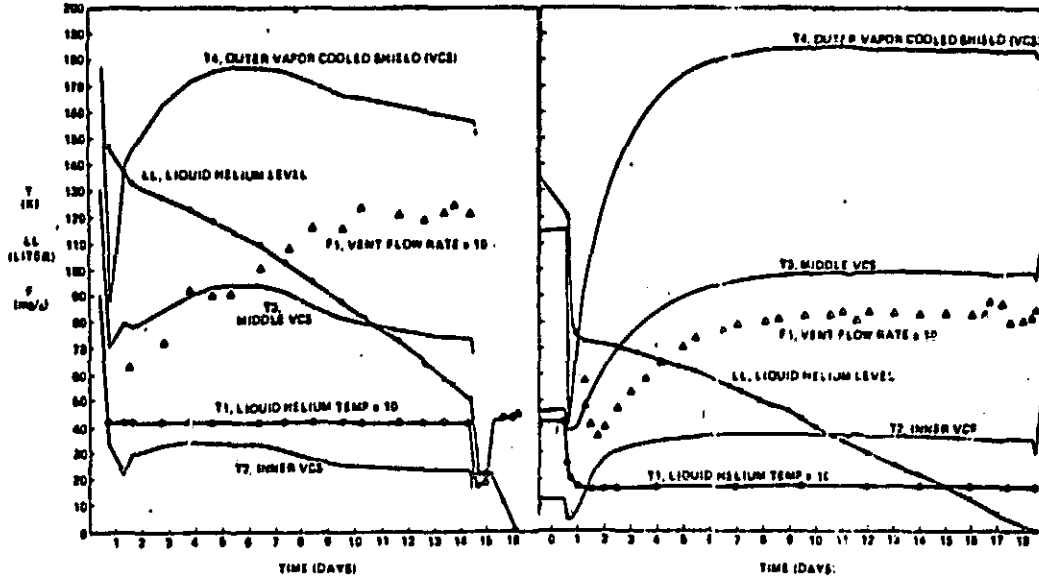


FIGURE 2. STEADY STATE PERFORMANCE TEST, HELIUM II

FIGURE 3. STEADY STATE PERFORMANCE TEST, HELIUM II

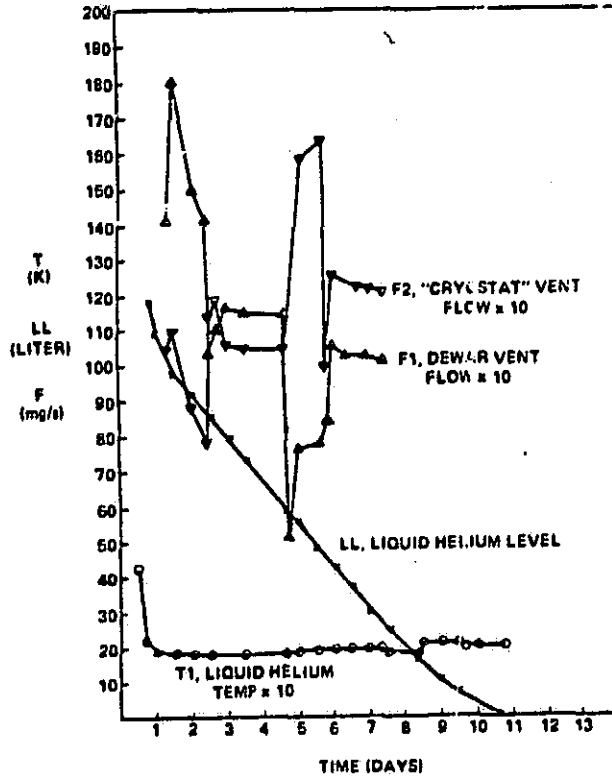


FIGURE 4. DIVIDED VENT FLOW TEST, HELIUM II

APPENDIX E

1983 SPACE HELIUM DEWAR CONFERENCE

CRYOGENIC PERFORMANCE TESTING OF THE INFRARED TELESCOPE (IRT) FOR SPACELAB 2

E.W. Urban, D. Ladner, J. Jolley, and M.D. Armstrong
NASA/Marshall Space Flight Center
Huntsville, Alabama 35812

J. Hendricks and G. Karr
The University of Alabama in Huntsville
Huntsville, Alabama 35899

INTRODUCTION

The Small Helium Cooled Infrared Telescope (IRT), to be flown on the Spacelab 2 mission in March, 1985, employs a novel cryogenic system consisting of a fixed superfluid helium dewar and a separate articulated dewar, called the cryostat, which contains the infrared optics. The cryostat is cooled by cold helium vapor delivered across a rotary connection from the dewar. This design, dictated by performance and cost constraints, and the special requirements for prelaunch servicing in the Space Shuttle have led to a number of unusual test conditions and performance results.^{1,2,3,4}

The IRT, which is a joint venture of the Smithsonian Astrophysical Observatory, the University of Arizona and MSFC, is now fully assembled at MSFC and cryogenic performance testing is about to begin. The two cryogenic subsystems having previously been tested separately. This paper reviews the system performance requirements, design and the results of testing to date.

SYSTEM DESCRIPTION

A model of the IRT is shown in Figure 1 and a schematic is shown in Figure 2. The 200 liter dewar subsystem, consisting of a dewar vessel and a transfer assembly containing flow control plumbing, is fixed to the main experiment structure. The cryostat subsystem, consisting of the cryostat, the optical components, vacuum cover and sunshade, is mounted in a set of bearings and is scanned from side to side across the sky at 6 degrees per second by a scan drive motor. The separation of the two cryogenic

subsystems was dictated by this scanning motion, since we could not tolerate the continuous fluid sloshing which would result from scanning the dewar.

In the following, we will describe the two cryogenic subsystems more fully, the results of subsystem performance tests, and predictions of prelaunch and mission lifetimes.

CRYOSTAT

The cryostat was purchased from Cryogenic Associates (CA) to a specification which defined and controlled the mechanical/thermal interfaces, but which left the detailed design and fabrication process to CA's discretion, and placed on them no burden of meeting a minimum performance goal. As a result, the cryostat cost was quite low by aerospace standards. Figure 3 is a schematic of the cryostat subsystem, the cryostat being that part below the vacuum cover and shroud. It employs standard fabrication methods with glued aluminum to G11 fiberglass-epoxy joints, and four aluminum vapor cooled shields (VCS) which are wrapped with NRC-2 multilayer insulation.

Cold helium gas enters the cryostat through a rotary connection, described below, on the scan axis, cooling first a cold finger provided to CA by the University of Arizona. The focal plane assembly, containing ten infrared detectors, field optics and preamplifiers, is fastened to the cold finger and, during infrared observing periods, must remain at a temperature of 3.0 K or less. The cold gas next enters an aluminum heat exchanger (8 K) and structural ring, which is glued to a large diameter fiberglass-epoxy tube glued in turn to the next warmer heat exchanger ring (60 K). The lower section of the IR telescope with mirror is bolted to the 8 K ring, and it is surrounded by the innermost VCS welded to the 8 K ring.

The cold gas next enters the 60 K heat exchanger ring, to which the upper telescope tube is bolted and a VCS is welded. The upper telescope tube must operate during scientific observations at a temperature no warmer than 60 K to keep its radiant load on to the lower telescope tube less than about 50 mW. At 60 K the upper tube absorbs about 1.1 W from the sunshade.

After leaving the 60 K heat exchanger, the helium gas passes through two additional heat exchanger rings, to each of which is welded a VCS, and then exits the cryostat. It is then conducted across the rotary interface to a flow control valve, V1.

To reduce the conduction of heat between adjacent heat exchanger rings in the cryostat, the venting gas passes through stainless steel tubing. An aluminum-to-stainless steel transition at the inlet and outlet of each ring joins the dissimilar tubing.

The two telescope tube/baffle sections are installed through the large open top of the cryostat which is exposed when the vacuum cover is removed. The focal plane is then fastened to the cold finger and aligned with the mirror through an access port in the side of the cryostat. The access port consists of removable, MLI-covered plates in three of the four VCS, and an external vacuum seal port carrying hermetic electrical connectors. The electrical cable bundle from the focal plane is heat stationed on each VCS at the access port.

The cryostat was tested thermally prior to and following the installation of the optical components. Temperatures of the three coldest VCS and of the cold finger are measured by germanium resistance thermometers (GRT) and platinum resistance thermometers (PRT). A dewar substitute device was connected to the gas inlet appendage to deliver a controlled flow of 2-3 K gas to the cryostat. This device was difficult to control and we could not be certain of the quality of the fluid reaching the cold finger. The optical components cooled and approximately stabilized at acceptably low temperatures when the mass flow rate was estimated to be about 15 mg/s. This flow rate is used in the system performance prediction made below. A more precise determination of the cryostat performance will be made during the system cryogenic tests soon to be started.

DEWAR SUBSYSTEM

The dewar, which is the lower part of the subsystem, shown in Figure 4, was also purchased from CA in the same mode as was the cryostat. The inner liquid vessel, which has an internal volume of 250 liters, is suspended from a top plate by a fiberglass/epoxy and aluminum tube, and is restrained at the bottom by three fiberglass/epoxy tension straps identical to those used in the Infrared Astronomical Satellite dewar. Three MLI-wrapped aluminum VCS with nominal design temperatures of 20 K, 60 K and 120 K surround the liquid container, connect to the neck structure of the aluminum rings and extend up within the neck to interface rings where the TA VCS are connected. Straight fill and vent tubes extend from above these interface rings through the center of the neck tube, terminating at the bottom and top, respectively, of the liquid vessel.

Since the dewar could not be operated without the Transfer Assembly (TA), the upper part of the subsystem (Figure 4), being in place, the dewar was also purchased with no cryogenic performance specifications. The basic structural and thermal design was jointly controlled by MSFC and CA, but fabrication details were at CA's discretion. Only vacuum integrity tests and a warm proof pressure test of the dewar were required to be performed. No instrumentation was included in the dewar.

The most complex cryogenic element of the IRT system is the TA, which was designed, fabricated and installed by the University of Alabama in Huntsville (UAH) group. The TA consists of an outer aluminum case and dome which bolt to and complete the dewar vacuum jacket; three nested aluminum tubs, each having a heat exchanger channel around its top

circumference, and each bolting to one of the dewar VCS extensions; and a stainless steel plumbing module within the inner tub. The module contains two welded aluminum burst diaphragms, three bellows sealed manual valves, a porous plug^{5,6} module with thermometers, a helical gas line to carry the cryostat cooling gas, a gas manifold and a charcoal cryopump. Several individual components are removable and the entire plumbing module can be removed from the TA. All demountable joints are Varian Mini-conflat ultra-high vacuum flanges with copper gaskets. As in the cryostat, stainless steel tubing connects the aluminum heat exchangers, with Al-SS transitions providing the connections.

When the dewar subsystem was initially assembled, a superconducting liquid level probe and a GRT were inserted down the vent line into the dewar, the wiring being brought out through a TA cable bundle together with wires from thermometers and a heater in the porous plug module and a thermometer on each VCS tub. This vent line and level probe arrangement were adequate to permit filling of the dewar in the upright attitude, after which the dewar could be turned on its side into the launch attitude. A vertical loop (trap) in the vent tube within the TA was then expected to prevent bulk liquid from reaching the porous plug prior to superfluid conversion, or if venting was interrupted after conversion and prior to launch.

After several subsystem performance tests had been made, as discussed below, we learned that prelaunch servicing at the Kennedy Space Center would have to be performed on the launch pad with the dewar lying on its side. Clearly we could only load the 250 liter vessel half full in that attitude because the original entrance to the vent tube was on the central axis of the dewar, as noted on Figure 4. With the tight performance margins and uncertainties in launch holds, we elected to modify the dewar vent to permit loading more fluid. Accordingly we removed the TA plumbing module and the dewar depth probe with thermometer, replacing the latter assembly with a new erectable vent line and short depth probe, having the configuration shown in Figure 4. It is now possible to fill the dewar to about 200 liter when the system is either in the launch attitude or upright. The dewar must be at least half full before the level probe begins to register. Prior to that time during filling we can determine the status of fluid flow into the dewar only by monitoring T1, which is a calibrated GRT, and Vac Ion Gauge 1, which is mounted on the TA and gives a sensitive indication as to when liquid is flowing in the fill lines within the TA.

The porous plug,^{5,6} also shown in Figure 4, is the liquid/vapor phase separator. It is 1.28 cm diameter, 0.64 cm thick porous stainless steel with a 0.5 μ m filtration grade pores, welded into a stainless steel holder. GRT T5 is located on the liquid or upstream side of the plug, while GRT T6 and a 130 mW resistive heater H3 are mounted against the vapor or downstream side of the plug.

The three manual valves are V5, which bypasses dewar vent flow around the porous plug during servicing or conversion; V7, the cold fill valve, which isolates the warm end of the fill circuit from the cold environment; and V17, which bypasses flow from the fill line directly to the vent line and thus permits fill line chilldown during topoff operations without disturbing the liquid in the dewar. All three valves are actuated by retractable rotary shafts. When an actuator is inserted into its valve it first depresses a spring-loaded detent lock, then engages the valve proper. A nut on the warm end of the actuator permits accurate closure torques to be applied. A valve closure torque of 9.0 inch-pounds has been found to give repeatable, superfluid tight seals.

When the actuators are withdrawn MLI flaps on each VCS blanket close to reduce radiation loads on the cold apparatus. A valve actuator cover is then installed. It holds the three actuators in the retracted position and can be evacuated to eliminate possible air leakage into the TA guard vacuum past the actuator gland during the vibration of launch.

The rotary joint connection between the dewar and the cryostat, identified in Figure 2, permits the scanning motion of the cryostat and the delivery of the cold gas stream to the cold finger, while maintaining a high vacuum seal for pre-launch testing and servicing. A Ferrofluidic high vacuum rotary seal connects the cryostat and the TA case, which therefore share a common vacuum. An MLI-wrapped extension of the inner TA VCS protrudes through the bore of the rotary seal and nests without contact between two of the cryostat VCS extensions. The MLI wrapped gas line runs along the center of the shield extension which is the cryostat rotation axis. The $+45^\circ$ rotation of the cryostat is accommodated in a 10 turn helical winding of the gas line within the TA plumbing module.

DEWAR SUBSYSTEM THERMAL PERFORMANCE EVALUATIONS

A series of thermal performance evaluations (TPE) were conducted with the dewar subsystem and without the cryostat. The first five TPES's were performed before the new curved vent line was installed, and two more were done afterward to verify the modifications. From these tests we established the steady state performance of the dewar subsystem by itself with normal liquid helium (LHe) and with superfluid (SHe) both in the upright attitude and tilted to various angles to simulate launch and zero-g conditions. In addition, we simulated the cooling of the cryostat. A complete description of this TPE series will be available soon. In this paper we discuss a number of interesting highlights and the predicted prelaunch and on-orbit performance of the complete cryogenic system.

Figure 5 is a summary of TPE I, performed with the dewar upright and with normal helium. Plotted as a function of time in days are the bath temperature, T1; the temperature of the three VCS, T2, T3, and T4, respectively; the measured liquid level (LL) and the measured vent flow rate. As LHe filling proceeded, the VCS subcooled due to the high vent

During TPE V we rotated the dewar into the horizontal or launch attitude for the first time and subsequently, as part of the porous plug performance test, we inverted the system. Although venting was only through the dewar VCS, the average liquid evaporation rate was 21 mg/s, confirming our suspicion that the dewar heat load had increased significantly. In spite of the anomalous heat load we were able to obtain considerable porous plug and system performance data.

The geometry of the plumbing made the low gravity simulation somewhat difficult. Consider Figure 4 with the original vent line entrance, the plug situated about 90 cm from the liquid vessel, and the vertical "fluid trap" seen in Figure 4, in the fluid line just upstream of the plug. In the launch attitude, up is to the left. To reach the plug liquid had to flow over the trap due either to the net volume in the vessel or to the tilt angle of the apparatus or both. To simulate low gravity behavior the hydrostatic head of fluid in the system had to be near zero. Thus a test in this orientation would require first rotating the dewar far enough to pour liquid over the trap and establish a fluid column, then rotating back to reduce the head. Figure 8 shows a typical set of plug and flow data in this orientation. The tilt angle θ had to be increased to about 98° from vertical before the plug became wet and the flow rate increased dramatically. The hydrostatic head (in parentheses) was 18.5 cm or 1.8 torr, plug temperatures T5 and T6 were unstable and were warmer than the bath T1, in the vessel, which was warming slowly. Then, as θ and the head were reduced, the plug temperatures became stable and cooler than the bath which began cooling. The downstream side of the plug (T6) was colder than the upstream side (T5).

Figure 9 shows the same parameters when the system was inverted making the trap a reservoir, rather than an obstacle. Here T5 remained warmer than the bath and T6, initially colder than T5, suddenly became much warmer than T5 and remained so while the bath and T5 cooled. In both of these cases with a total flow rate of more than 20 mg/s the porous plug operated as a fluid restraint and cooled the bath, so long as the hydrostatic head was less than about 1.5 torr.

Following TPE V the system was modified as indicated earlier, to incorporate the curved vent line, short liquid level probe, new GRT thermometers, an adsorption cryopump, and a Vac-ion gauge on the TA case. The suspected plumbing leak was located and was repaired by means of Stycast 1266 epoxy. In addition the valve stems which had permitted air to enter the plumbing during TPE I were reinstalled with improved seals.

TPE VI was intended to verify all of the modifications and repairs to the system and to measure performance in the presence of a more realistic parasitic heat load. The system was filled with liquid while in the launch attitude, thus confirming our ability to load the experiment on the launch pad. The first phase of the TPE was a steady state performance test during which the temperatures and flow rate tracked those measured in TPE II to better than 10%. Early in the test a prototype flight flowmeter was connected to the experiment; an unsuspected vacuum leak in the device

PRECEDING PAGE BLANK NOT FILMED

permitted entry of enough air to contaminate the porous plug, though not to abort the test. As a result, the balance of this TPE consisted of a second divided flow test, shown in Figure 10. At a cryostat equivalent mass flow rate of 10.0 mg/s, the dewar flow rate settled at 5.0 mg/s for a total flow rate of 15.0 mg/s. T2, the inner vapor cooled shield temperature, was 63 K compared with its earlier value of 38-42 K (TPE II and VI) when all vent flow (~ 8.5 mg/s) was through the dewar VCS.

The primary objective of TPE VII was to determine the porous plug performance, which could not be measured in the previous TPE, as explained above. First, during initial conversion to superfluid the plug bypass valve was closed when T1 = 2.8 K and the mass flow rate was still greater than 300 mg/s, in order to determine whether the system could be repumped to superfluid through the plug alone, if warmup should occur at a time in the prelaunch schedule beyond which we could not operate the cold manual valves. The plug did in fact cool and carry the full flow as the bath continued to cool to and below the lambda point.

Figures 11 and 12 illustrate typical data taken with the system in the inverted attitude. In this case up is to the right in Figure 4 and the trap is below the plug. At large tilt angles and high hydrostatic heads (not explicitly shown in the figures) the plug temperatures were unstable and the bath was warming. We conclude that superfluid was being forced through the plug. As the angle and head were reduced, the plug temperatures became stable and the bath and flow rate decreased smoothly. It is noteworthy that in this and similar conditions the upstream side of the plug (T5) was colder than the bath, indicating a small thermal resistance existed in the long vent tube between the bath and the plug, and the downstream side of the plug (T6) was warmer than T5. This last fact suggests that the liquid/vapor interface had receded into the plug and the evolving gas was then warming slightly. The pressure dependence of this process is seen in Figure 12. When the tilt angle and head were increased very slightly, T6 abruptly cooled, the interface having been pushed farther through the plug. More detailed analyses of these results are found in the complete TPE series report.⁷

SYSTEM LIFETIME PREDICTIONS

Figure 13 is a summary plot of IRT system mass flow rates as a function of the divided flow ratio, $s = \text{dewar flow rate}/\text{total flow rate}$. The dashed lines are analytical predictions of performance based on early calculations of the expected thermal characteristics of the dewar and cryostat. They predicted that the steady state stand-alone ($s = 1$) dewar flow rate, F1, would be about 6.5 mg/s, and that to deliver 15 mg/s to the cryostat, F2, the dewar would receive less than 4 mg/s.

The points shown are measured or estimated steady state data from the various TPE's. Only TPE VI gave reliable divided flow data at an acceptable parasitic heat input. The solid curves are fits to the TPE VI points and indicate that, if the cryostat requires F2 = 15 mg/s, then F1 = 5 mg/s and $s = .25$. The resulting total flow of 20 mg/s or 12 liters/day

means that if the dewar can be filled to 150 liters of SHe at final prelaunch servicing, full cooling could be delivered to the cryostat continuously for 12.5 days. If final servicing is completed 48 hours before launch, then we will have a three day margin of liquid helium for the seven day Spacelab 2 mission. If, on the other hand, the cryostat requires 20 mg/s to keep the detectors cold enough, then $F_{total} = 24$ mg/s or 14.4 liters/day, and the margin is reduced to 1.4 days for continuous, full cooling.

In principle the fluid margin can be increased by changing the settings of valves V1 and V2 and reducing cryostat flow during periods of the mission when infrared observations are not being made. This will move the system to larger values of s in Figure 13, permit the optical components to warm somewhat, and conserve superfluid helium. However it is not clear at this time how rapidly the infrared detectors and telescope components will recool to acceptable temperatures, when cryostat flow is again increased. Thus because of long thermal time constants we may have to maintain relatively high net flows and a narrow performance margin in order to insure that the infrared observations can be successfully accomplished.

CONCLUSIONS

In this paper we have reported briefly on the results of a series of seven thermal performance evaluations conducted over a period of 10 months on the Infrared Telescope Dewar Subsystem. A large number of test objectives were satisfied, including verification and refinement of complex operating procedures, and measurement of quantitative performance data for components and for the dewar subsystem. An important simulation was made of the effect on the storage lifetime of the complete system when cooling is delivered to the cryostat.

Assembly of the cryostat onto the dewar is in progress and will be followed by cryogenic performance tests on the complete system. The dewar subsystem TPE's reported here have served as a vital tool in preparing for efficient and safe conduct of the system tests and of the flight mission itself.

REFERENCES

1. The Spacelab 2 Infrared Telescope Cryogenic System, SPIE, Space Optics, 183, 40, 1979 with L. Katz, J. Hendricks and G. Karr.
2. Cryogenic Subsystem Performance of the Infrared Telescope for Spacelab 2. Proceedings of the Eighth International Cryogenic Engineering Conference (ICEC 8), Genoa, Italy, June 1980, with G. Karr, J. Hendricks, D. Ladner and L. Katz.
3. A Cryogenic System of the Small Infrared Telescope for Spacelab 2, Proceedings of Conference on Refrigeration for Cryogenic Sensors and Electronic Systems, Boulder, CO, October 1980 with L. Katz, G. Karr and J. Hendricks.

4. Development and Integration of the Infrared Telescope for Spacelab, Proceedings Intersociety Conference on Environmental Systems, San Francisco, July 1981, with L. Katz and R. Watts.
5. Superfluid Plug as a Control Device for Helium Coolant, Cryogenics 20, 266 (1980) with G. Karr.
6. See also porous plug papers, this conference.
7. NASA TR, to be published.

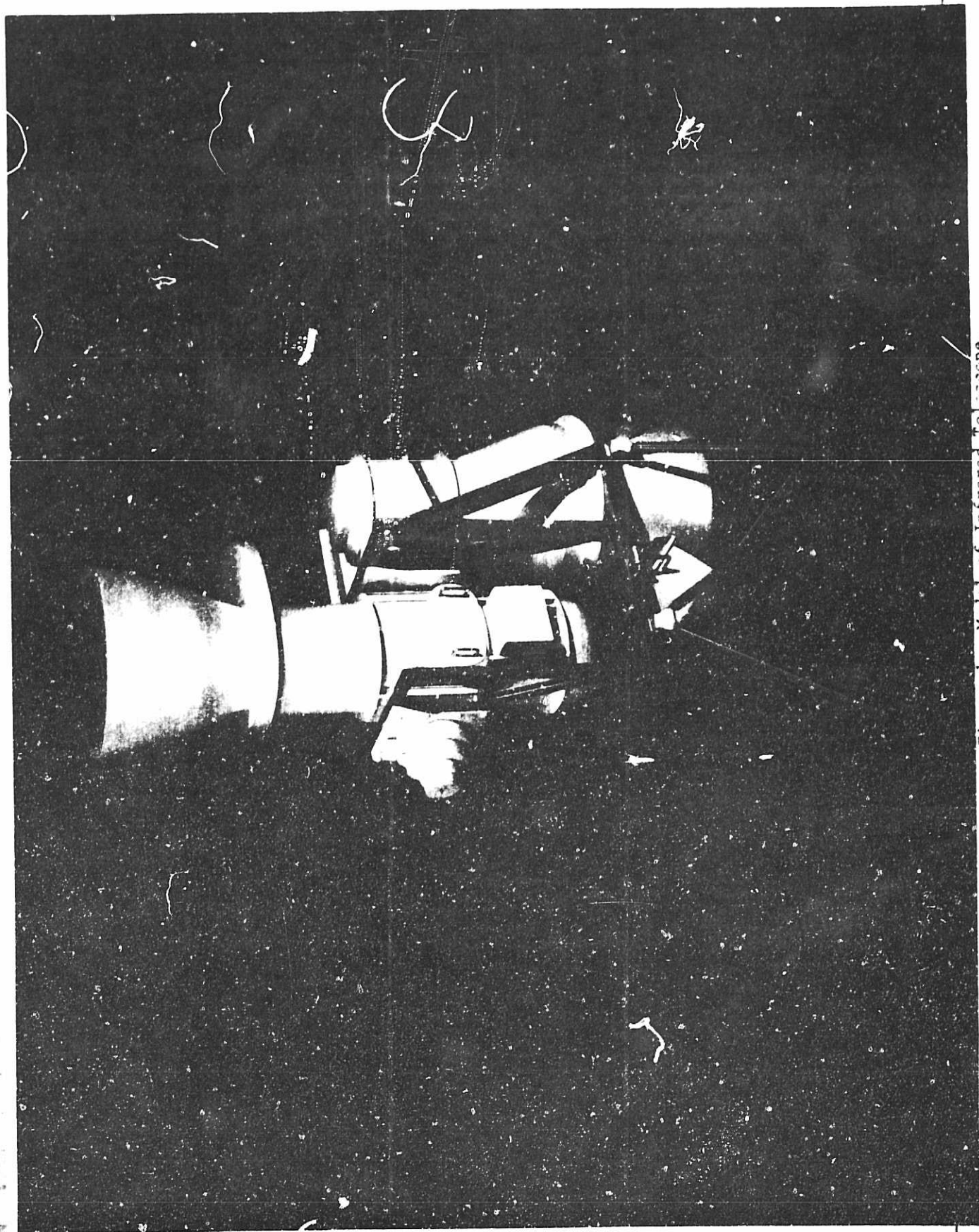
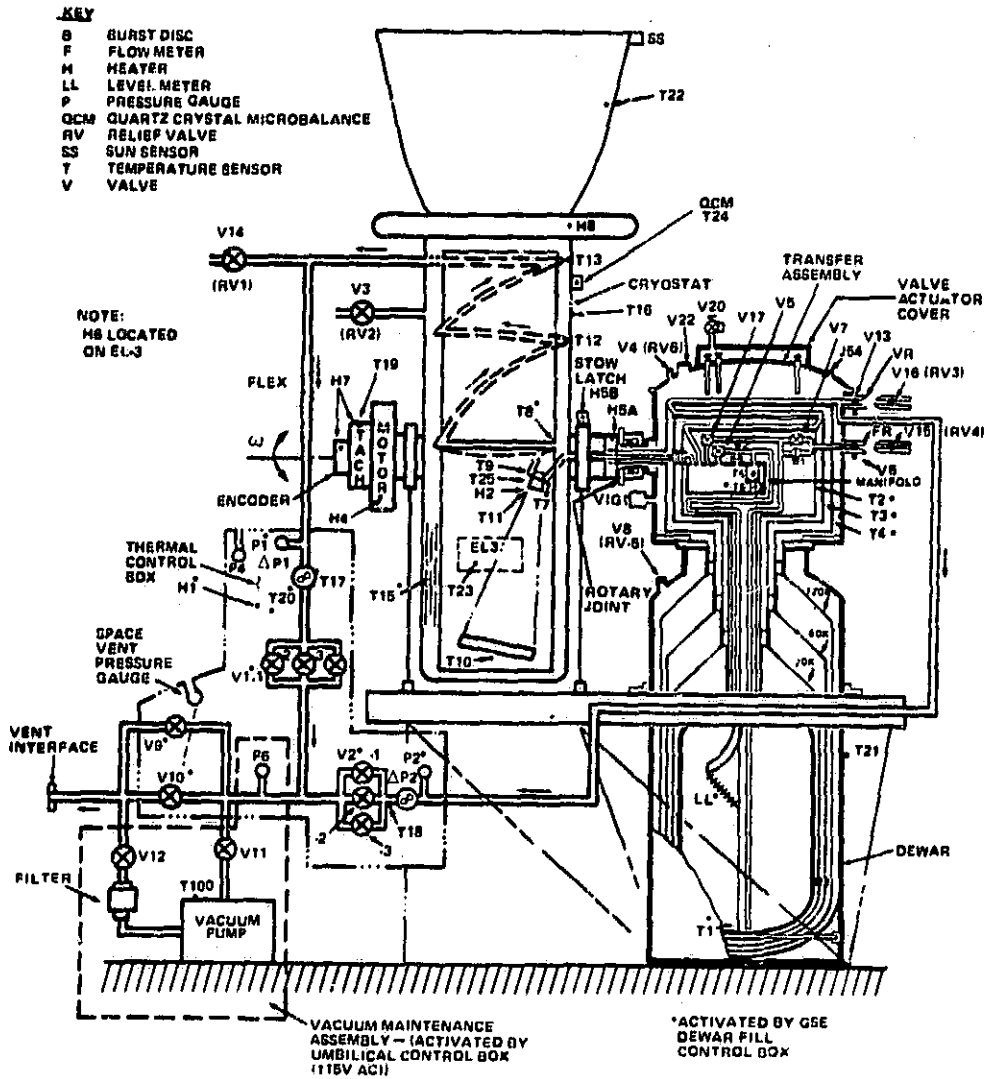


Figure 1. Model of Infrared Telescope.

HI
e

7

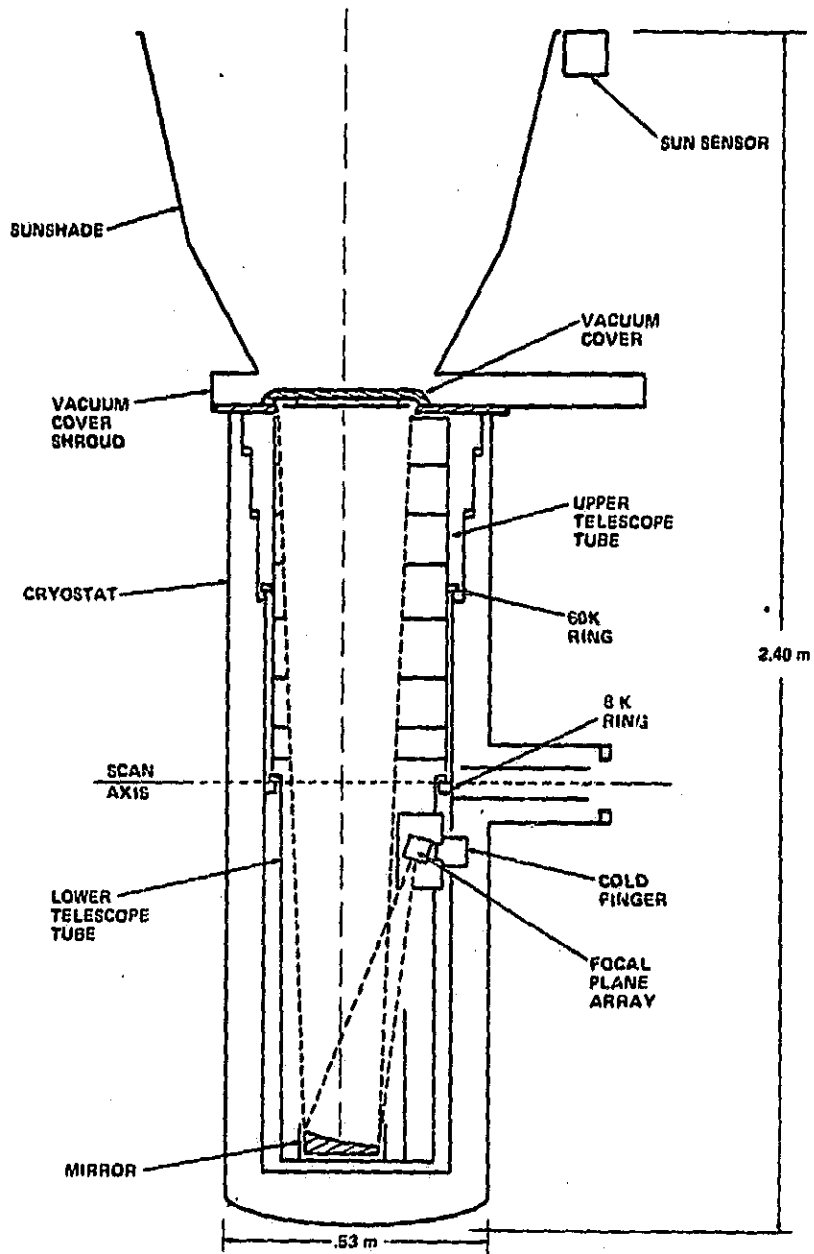
REV. 10/3/83



IRT CRYOGENIC AND INSTRUMENTATION SCHEMATIC

ORIGINAL FACED
OF POOR QUALITY

Figure 2. Schematic of IRT

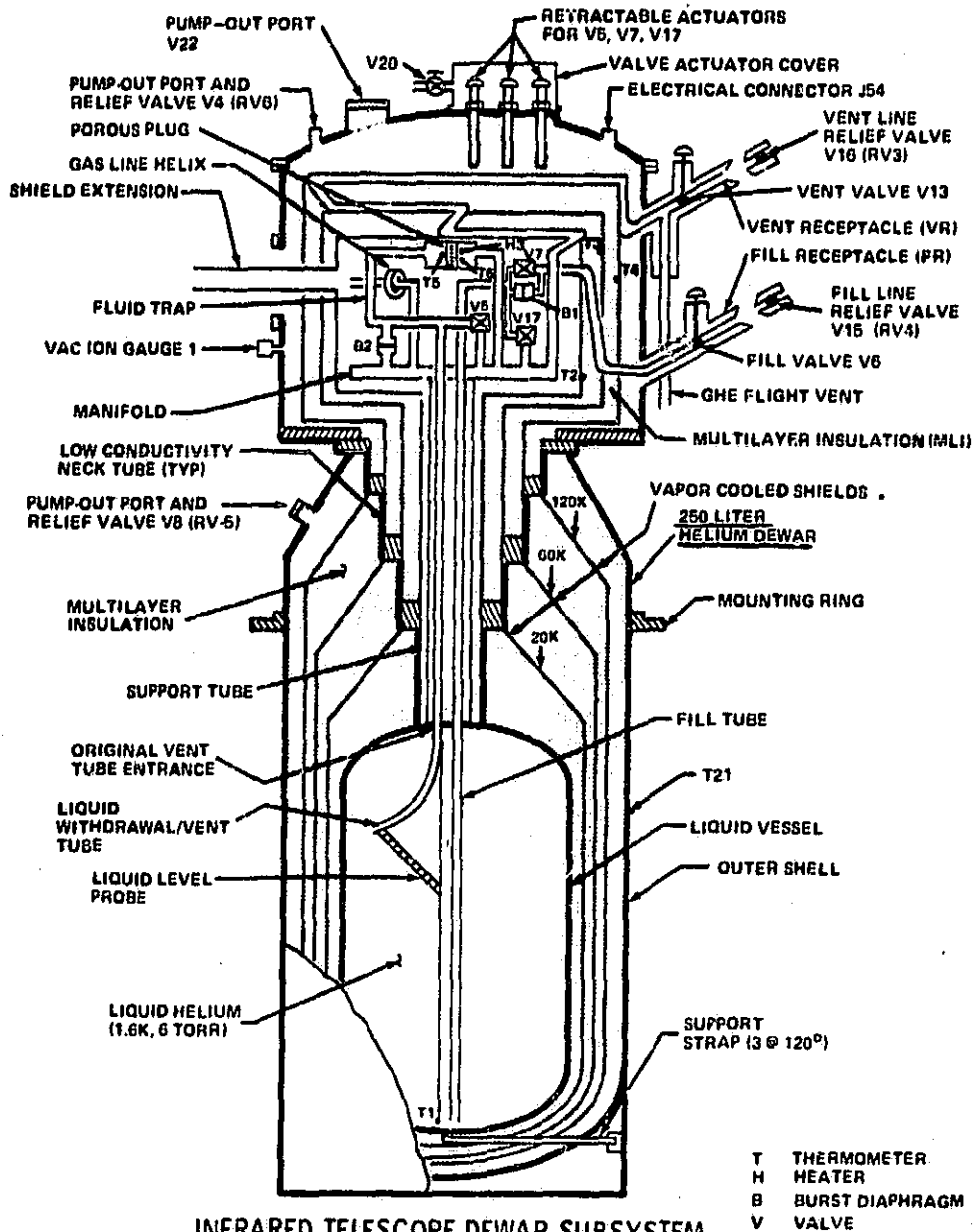


INFRARED TELESCOPE OPTICAL SYSTEM

Figure 3. Cryostat Subsystem Schematic

ORIGINAL PAGE IS
OF POOR QUALITY

REV. 10/3/83



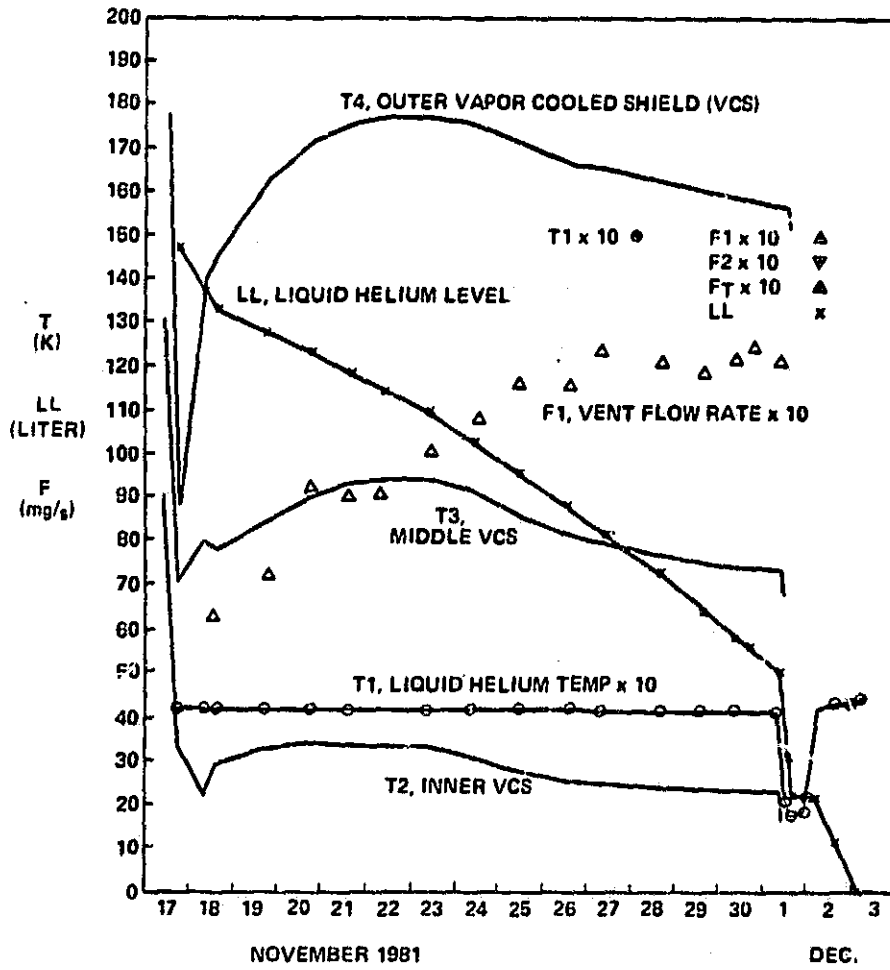


Figure 5. Summary of TPE I

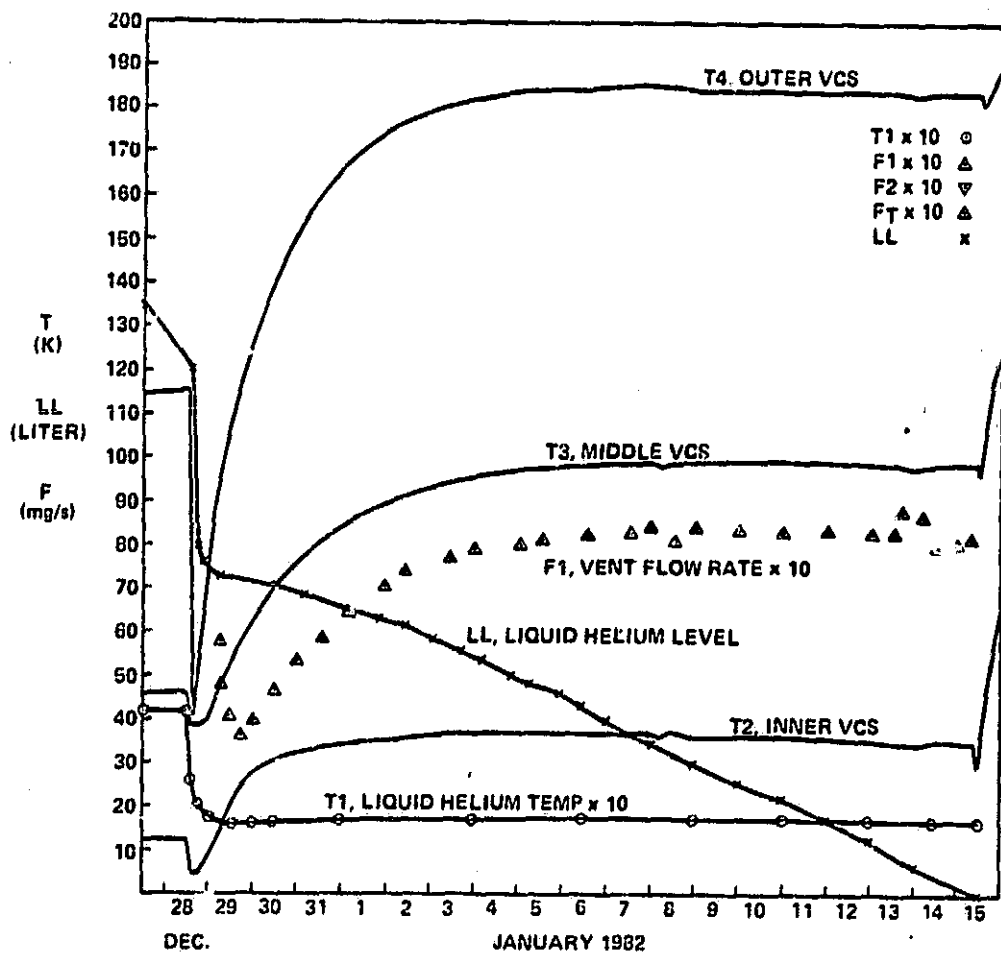


Figure 6. Summary of TPE II

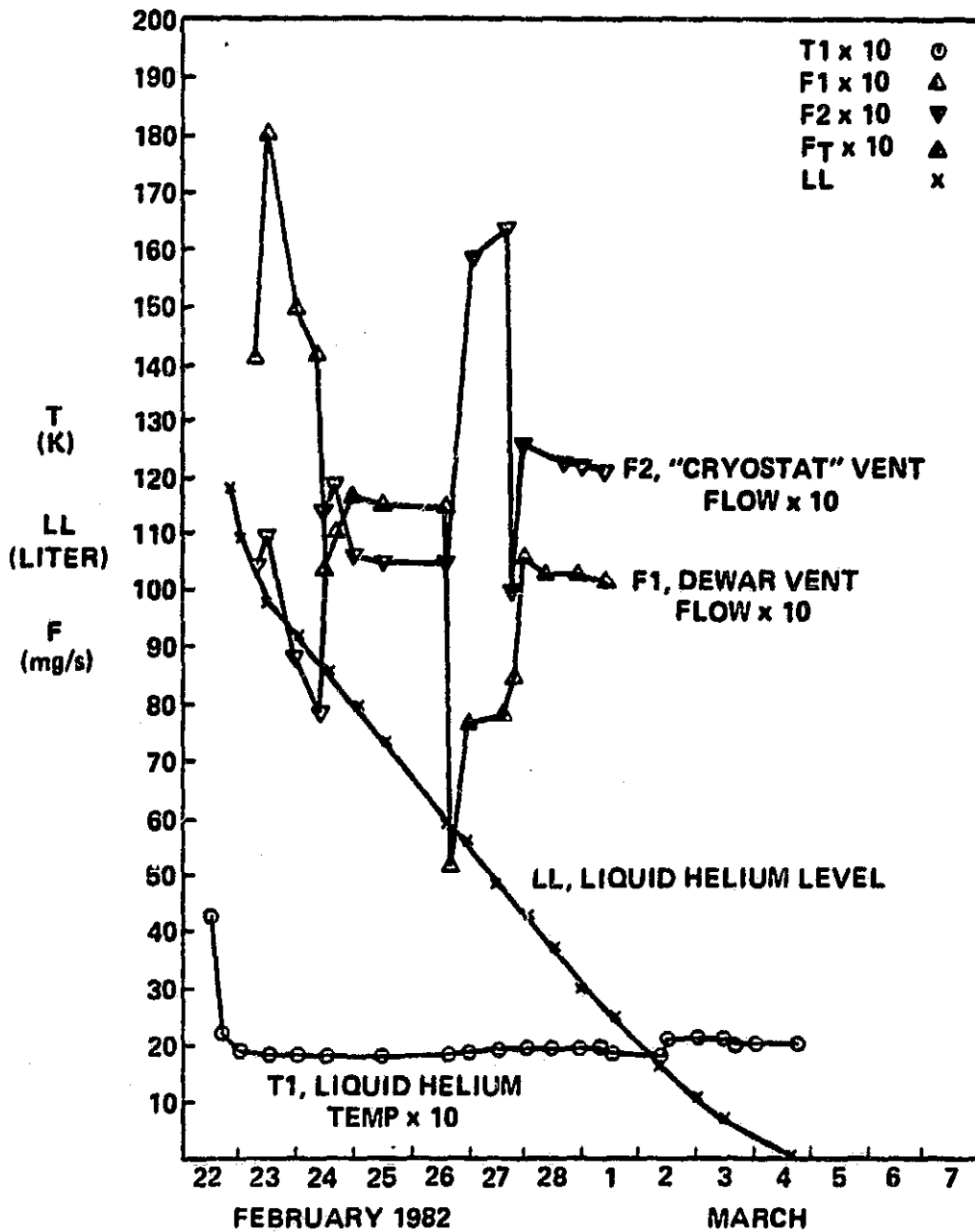


Figure 7. Divided Flow Test, TPE IV

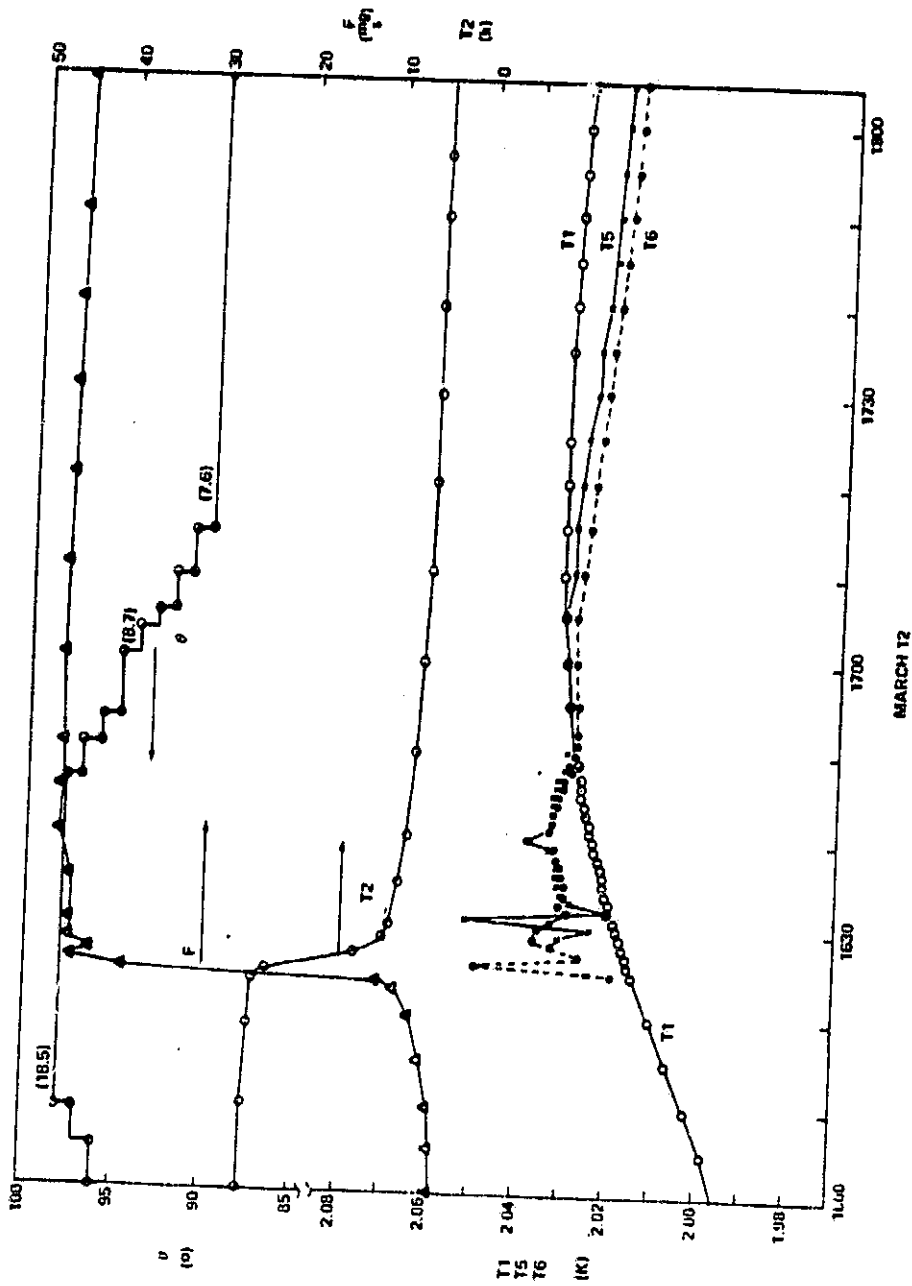


Figure 8. Porous Plug Data, TPE V, Part 1

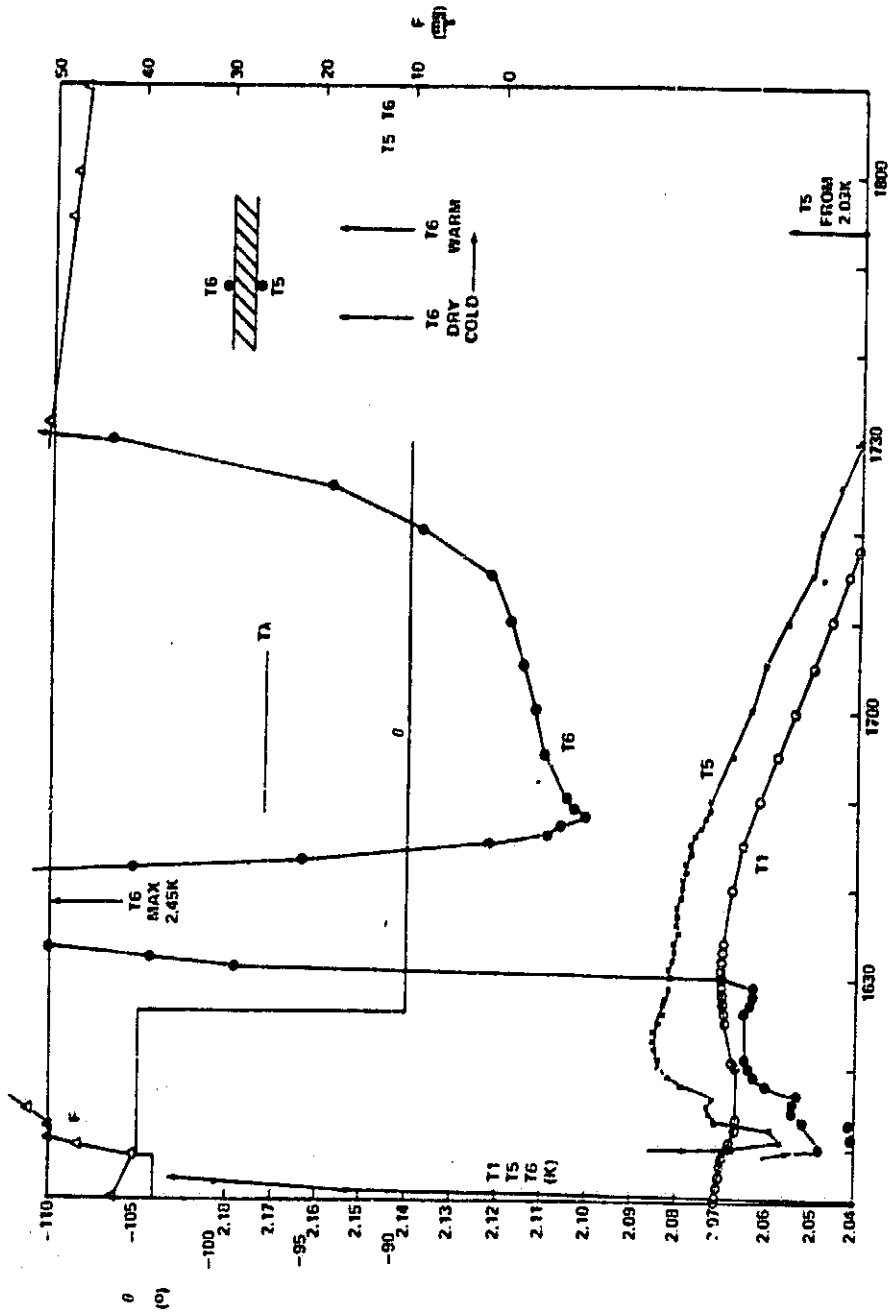


Figure 9. Porous Plug Data, TPE V, Part 2

URBAN, LADNER, JOLLEY, AND ARMSTRONG
HENDRICKS, AND KARR

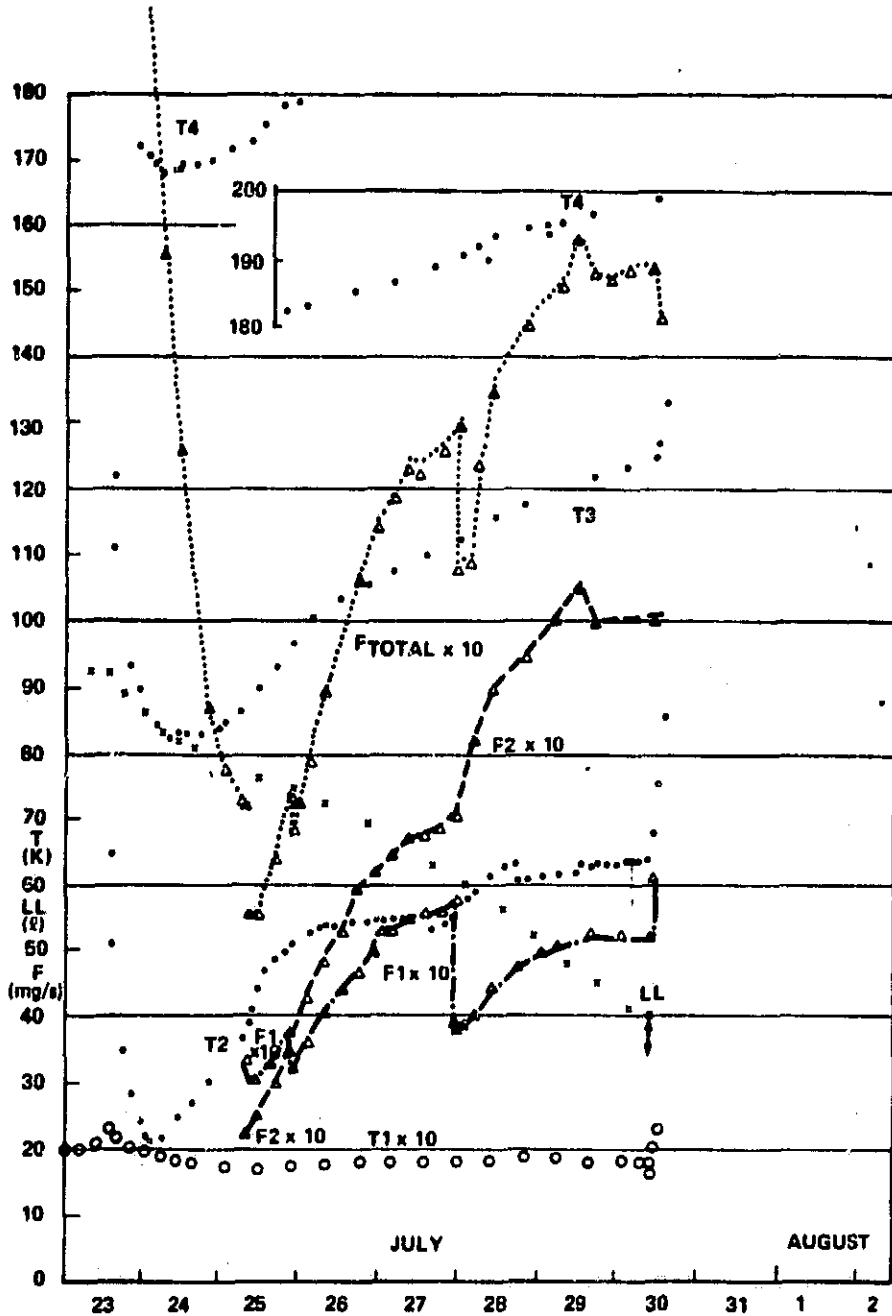


Figure 10. Divided Flow Test, TPE VI

ORIGINAL PAGE IS
OF POOR QUALITY

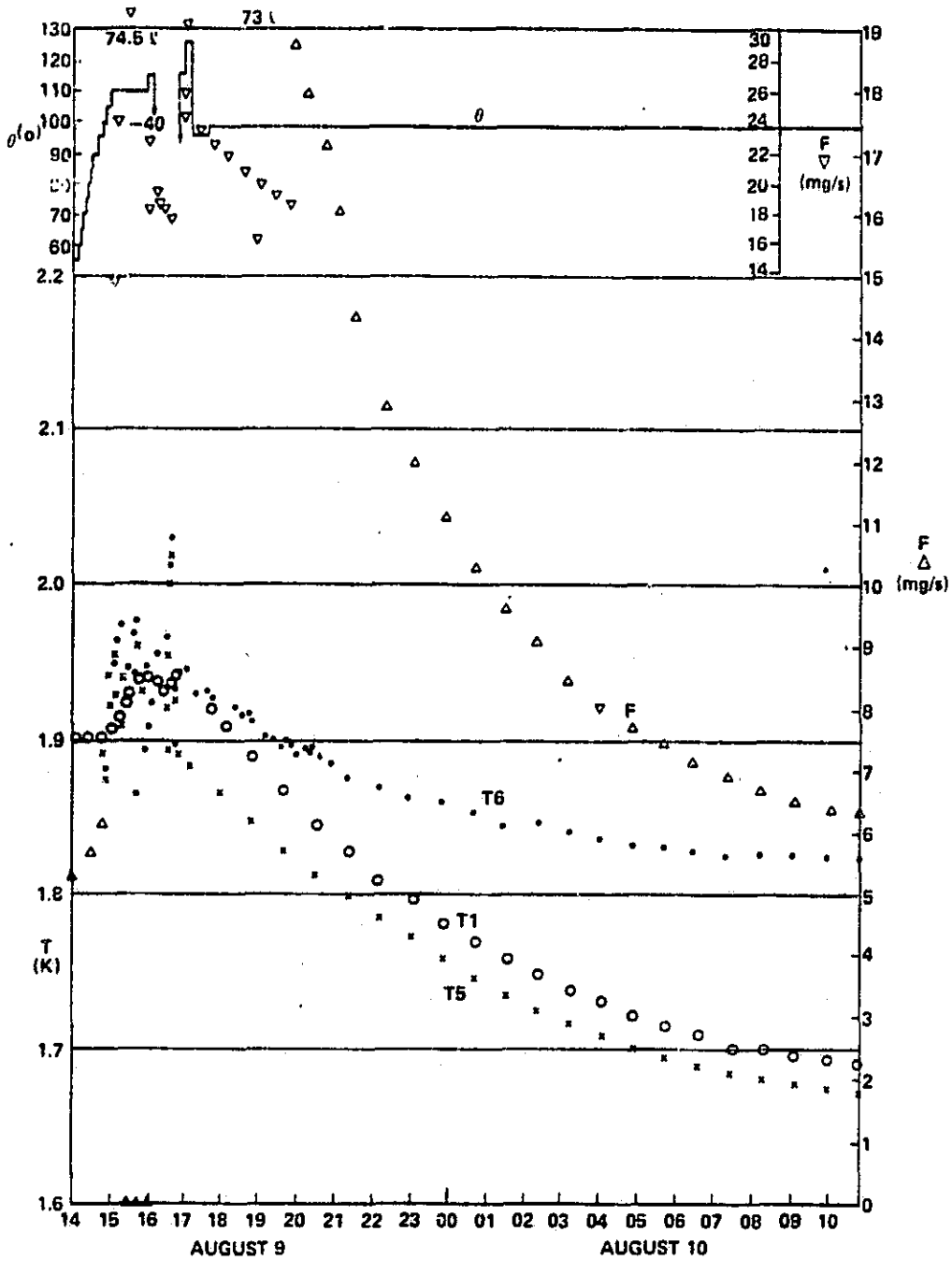


Figure 11. Porous Plug Data, TPE VII, Part 1

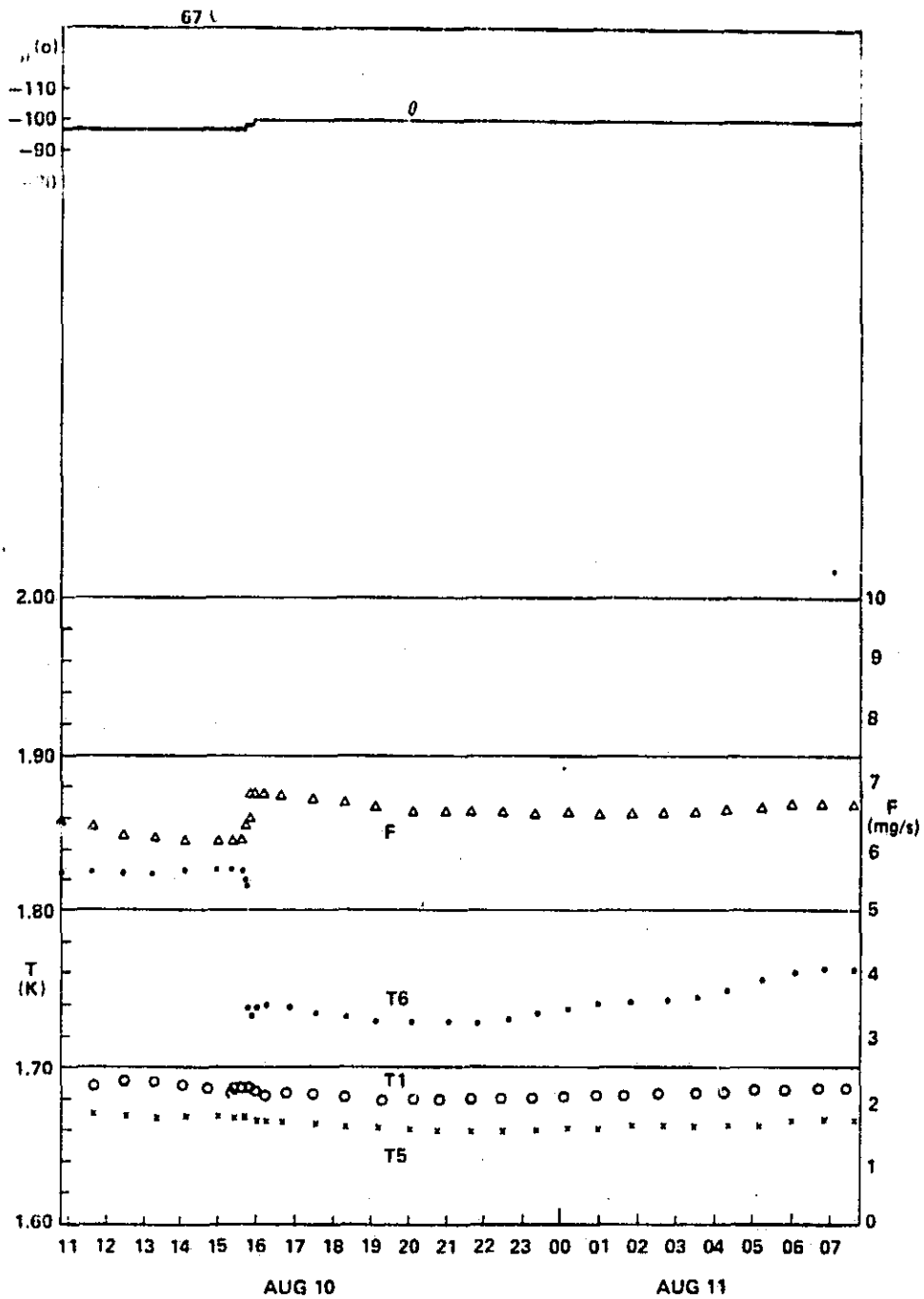
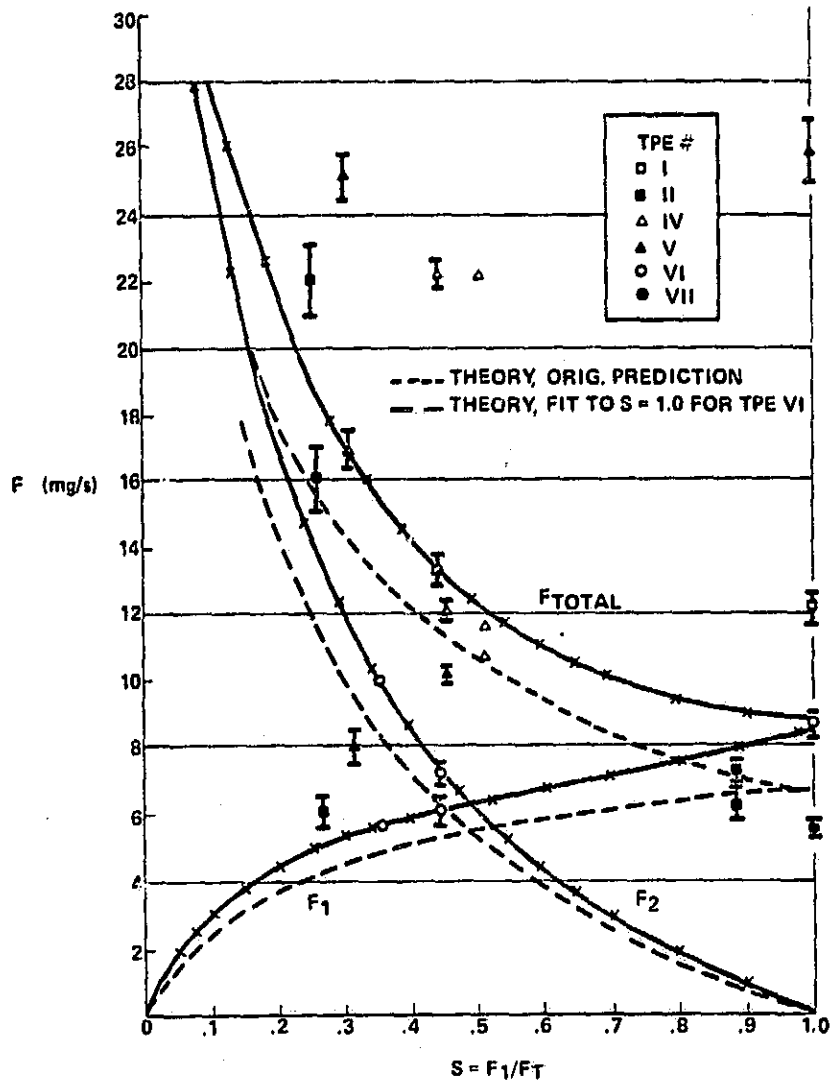


Figure 12. Porous Plug Data, TPE VII, Part 2



IRT SYSTEM MASS FLOWRATE vs. DIVIDED FLOW RATIO

Figure 13. Mass Flow Rate vs. Divided Flow Ratio

52 Bl
e

DESIGN AND PERFORMANCE OF TRANSFER ASSEMBLY
FOR THE INFRARED TELESCOPE FOR SPACE LAB 2

Gerald R. Karr and John B. Hendricks
University of Alabama in Huntsville
Huntsville, Alabama 35899

INTRODUCTION

The infrared telescope (IRT) for Spacelab 2 is of unique cryogenic design in that the approximately 2K He gas is delivered to the IR detectors from a superfluid supply dewar which is separate from the telescope/detector unit. The usual design of an infrared telescope system is for the telescope/detector unit to be an integral part of the dewar with the telescope/detector emersed into the helium bath. The IRT design has the advantage of decoupling disturbances in the liquid helium bath from the IR detector. Another advantage for IRT was that the telescope/detector design, fabrication, and testing could be carried out completely independent of the dewar development. The design of the IRT telescope/detector unit (called cryostat) was performed assuming that gaseous Helium at 2°K would be made available at the inlet to the cryostat at a flow rate that could be varied from zero to 40 mg/sec. The supply dewar was designed so that standard commercial construction methods could be used. The dewar contained no valves or heat exchanges in order to simplify the design and reduce costs. The interfacing of the storage dewar with the cryostat is the function of what is termed the transfer assembly. The transfer assembly (TA) provides for the essential IRT system functions listed in Table I. Table I also shows a list of devices contained in the transfer assembly which serve to provide the required function. In the following, we report on the design and performance of the various units of the IRT transfer assembly. Figure 1 is a schematic of the transfer assembly showing the major components, the flow passages and vacuum spaces.

TABLE I
TRANSFER ASSEMBLY FUNCTIONS AND DEVICES

<u>FUNCTIONS</u>	<u>DEVICES</u>
1. Phase separation of liquid gaseous Helium.	Porous Plug.
2. Control of flow rate of helium to IR detector.	Manifold.
3. Active and passive radiation shielding.	Heat exchangers (three) attached to shields and MLI.
4. Filling, venting, and top-off.	Thermally isolated cold valves (three) and vacuum jacketed warm valves (two).
5. Monitor performance.	Five germanium and one diode thermometer. One depth probe.
6. Vacuum integrity.	Electrical feed throughs with o-rings (warm), miniconflats (cold), rotating seals for gas line and shaft seals for cold valve operations, flexible bellows, cryopump.
7. Burst Protection.	Cold burst disks on two independent paths. Warm relief valves three.
8. Low thermal conduction between shields and to liquid volume.	Fiberglass necktube, long path length, stainless steel thin walled tubing and heat exchangers with transitions to aluminum.

Porous Plug Module

The porous plug serves as the phase separation device. The theory and performance of porous plug is discussed in another paper at this conference.¹ The plug employed in the IRT is 1/16" thick porous stainless steel of one inch diameter. The plug was welded into a plug module. The plug module has one inlet and one outlet terminated by mini-conflat flanges with copper gaskets. The plug module also has two instrumentation ports (one for each side of the plug) which are sealed using mini-conflat type flanges with copper gaskets. The instrument ports have devices for holding germanium thermometers against the plug surface under a spring force.

Plumbing Module

The plumbing module is a removable unit containing the gas manifold, cold valves, and cold burst disks. Figure 2 shows the plumbing module with the porous plug module attached. The TA manifold serves a variety of functions depending on the mode of operation. The manifold serves as the cold structural unit to which all the cold valves and plumbing are attached. The stainless steel manifold is bolted directly onto the central aluminum support tube which in turn is rigidly attached to the 200 liter aluminum liquid storage vessel. The gas side of the porous plug attaches to the manifold and the liquid side of the plug module attaches to the liquid supply line leading from the storage vessel. Gas from the porous plug flows into and through the manifold and out via two possible paths. One path out of the manifold leads to the helix which then delivers gas to the IR detector. The other path is through the dewar heat exchanges which cool the dewar and TA radiation shields.

The cold fill, vent (plug bypass), and dewar bypass valves are attached to the manifold allowing filling and vapor venting during fill operations. The porous plug is bypassed by the vent valve during the high vapor flow experienced during the filling and top-off operations. The dewar bypass valve allows for precooling of all the TA plumbing and heat exchanges prior to dewar top-off. Prior to launch, all cold valves are closed and the fill line is evacuated. The vacuum in the fill line is sealed at the warm end by a warm low pressure (3 psi) relief valve. A similar relief valve is placed on the vent line. During filling, top-off, and pump down activities the vent line is pumped via large capacity pumps connected directly to the vent line at the TA outer case. Prior to launch the TA vent line access is sealed with the warm relief while the low vent-line pressure is maintained by an onboard vacuum pump. Thermal isolation of the cold valves is achieved by using manually operated valve stems which are retractable through holes in the radiation shields. The holes are radiatively blocked with MLI flaps. A rotating and sliding vacuum seal is provided for the valve stems at the top of the TA.

One cold burst disk contained in the plumbing module provides a relief path should the plug fail to pass liquid or vapor. Another cold burst disk provides for a relief path past the fill line cold valve. The two burst disks relieve into the vent and fill lines respectively which are then relieved by the warm low pressure relief valves discussed above.

Helix Module

A device called the helix module is designed to provide for passage of the cold helium gas through the rotating interface between the TA and the cryostat. The helix module has mini-conflat inlet and outlet flanges with copper seals. Cold gas from the manifold travels

4

to the helix module inlet. The gas then travels through 1/8" stainless steel thin wall tubing wound in a helix of three inch diameter having ten turns. The helix is designed to allow for $\pm 45^\circ$ cyclic rotation along the axis of the helix. The number of helix windings was determined such that the stainless tube was stressed well below the fatigue limit.

Dewar Heat Exchanges Units

Gas may leave the manifold either through the helix or through the dewar heat exchanges. The control of the flow rates out these two paths is achieved by flow control valves on the vent lines of both the cryostat and the dewar. These flow control valves are motor operated and are at room temperature housed in a heated flow control box attached to the flight structure.

The dewar heat exchangers receive gas from the manifold at a flow rate determined by the external control valve settings. There are three dewar heat exchangers which cool the three dewar radiation shields. The heat exchanges consist of rectangular aluminum manifolds welded to aluminum tubs (see figure 3). Figure 3 shows the three tubs with the heat exchangers welded to the top of the tubs. The tubs are belted to concentric aluminum cylinders which are welded to the dewar radiation shields surrounding the liquid storage container. Figure 4 shows the three concentric cylinders which are visible at the dewar top flange. The dewar guard vacuum is separated from the transfer assembly vacuum by the fiberglass neck tube. The fiberglass neck tube serves also to support the liquid container, the radiation shields and the tubes supporting the heat exchanges.

The first dewar heat exchanger is a 0.95 by 3.3 by 86cm aluminum volume fed by 1/2" line having a transition to 1/2" stainless line for thermal isolation. The first heat exchanger is connected to the second heat exchanger through a 1/2" stainless steel line with transition to aluminum at each heat exchanger. A vacuum tight disconnect allows for the assembly or disassembly of the heat exchanger interconnects. The second and third heat exchange are of similar design to the first. The second heat exchange has an internal flow passage of 0.95 by 7.3 by 108cm length. The third heat exchanger has an internal flow passage of .95 by 9.8 by 128cm length. The design of the heat exchangers is based on a requirement to provide for efficient heat exchange while also having low pressure drop. The low pressure drop through the heat exchangers is necessary to provide efficient pumping during filling and top-off operations. For the range of flow rates through the heat exchanger systems, the flow is fully developed laminar with a constant Nusselt number, Nu, of near four. That is

$$Nu = \frac{hD_h}{k} \approx 4$$

where h is the film coefficient, D_h is the hydraulic diameter of the rectangular flow passage and k is the thermal conductivity of the gas. Under the conditions of fully developed laminar flow, the pressure drop is reduced to extremely low values as indicated by the following equation for pressure drop per unit length of that exchanger

$$\frac{dp}{dx} = \frac{32m\dot{\mu}}{\rho D_h^2 A}$$

where m is the flow rate, μ is the viscosity, ρ is the density, and A is the cross-section area of the flow channel. The equation reveals the importance of increasing the area to reduce the pressure drop while maintaining the heat transfer at a high level.

Transfer Assembly Performance

The assembled and flight ready transfer assembly is shown pictured in figure 5. The view seen in figure 5 shows the top of the TA with the three cold valve control stems visible. The external fill and vent valves can also be seen in figure 5. Performance testing has shown that all objectives have been reached by the design. Figure 6 shows temperature and flow data recorded during thermal performance testing. All the various TA modules performed as expected. The heat exchanger temperatures are found to have long time scale (days) damped oscillations to steady state. The heat exchange/shield systems have high heat capacity with low thermal conduction between the shields. Cold gas delivery to the cryostat has been shown to be adjustable from zero to 40 mg/sec at a delivery temperature of at least 2K². In summary, the TA appears to meet all specifications and should function as expected during the Space Lab 2 mission now scheduled for March 1985.

Acknowledgements

This work was supported in part under NASA/MSFC contract NAS8-32818.

References

1. J.B. Hendricks and G.R. Karr, Paper CB-6 (this conference).
2. G.R. Karr, J.B. Hendricks, E.W. Urban, L. Katz, and D. Ladner Proceedings of Eighth ICEC, June 1980, p. 38-42.

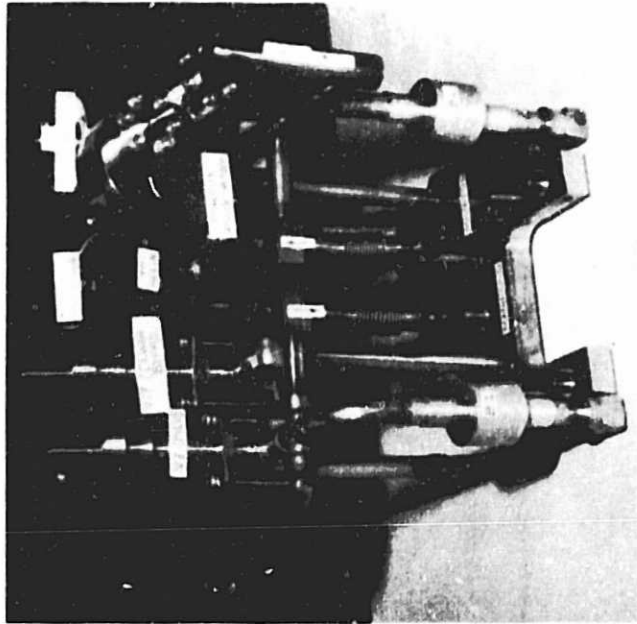


Figure 2. This photo of the plumbing module also shows the porous plug module attached. The two burst disks are shown labeled B1 and B2. The three cold valves are labeled as V7 (Fill), V17 (Dewar Bypass), and V5 (Plug Bypass). The manifold is labeled and serves as the support structure of the plumbing elements. The two bellows shown labeled with arrows are attached to the dewar fill line (arrow down) and the liquid withdraw line (arrow up).

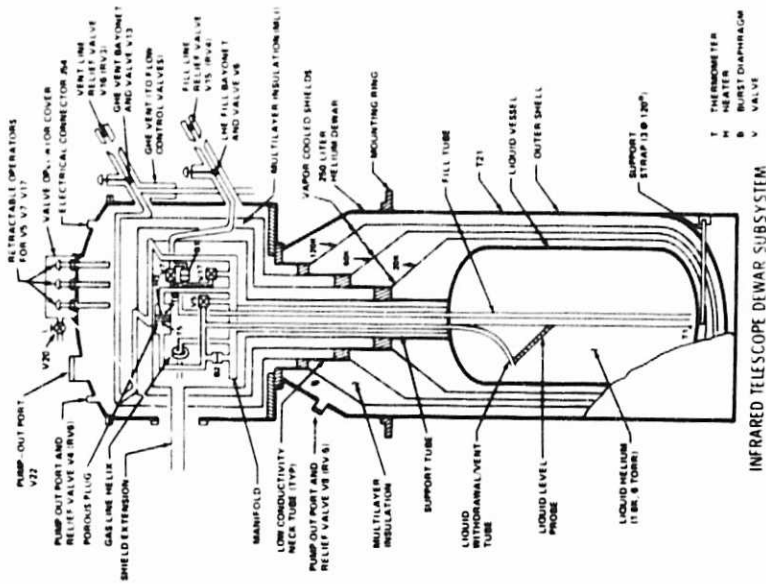


Figure 1. This schematic of the dewar subsystem shows how the transfer assembly interfaces with the storage vessel. The cryostat attached to the flange at the upper left hand of the schematic at the point labeled "Shield extension."

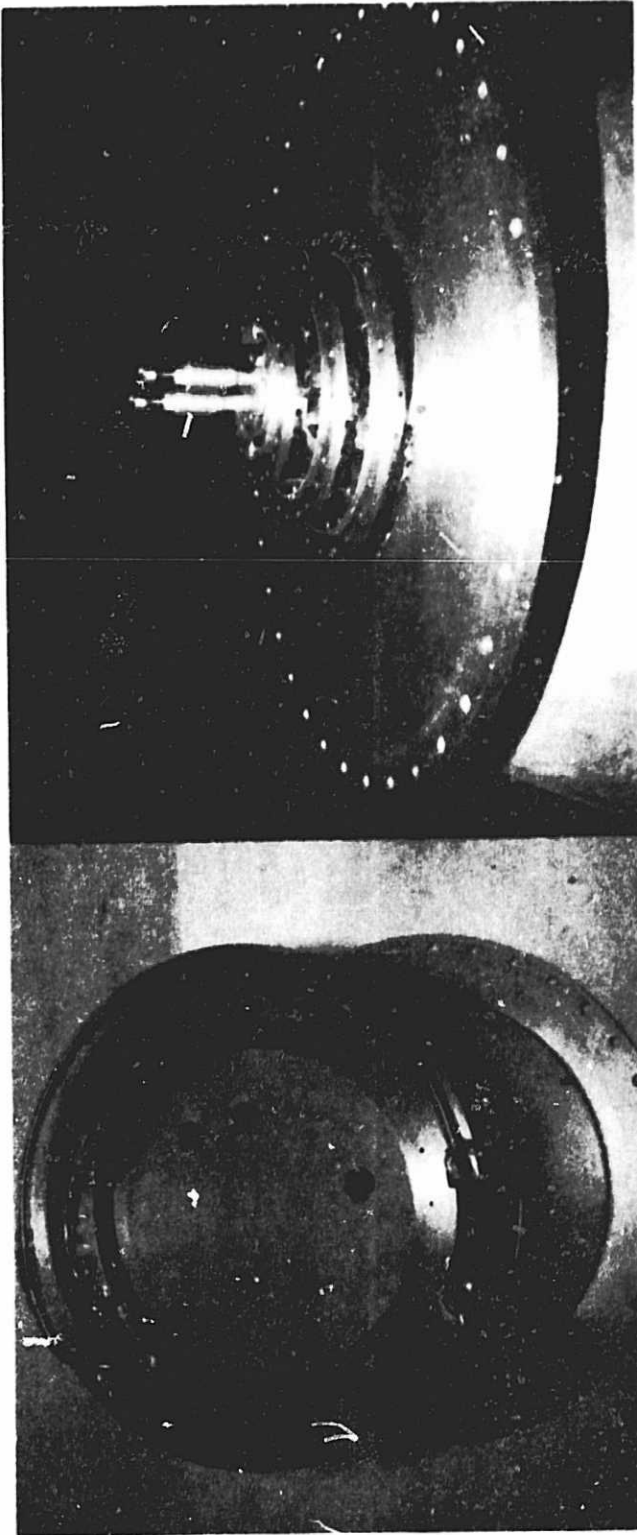


Figure 3. This photo shows the three heat exchangers as they are assembled onto the dewar. The MLI had not yet been applied when this photo was taken. The smallest heat exchanger has the coverplate attached showing the holes which allow for passage of the cold-valve operators. MLI blankets and similar cover plates are attached to the second (mid-sized) and third (largest) heat exchanger. The photo also shows the $\frac{1}{2}$ " interconnect lines and the vent line flange.

Figure 4. This photo shows the dewar top flange (large bolt circle) with the three concentric tubes which attach directly to the dewar shields. The three heat exchangers shown in Figure 3 attach to the three concentric rings shown in this photo. The two tubes in the center pass through a central column which supports the plumbing module which bolted attachment at the manifold (see Figure 2). The two tubes also attach to the plumbing module to serve as the fill and liquid withdraw line.

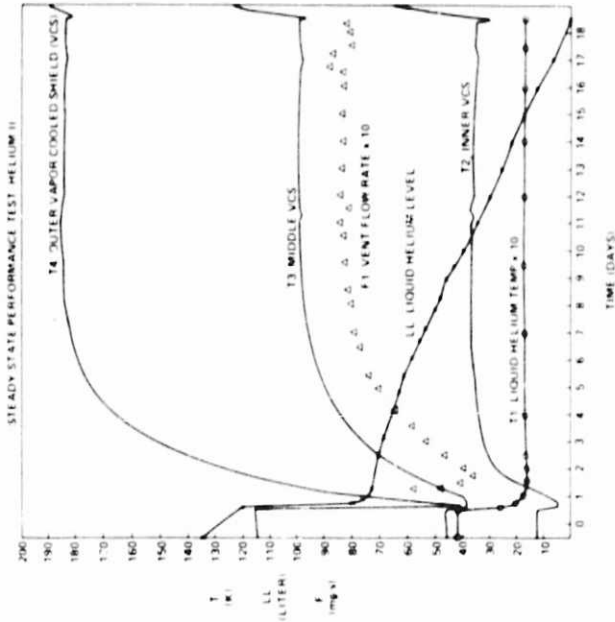


Figure 6. The performance of the transfer assembly is illustrated in this figure which shows the temperatures of the three heat exchangers as a function of time during a pump down to 1.6K. The flow rate leveled off a 8 mg/sec after 8 days. The shield temperatures leveled off to approximately 38K, 98K, and 180K representing steady state operation of the inner, middle, and outer heat exchangers.

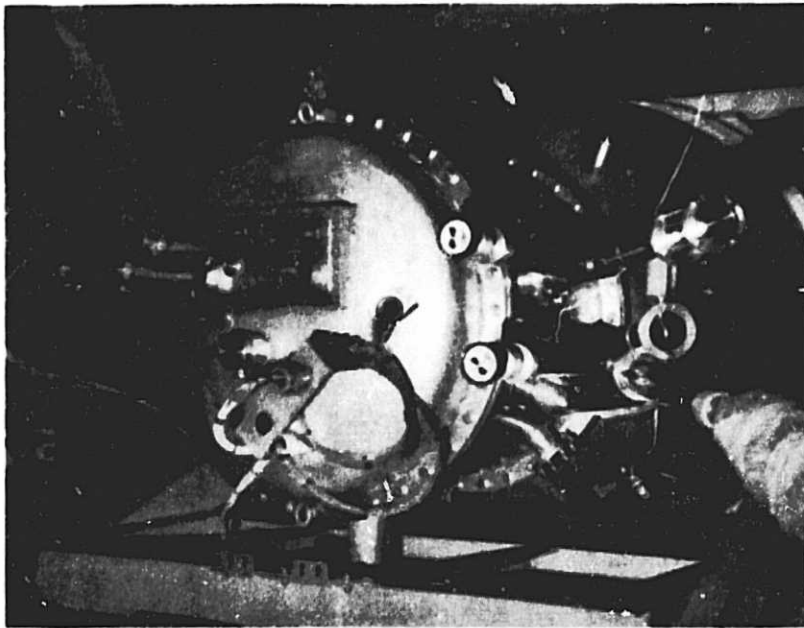


Figure 5. Top view of assembled transfer assembly onto the flight dewar. The three cold-valve control stems are visible on the dome. The fill and vent lines are in the foreground. The vent line has a pumping line attached while the fill line has a low pressure relief valve attached as will be the case for flight.

APPENDIX G

THE INFRARED TELESCOPE ON SPACELAB 2

J.B. Hendricks[†], G.R. Karr[†], E.W. Urban* and D.R. Ladner*

[†]The University of Alabama in Huntsville; Huntsville, AL 35899 USA

*NASA, Marshall Space Flight Center; Huntsville, AL 35812 USA

I. Introduction

The Infrared Telescope (IRT) for Spacelab 2 is now scheduled to be flown in April, 1985. The experiment has been integrated into the Spacelab 2 payload and has passed all cryogenics testing. This paper briefly describes the experiment concept, the theory of operation, the performance during ground operations as compared to theory, and finally we discuss the pre-launch servicing that is planned.

II. Experiment Concept

The concept for cooling the IRT is unique in that the liquid helium cryogen is contained separately from the telescope. The liquid helium is maintained in a superfluid state and only the cold vapor is supplied to the telescope detector block. This concept allowed for the telescope to scan relative to the shuttle while the large volume of liquid helium can remain fixed relative to the shuttle. The concept allows for considerable isolation of the detector block from any motions and pressure changes that may occur in the liquid helium. The storage dewar and cryostat are shown in Figures 1 and 2 respectively. The reader is referred to references /1,2,3/ which describe the two subsystems in greater detail.

In order to reduce costs and to make delivery schedules, the dewar and cryostat were designed to be developed separately and the basic units were purchased commercially and contained no moving parts or active elements. All the plumbing complexity is built into the upper section of the dewar subsystem called the transfer assembly. The transfer assembly (TA) contains the following major components.

- a. Porous plug for phase separation of helium.
- b. Plumbing manifold for control of helium vapor flow.
- c. Heat exchangers attached to radiation shields of the dewar.
- d. Three cold valves and two warm valves for filling, venting and top-off servicing of the dewar.
- e. Instrumentation for monitoring temperatures at six locations and measuring the depth of liquid helium in the dewar.
- f. Rotating vacuum-tight seals to allow rotation of the cryostat relative to the dewar and to provide for manual operation of cold valves.
- g. Two burst disks to provide independent burst paths and designed to operate at helium temperatures.
- h. Activated charcoal absorber.

The above major components were all designed to be assembled as separate components which could be easily exchanged should some component fail. The modular design concept has proven to be an advantage in that some units have had to be replaced for various reasons during the build-up of the experiment. All the major components are connected via high vacuum seals proven to be leak-tight at helium temperatures.

III. Theory and Simulation of Operation

The thermal performance of the entire IRT system was first simulated in order to guide the design and development of the experiment. A computer program was constructed based on an energy balance at various stations in the system. Each of the system heat exchangers were required to satisfy a heat balance equation given by

$$\dot{m}_k c_p (T_n - T_{n-1}) = \sum_i C_{i,n} (T_i - T_n) + \sum_i R_{i,n} (T_i^4 - T_n^4) \quad (1)$$

where \dot{m}_k represents either the dewar flow (\dot{m}_1) or the cryostat flow (\dot{m}_2), c_p is the specific heat of the helium gas, $C_{i,n}$ represents the conduction heat transfer coefficient between the heat station at T_i and the heat station at T_n , and $R_{i,n}$ represents the radiative heat transfer coefficient between the i^{th} and the n^{th} heat station. The primary conduction and radiation paths for each heat exchanger is between those heat stations directly above and below in temperature. Notable exceptions to this pattern is the radiation onto the lower telescope tube during times that the vacuum cover is closed and certain support straws that have conduction paths through neighboring heat shields. The total mass flow rate ($\dot{m} = \dot{m}_1 + \dot{m}_2$) is governed by the heat balance for the dewar liquid vessel given by

$$\dot{m}L = \sum_i C_{1,i} (T_i - T_1) + \sum_i R_{1,i} (T_i^4 - T_1^4) \quad (2)$$

where L is the latent heat of vaporization of liquid helium at temperature T_1 . A set of equations can then be developed for the dewar system given by Equation 2 for the inner vessel and three equations of the type given in Equation 1 to represent the heat balance of the three heat exchangers. Equation 1 applied to the dewar will have $\dot{m}_1 = s\dot{m}$ where s represents the fraction of total helium boil off sent to the dewar heat exchangers. Assuming that the outer case temperature is given and the liquid helium temperature T_1 is given, we obtain, for the dewar, a set of four equations in four unknowns of the form

$$R_i(\dot{m}, T_2, T_3, T_4) = 0, \quad i = 1, 4 \quad (3)$$

where $T_2, T_3,$ and T_4 are the unknown temperature of the three dewar heat exchangers.

The cryostat will receive a mass flow of $\dot{m}_2 = (1-s)\dot{m}$ where \dot{m} is determined from the solution to Equation 3. Thus, the cryostat has a set of type 1 equations representing the heat balance of the four heat exchangers given by

$$R_i(T_6, T_7, T_8, T_9) = 0, \quad i = 5, 6, 7, 8 \quad (4)$$

The dewar and cryostat sets of equations can be solved separately and in a similar fashion. The equations are found to be algebraic and non-linear which requires that an iterative technique be used for numerical solution. A Newton-Raphson method was chosen in which the residuals given in Equations 3 and 4 are differentiated with respect to the given unknowns to form, for each R_i , the following equation

$$\frac{\partial R_i}{\partial Y_1}(\delta Y_1) + \frac{\partial R_i}{\partial Y_2}(\delta Y_2) \dots = -R_i \quad (5)$$

where Y_i represents the unknowns. This set of equations is solved for the corrections, δY_i , to be used to provide a new value of Y_i at the n^{th} iteration, given by,

$$Y_i^{(n)} = Y_i^{(n-1)} + (\delta Y_i)^{(n)} \quad (6)$$

The above procedure was found to converge rapidly.

IV. Pre-Launch Performance

The dewar and cryostats were tested separately, and as a system during a one year period. Figure 3 summarizes the performance and also shows the comparison with the simulation discussed above. In general, the performance is much as predicted. The total heat leak into the system is only a little higher than predicted and no effort has been made to identify the source. A more complete discussion of the performance of the system during the various thermal performance experiments is described in a previous paper.

V. Pre-Launch Ground Operations

The pre-launch operations required for the IRT are summarized in Figure 4. The figure shows a nominal March 29 launch and approximately two months of preparation.

The preparation begins with a long duration pumping of the guard vacuums for both the cryostat/TA vacuum and the separate dewar vacuum. The vacuum guards are pumped through 3 inch pumping ports. The first filling of the dewar is designed to cool and stabilize the system during the period between the beginning of loading of the Spacelab 2 (SL2) payload into the shuttle and the beginning of operations in the vertical assembly building (VAB). At the beginning of the VAB operation, the IRT is topped-off with enough liquid helium to last during the entire period of VAB and pad operations. The dewar is lying with its longitudinal axis horizontal. This horizontal mode of filling and venting had not been planned during the early phases of the IRT development and required that the curved vent tube shown in Figure 1 be added.

Two days prior to launch, when the shuttle is in the launch pad, the dewar is pumped-on to convert the helium to superfluid. The dewar is then topped-off with liquid using low pressure top-off techniques. After the low pressure top-off, the liquid is again converted to superfluid, in preparation for launch.

During orbital operations, the helium flow rate is expected to be less than 30 mg/s which will give adequate lifetime operation of the telescope throughout the nominal seven day mission. The helium flow rates through the dewar and cryostat will be monitored and controlled from the ground throughout the mission.

References

1. Urban, E.W., D. Ladner, J. Jolley, M. Armstrong, J. Hendricks, and G.R. Karr, "Cryogenic Performance Testing of the Infrared Telescope (IRT) for Spacelab 2," To be published in the Proceedings of the 1983 Space Helium Dewar Conference and Workshop, August 23-26, 1983.
2. Karr, G.R., and J.B. Hendricks, "Design and Performance of Transfer Assembly for the Infrared Telescope for Spacelab 2" *Adv. in Cryo. Eng.*, Vol. 29, (1984).
3. Karr, G.R., J.B. Hendricks, E.W. Urban, and D. Ladner, "Performance of the Superfluid Dewar Subsystem for the Spacelab 2 Infrared Telescope" Ninth International Cryogenic Engineering Conference - International Cryogenic Materials Conference and Exhibition, May 11-14, 1982, Kobe, Japan.

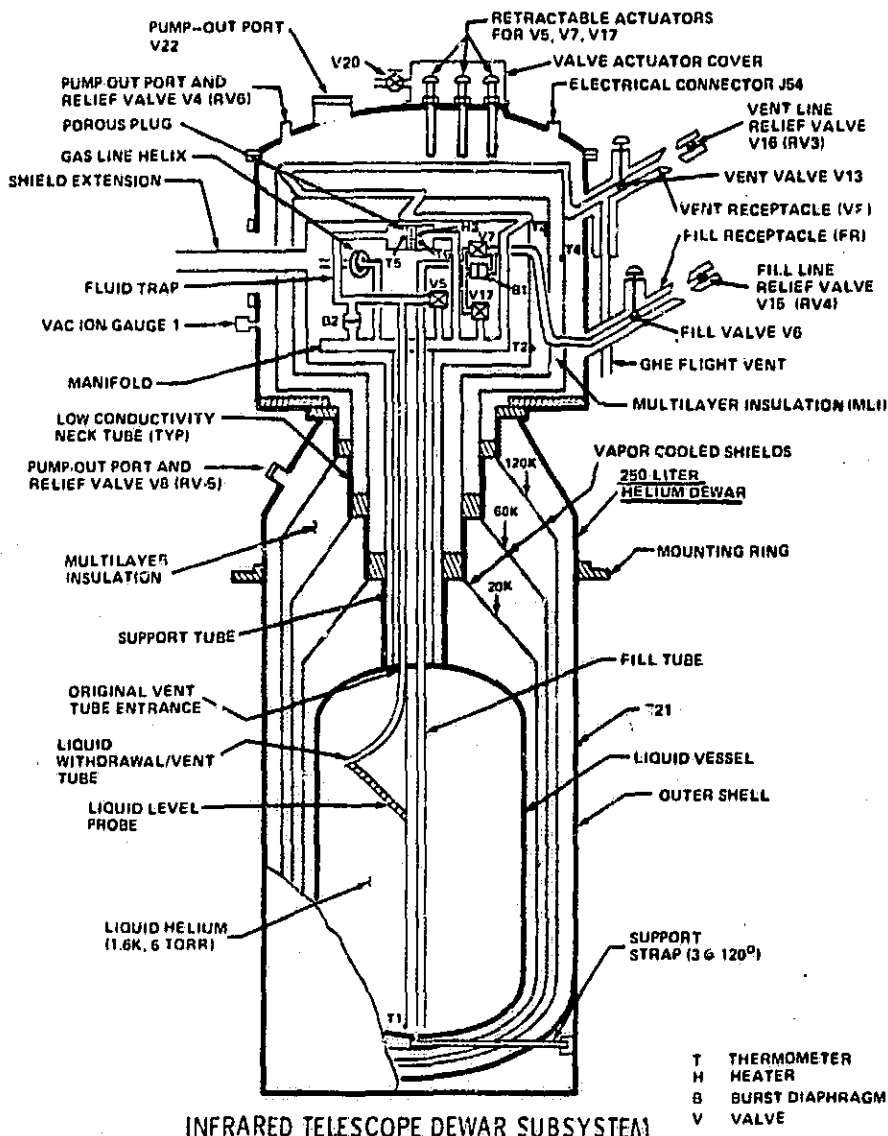
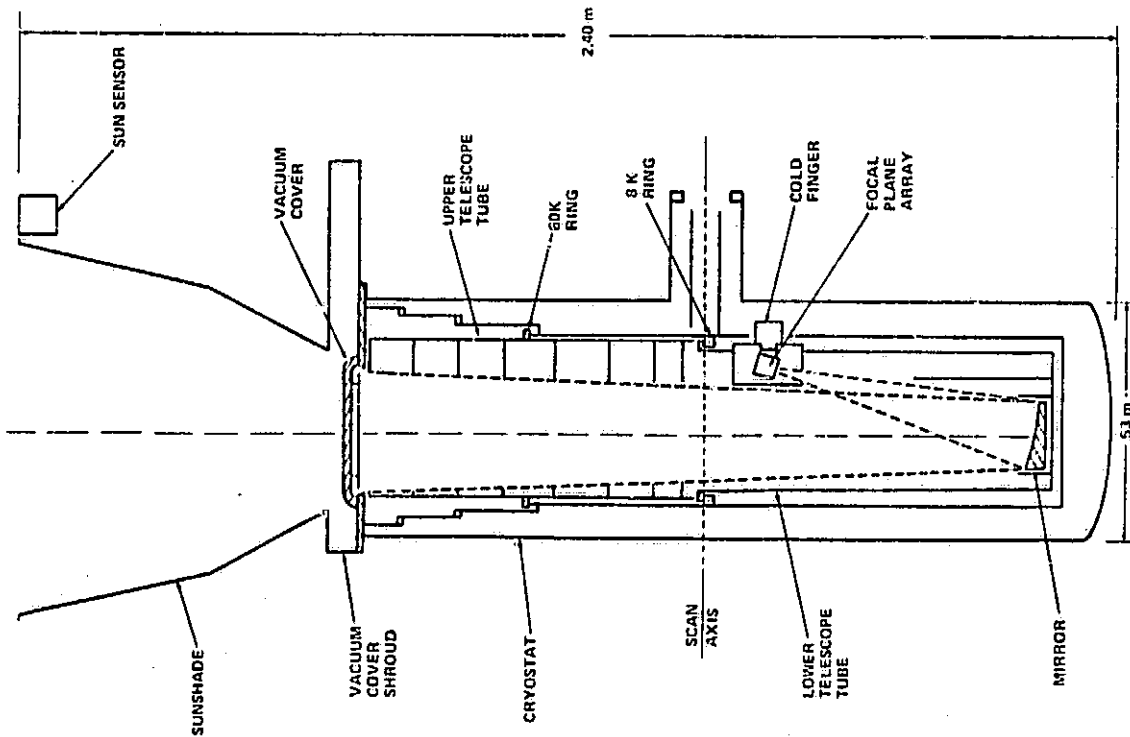
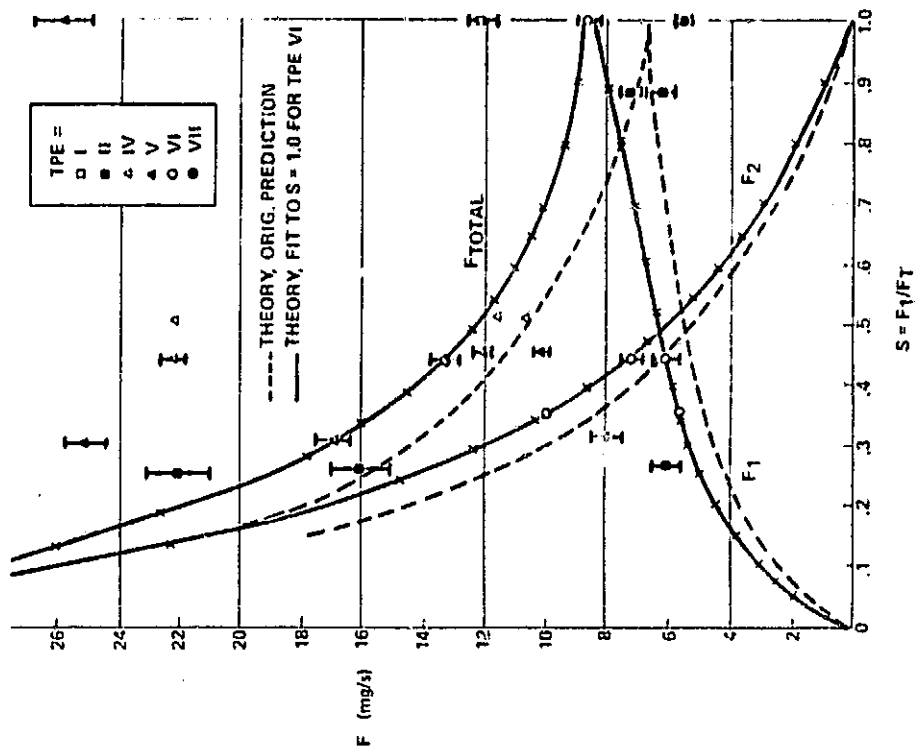


Figure 1. Dewar Subsystem Schematic



INFRARED TELESCOPE OPTICAL SYSTEM

Figure 2. Cryostat Subsystem Schematic



IRT SYSTEM MASS FLOWRATE vs. DIVIDED FLOW RATIO

Figure 3. Mass Flow Rate vs. Divided Flow Ratio.

JANUARY 20 21 22 23 24 25 26 27 28 29 30 31
 FEBRUARY 1 2 3 4 5 6 7 8 9 10 11 12 13 14 15 16 17 18 19 20 21 22 23 24 25 26 27 28 29 30 31
 MARCH 1 2 3 4 5 6 7 8 9 10 11 12 13 14 15 16 17 18 19 20 21 22 23 24 25 26 27 28 29 30 31
 APRIL 1 2 3 4 5 6 7 8

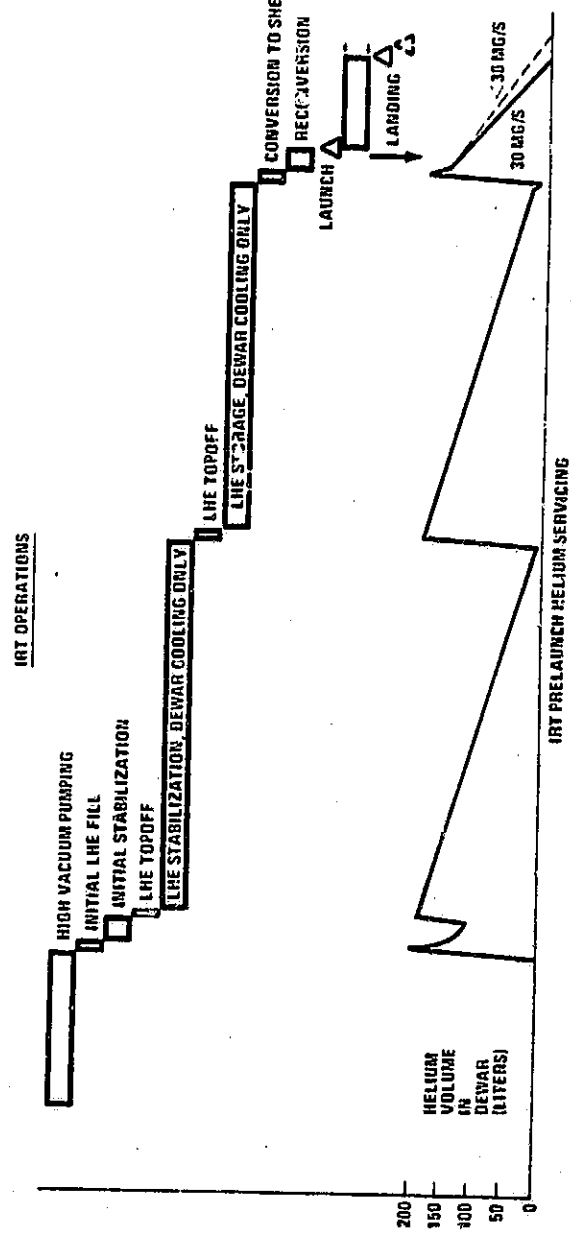
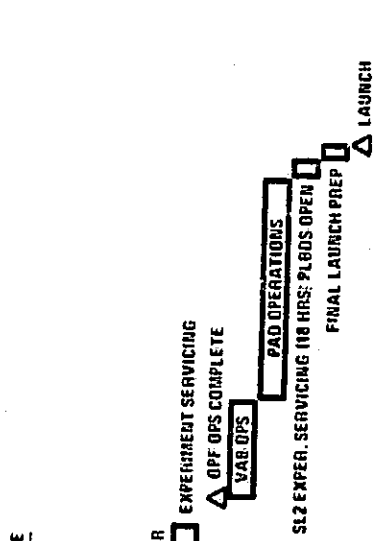


Figure 4. Nominal Ground Operations Schedule for IRT.